

# DISSERTATION

submitted to the  
Combined Faculties for the Natural Sciences and for Mathematics  
of the Ruperto–Carola University of Heidelberg, Germany  
for the degree of  
Doctor of Natural Sciences

presented by

Diplom–Physiker Tobias Baier  
born in Nürnberg

Oral examination: December 17, 2002



A RENORMALISATION GROUP APPROACH  
TO THE HUBBARD MODEL

Referees: Prof. Dr. Christof Wetterich  
Prof. Dr. Michael G. Schmidt



# Renormierungsgruppenzugang zum Hubbard Modell

## Zusammenfassung

Nach der Entdeckung der Hochtemperatursupraleiter hat das zweidimensionale Hubbard Modell als mögliche Beschreibung dieser Materialien verstärkte Aufmerksamkeit auf sich gezogen. Intensive Studien ergaben, daß dessen Phasendiagramm in der Tat einige Eigenschaften dieser Materialien widerspiegelt. Wir untersuchen das zweidimensionale Hubbard Modell mit Hilfe von exakten Renormierungsgruppengleichungen. Dafür formulieren wir die rein fermionische Theorie in einer Form, in der bosonische Felder die Wechselwirkung zwischen den Fermionen vermitteln. Ein symmetriebrechendes Kondensat äußert sich dann in einem nichtverschwindenden Erwartungswert für eins dieser bosonischen Felder. Allerdings wird durch die (partielle) Bosonisierung eine unphysikalische Freiheit in der Wahl der Kopplungen induziert, die von der Möglichkeit herrührt, Fierz-Transformationen durchzuführen. Diese Willkür spiegelt sich in nicht eindeutigen Mean-Field-Resultaten wieder. Die Renormierungsgruppe ist in der Lage, durch korrekte Berücksichtigung des Renormierungsgruppenflusses der Kopplungen, die Invarianz unter unterschiedlichen Wahlen der Anfangskopplungen wiederherzustellen. Indem wir dem Fluß der Kopplungen in die gebrochene Phase folgen, können wir eine Möglichkeit aufzeigen, das Mermin-Wagner-Theorem mit der Beobachtung antiferromagnetischer Ordnung bei nichtverschwindender Temperatur zu vereinbaren.

## A Renormalisation Group Approach to the Hubbard Model

### Abstract

After the discovery of high temperature superconductors the two dimensional Hubbard model has attracted a lot of attention as a description of these materials. Intensive studies have revealed that indeed its phase diagram shows features known from high temperature superconductors. We study the two dimensional Hubbard model with the aid of exact renormalisation group equations. For this purpose we rewrite the purely fermionic theory in a form where bosonic fields mediate the interaction between fermions. A symmetry breaking condensate then manifests itself in a nonvanishing expectation value for one of these bosonic fields. However, the bosonisation procedure induces an arbitrariness in the couplings between fermions and bosons due to the possibility to perform Fierz transformations. This arbitrariness is mirrored in ambiguous mean field results. By properly taking into account the running of the couplings, the renormalisation group is able to restore the invariance under equivalent choices of initial couplings. By following the flow into the broken phase we show how one may reconcile the Mermin-Wagner theorem with the observation of an antiferromagnetic long range order at nonvanishing temperatures.



# Contents

<b>1</b>	<b>Introduction</b>	<b>1</b>
1.1	High temperature superconductors . . . . .	2
1.2	Effective theories . . . . .	4
1.3	The Hubbard model . . . . .	6
1.4	Dissertation outline . . . . .	9
<b>2</b>	<b>The partition function</b>	<b>11</b>
2.1	Quantum many particle systems . . . . .	11
2.2	Coherent state path integral . . . . .	13
2.2.1	Coherent states . . . . .	13
2.2.2	Path integral formalism . . . . .	15
2.2.3	Application to the Hubbard model . . . . .	17
2.3	Partial bosonisation . . . . .	20
2.3.1	$d$ -wave operators . . . . .	24
2.3.2	Introducing sources for bosonic fields . . . . .	25
2.4	The effective action . . . . .	26
<b>3</b>	<b>A mean field calculation</b>	<b>28</b>
3.1	Calculation of the effective potential . . . . .	29
3.2	Spontaneous symmetry breaking . . . . .	32
3.2.1	Numerical results . . . . .	34
3.3	Comparison with Hartree–Fock equations . . . . .	38

<b>4</b>	<b>Exact renormalisation group equations</b>	<b>42</b>
4.1	The average effective action . . . . .	42
4.2	A flow equation . . . . .	44
4.3	A standard example: the effective potential in $O(N)$ theories . . . . .	47
<b>5</b>	<b>Loop calculations</b>	<b>49</b>
5.1	The bosonic propagator to one loop order . . . . .	49
5.2	Four fermion terms . . . . .	53
<b>6</b>	<b>Renormalisation group analysis</b>	<b>56</b>
6.1	Rebosonisation of fermionic interactions . . . . .	56
6.2	First truncation: Antiferromagnetic behaviour close to half filling . . .	58
6.2.1	Choice of the regulators . . . . .	60
6.2.2	The flow equations at half filling . . . . .	61
6.2.3	Numerical results . . . . .	66
6.2.4	The flow equations for $\mu \neq 0$ . . . . .	70
6.2.5	Numerical results . . . . .	71
6.3	Second truncation: Parametrisation dependence in the bosonised theory	72
6.3.1	The flow equations . . . . .	73
6.3.2	Numerical results . . . . .	74
<b>7</b>	<b>Conclusions</b>	<b>77</b>
<b>A</b>	<b>Conventions and notation</b>	<b>79</b>
<b>B</b>	<b>Useful formulae</b>	<b>80</b>
B.1	Pauli matrices . . . . .	80
B.2	Matrix relations . . . . .	81
B.3	Matrices containing Grassmann numbers . . . . .	81
B.4	Gaussian integrals . . . . .	83
B.5	Loop calculations . . . . .	84
B.5.1	Fermion-loop corrections in pure fermionic theory . . . . .	84
B.5.2	Mixed bosonic and fermionic fields . . . . .	85



**Bibliography**

**88**



# Chapter 1

## Introduction

The investigation of strongly correlated fermion systems has been a main interest of theoretic solid state physics for a long time. Of course it is much too difficult to study these materials in a detailed microscopic theory taking into account all core atoms as well as their electron shells and energy bands. Furthermore, it is questionable if these are really the relevant degrees of freedom for an adequate description of such materials. Instead, one is forced to construct idealised models that on the one hand are simple enough to be manageable by calculations but on the other hand at least qualitatively capture the characteristic features of the system. By investigating such models one gains insight into the general mathematical structures of these many particle systems but may also advance the understanding of the experimental behaviour of many materials.

One such model is the Hubbard model that has recently attracted increased attention since it was proposed to be a good candidate for the description of high temperature superconductors. These materials were found about 15 years ago and raised great expectations for their technical applicability. Not all of these hopes have been met in practice, but a lot of applications have been found. Among these are sensitive sensory devices for the detection of magnetic fields (SQUIDs), high frequency transmitters for mobile and satellite communication and first applications in power transmission and storage. Nevertheless, the origin of many properties of these materials still lie in the dark. A further understanding of these aspects should result into widening the spectrum of applications of such materials. However, even the Hubbard model, which on a first glance seems to be of comparatively simple structure, has proved to be reluctant to reveal its secrets. Recent work has shown that the phase structure exhibited by the Hubbard model may be very complex and indeed mirror many properties of high temperature superconductors.

Among the most promising current approaches to the Hubbard model are renormalisation group techniques. The object of this work is to further develop a frame-

work for the application of renormalisation group methods in the context of the Hubbard model but which also may prove useful for the understanding of similar models in solid state physics. For this purpose we will apply techniques that have proven to be valuable in the study of fermionic models of strongly interacting particles. Before turning to a description of the renormalisation group idea and the Hubbard model let us take a look at the features that – apart from the exceptionally high transition temperature into the superconducting state – make high temperature superconductivity such an interesting field. For a recent review of this topic see [15].

## 1.1 High temperature superconductors

The first high temperature superconductor was found in 1986 by Georg Bednorz and Alex Müller [8]. They performed experiments on a certain ceramic material with chemical composition  $(\text{La, Ba})_2\text{CuO}_4$  and reported a transition temperature  $T_c$  into the superconducting state of approximately 35K. This was about 50% larger than the highest transition temperature measured up to then and their result triggered a tremendous experimental rush. In the next few years higher and higher transition temperatures were discovered in materials with a similar structure, including the famous yttrium barium copper oxides (YBCO) with a  $T_c$  above the boiling point of liquid nitrogen. The current world record is a transition temperature of 134K found in a mercury based copper oxide at room pressure.

The common feature of all these materials is that they are composed of layers of copper oxide ( $\text{CuO}_2$ ) planes, hence their name *cuprates*. Because of this layered structure their properties are very anisotropic. The layers are separated by blocks containing other atoms, e.g.  $\text{La}_2\text{O}_2$ -blocks in  $\text{La}_2\text{CuO}_4$ . By replacing atoms in these blocks one may add holes (p-doping) or electrons (n-doping) to the  $\text{CuO}_2$  planes and change their electric properties. For example in  $(\text{La}_{2-x}\text{Ba}_x)\text{CuO}_4$  a fraction  $x$  of the La atoms have been replaced by Ba atoms thereby adding holes to the planes. A typical phase diagram of a high temperature superconductor is shown in figure 1.1. The doping level refers to the fraction of atoms replaced, i.e.  $x$  in the above example.

For the undoped material one finds a strong antiferromagnetic interaction between the Cu atoms in the planes which below a few hundred Kelvin leads to a long range order. In this case the material is an insulator. Increasing the level of doping results in a vanishing of the antiferromagnetic long range order and the emergence of a region where the system is in the superconducting state. Below and above the optimal doping, i.e. at the doping level where the highest critical temperature for the superconducting transition is achieved, the material is said to be under- and over-doped respectively. However, the antiferromagnetic and superconducting regions are

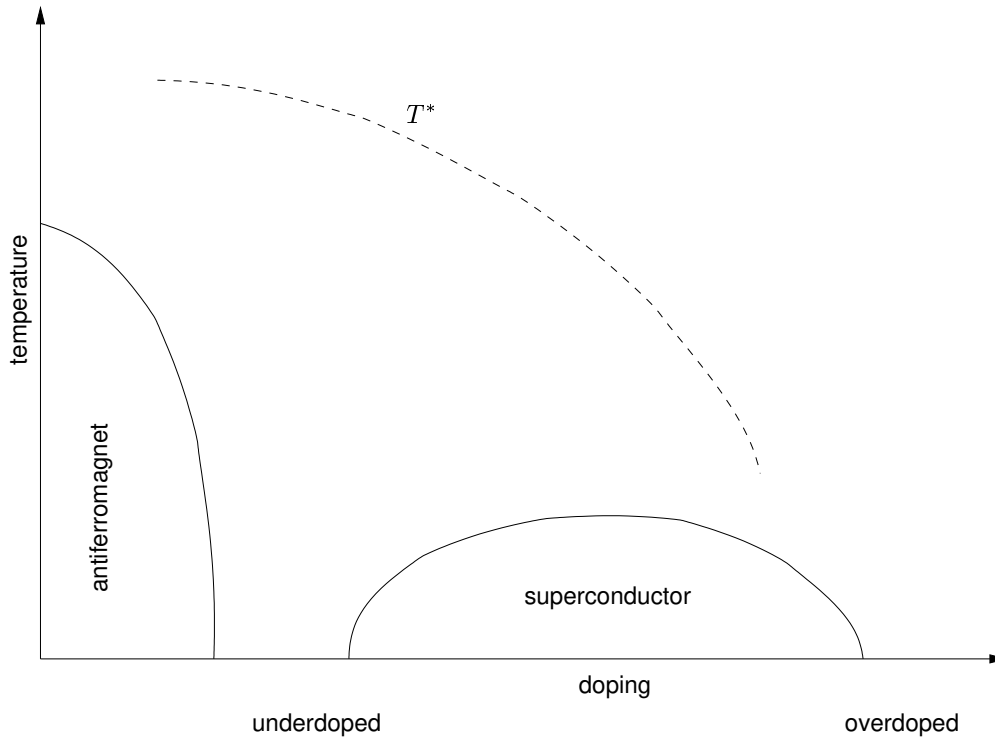


Figure 1.1: Schematic phase diagram of a cuprate superconductor.

not the only interesting features in the phase diagram. Notably in the underdoped regime and below a temperature  $T^*$  one observes unusual thermal and transport properties. These are associated with a “pseudo energy gap”. The endpoints of this  $T^*$  line are still heavily disputed. Furthermore the transition into this region seems to be rather a crossover than a real phase transition. The nature of this gap, however, remains hitherto completely obscure, even if a variety of possible explanations have been put forward including various kinds of charge and spin density waves, alternating circular currents in the unit cells or a preformation of hole-hole pairs that later condense into the superconducting state (see [7] for a review).

A common feature of all superconductors is that the electrons somehow overcome their mutual electrostatic repulsion to form Cooper pairs. Breaking such a pair of electrons costs energy – in other words there is an energy gap between the paired and unpaired electron states. Since these pairs do not have to obey the Pauli exclusion principle they may condense into a single quantum state below a certain temperature. The superconducting state may then be described by a macroscopic wave function. The condensate breaks the  $U(1)$  symmetry and from this the unusual properties of superconductors like the supercurrent or the Meissner and Josephson effects can be derived [42].

When a superconductor is cooled below its critical temperature and put into a

magnetic field or vice versa the field is expelled from the inside of the superconductor (Meissner effect). The external magnetic field is then compensated by supercurrents on the surface of the material. However, when the magnetic field is too large the energy cost for maintaining these surface currents may be larger than the energy gained by condensating into the superconducting state. The superconductor may then either completely return to its normal state (type I superconductor) or, if it is energetically favourable to have boundaries between the superconducting and normal ordered phase, choose to develop flux tubes, i.e. regions of material in the normal state that the magnetic field can penetrate while the rest of the material stays in the superconducting state (type II superconductors). In the latter case it will take much larger magnetic fields to completely break up the superconducting state. The cuprate superconductors are of the second kind.

In conventional superconductors the attractive force responsible for the pairing between the electrons is mediated by lattice vibrations (phonons). The electrons form pairs of vanishing total angular momentum, i.e. a rotationally invariant state or an  $s$ -wave. This is the simplest case of BCS theory [6] that explains how the superconducting condensate forms when an attractive force is present between electrons. However, pairs with other values of the angular momentum are possible and indeed it has been shown experimentally [40, 37] that in high temperature superconductors the pairs are in a state with  $d$ -wave symmetry. This means that the gap function  $\Delta(\mathbf{k}_F)$ , which is the order parameter for superconductivity, changes its sign on the Fermi surface (the energy gap  $|\Delta(\mathbf{k}_F)|$  thus has zeroes on the Fermi surface). However, the mechanism for the pair correlation in these materials is still unknown. It is speculated that an understanding of the pseudogap region might shed some light on the nature of this mechanism.

## 1.2 Effective theories

One of the deepest insights into quantum field theory is the observation that all theories we know should be considered as effective theories derived from some underlying theory by a kind of averaging procedure. For condensed matter physics this observation may seem very obvious, but the notion is indeed much more general and can be quantified and applied for calculations. These ideas were put forward in the most stringent form in the 1970<sup>ies</sup> although the basic notions had already pervaded the literature for quite a while [45].

Consider a theory defined at some energy scale  $\Lambda$  by its action  $S_\Lambda$  containing masses and couplings collectively denoted by  $g_\Lambda$ . The scale  $\Lambda$  serves as a cutoff: path integrals are only performed for modes corresponding to energies below  $\Lambda$ . In solid state physics this cutoff might correspond to a momentum of the order of the inverse lattice distance. Now suppose we are interested in physics at energy scales  $\Lambda' \ll \Lambda$ ,

for example when measurements are performed with a spatial resolution of the order of  $1/\Lambda'$ . In this case we may as well integrate out the large energy modes and obtain a new effective theory defined at the new energy scale  $\Lambda'$  through an action  $S_{\Lambda'}$  and couplings  $g_{\Lambda'}$ . To do this, split the fields in the path integral into high energy ( $\phi_{>}$ ) and low energy ( $\phi_{<}$ ) modes:

$$\begin{aligned} \int \mathcal{D}\phi \exp(-S_{\Lambda}[\phi]) &= \int \mathcal{D}\phi_{>} \mathcal{D}\phi_{<} \exp(-S_{\Lambda}[\phi_{>}, \phi_{<}]) \\ &\equiv \int \mathcal{D}\phi_{<} \exp(-S_{\Lambda'}), \end{aligned} \quad (1.1)$$

where  $\phi_{>}$  ( $\phi_{<}$ ) vanishes for energies  $E < \Lambda'$  ( $E > \Lambda'$ ). In the last line we have put

$$\exp(-S_{\Lambda'}[\phi]) = \int \mathcal{D}\phi_{>} \exp(-S_{\Lambda}[\phi_{>}, \phi_{<}]). \quad (1.2)$$

The new (Wilsonian effective) action  $S_{\Lambda'}$  describes the *same* physical system and in particular one will obtain the same Green functions. However, loop-integrals now have to be performed up to the new cutoff only. In particular *at* the scale  $\Lambda'$  tree level diagrams suffice. This also answers the question where  $S_{\Lambda}$  came from in the first place: it is itself derived from a more fundamental theory by mode elimination. Iterating the above procedure one obtains a sequence of actions  $S_1, S_2, S_3 \dots$ . Each step is called a *renormalisation group transformation*. One often depicts this procedure by plotting the *flow* of the couplings  $g_i$  in parameter space. These trajectories are the so called *flow lines*.

Instead of integrating over a finite energy interval as above one may as well consider infinitesimal intervals. One then obtains a differential equation describing the change of the action dependent on the energy scale. Such differential equations are termed *renormalisation group equations* or just *flow equations*. They describe an infinite system of coupled differential equations for the couplings  $g$

$$\Lambda \frac{\partial}{\partial \Lambda} S[\phi] = \mathcal{B}(S[\phi]), \quad \Lambda \frac{\partial}{\partial \Lambda} g = \beta(g) \quad (1.3)$$

and define the famous *beta functions*.

The renormalisation group equations may be viewed as a kind of magnifying glass. For large values of the cutoff one is able to distinguish details on small length scales. Following the flow towards a smaller cutoff is equivalent to averaging over larger and larger regions in space, in this way smearing out the small scale features. In applying the renormalisation group one is able to interpolate between a microscopic description and an effective theory suitable for length scales on which typical experiments are performed.

A beautiful example of an effective theory is the Landau theory of Fermi liquids that with a few basic assumptions can account for many thermodynamic and transport properties of conductors [30]. Though formulated long before renormalisation theory was developed it may be cast into the language of this formalism (see [38, 35] and references therein). From a microscopic viewpoint any electron in a conductor will feel a complicated potential from all its surroundings. Landau assumed that at least the low lying excitations, i.e. particles near the Fermi surface, are complicated bound states of electrons that again behave like fermions. These “dressed” or “renormalised” particles, called *quasiparticles*, are then assumed to be essentially free. In other words the complicated interactions between electrons have been “integrated out” and now can be traced in a few parameters such as an altered electron mass or some weak residual interaction. This view explains the success of the independent electron approximation (or rather independent quasiparticle approximation) in reproducing so many properties of a conductor.

However, quasiparticles composed of electrons do not even have to be fermionic. In the BCS theory of superconductivity two electrons (or rather fermionic quasiparticles in the above sense) form a bound state that acts as a whole like a boson<sup>1</sup>. Viewed on sufficiently large length scales we may as well give this bosonic state an independent meaning and treat it as a single particle just as the fermionic quasiparticles above. This shows that what we consider as a “fundamental particle” may be scale dependent. Far below a *compositeness scale* these particles may behave like fundamental particles, whereas above this scale we observe a composite object.

Of course this has a close relation to particle physics. At sufficiently high energies the fundamental particles in strong interactions are quarks and gluons. However, at low energies the relevant degrees of freedom are rather baryons and mesons, i.e. composite objects from a microscopic point of view.

### 1.3 The Hubbard model

The Hubbard model was independently introduced in the 1960<sup>ies</sup> by Hubbard, Kanamori and Gutzwiller [25]. However, the most extensive calculations in this model were first performed by Hubbard and therefore his name is associated with it. It has proven to be valuable for the modelling of a wide class of phenomena in solid state physics. Initially, it was applied to the description of electric properties of solids with narrow energy bands (e.g. transition metals), but soon it was also used for the study of magnetic ordering and the metal insulator transition (Mott

---

<sup>1</sup>In two dimensions one can even give a meaning to states that pick up *any* phase factor under interchange of two (quasi)particles and are thus termed “anyons” [17]. They do not seem to play a role in cuprates, however.



transition). More recently the model has become very popular for understanding high temperature superconductors [1]. There is little doubt that the model is much too simple to describe any actual solid faithfully, nevertheless it is a kind of minimal model that takes into account the quantum mechanical motion of the electrons and their mutual repulsive interaction which seem to be the dominating features in many solids.

Despite its apparent simplicity the model has proven to be hard to solve even approximately. An exact solution has been found in one dimension only [31], while in larger dimensions very few exact results are known – mostly in extreme regions of the parameter space (see [39, 33] for reviews). A vast amount of calculational techniques have therefore been applied to the Hubbard model over the years. Unfortunately none of these have turned out to be universally applicable to all aspects of the model and they do not agree on more than some basic features.

In the Hubbard model the electrons are assumed to be very tightly bound to the core atoms of the crystal, i.e. we declare that electrons only live on the sites of some lattice. We further assume that only a single non-degenerate orbit on each atom plays a significant role for the low energy properties of the solid. This means that only two electrons with opposite spin can reside on a single lattice site. Of course these electrons will feel a strong repulsive Coulomb force. We will take this interaction to be very effectively screened so that only electrons on the same lattice site are affected. Another important ingredient is their ability to move around in the lattice by tunnelling from atom to atom.

The Hamiltonian of the Hubbard model is very conveniently formulated in terms of creation and annihilation operators:

$$H = \sum_{ij,\sigma} t_{ij} a_{i,\sigma}^+ a_{j,\sigma} + U \sum_i n_{i,\uparrow} n_{i,\downarrow}, \quad (1.4)$$

where  $a_{i,\sigma}^+$  and  $a_{i,\sigma}$  are creation-/annihilation-operators for an electron at site  $i$  with spin  $\sigma$  and obey the usual anticommutation relations  $\{a_{i,\sigma}^+, a_{j,\tau}\} = \delta_{ij} \delta_{\sigma\tau}$ .  $n_{i,\sigma} = a_{i,\sigma}^+ a_{i,\sigma}$  is the particle number operator.  $t_{ij}$  is the probability for an electron to tunnel from site  $i$  to site  $j$  and the  $U$ -term mimics the screened Coulomb like interaction. The first part of this Hamiltonian is often referred to as the *hopping term*. All physical information in the Hamiltonian resides in the topology of the lattice and the parameters  $t_{ij}$  and  $U$  or rather their dimensionless ratios  $t_{ij}/U$ . However, we also need the number of electrons per lattice site and the temperature if we are interested in thermodynamics.

Many different lattice topologies have been investigated. However, we will restrict ourselves to a square lattice in two dimensions appropriate for the modelling of high temperature superconductors. Because of the highly anisotropic structure of cuprates, electrons are strongly favoured to move inside of the  $\text{CuO}_2$  planes. It is

believed that the coupling between different layers is weak and that the basic pairing mechanism resides in the planes. Moreover one can show that the hopping between copper and oxygen atoms may be modelled by a simple square lattice (see [37] and references therein).

The “hopping parameters”  $t_{ij}$  are chosen such that tunnelling is only possible between closely neighbouring sites:

$$t_{ij} = \begin{cases} -t & \text{for nearest neighbours (NN)} \\ -t' & \text{for next to nearest neighbours (NNN)}, \\ 0 & \text{otherwise} \end{cases} \quad (1.5)$$

where  $t'$  is much smaller than  $t$ . The overall sign of the parameters is conventional but their relative sign plays a role. In the interaction term, however, one has to choose  $U > 0$  in order to model a repulsive interaction.

The special case referred to as *half filling*, where the number of electrons on the lattice equals the number of lattice sites, is especially interesting as this corresponds to an undoped cuprate and furthermore some exact results are known. These results are particularly valuable as numerical simulations can be compared to them and have to pass this test. It is known that for sufficiently large  $U$  and at half filling the ground state of the Hubbard model is antiferromagnetic. This agrees with the observed antiferromagnetism of undoped superconductors. Therefore one would assume that for low enough temperature the two dimensional Hubbard model describes an antiferromagnet.

However, there is an even more general result known as the Mermin-Wagner theorem [32, 33] which states that for one and two dimensional theories with a continuous symmetry no long range order is possible in the two point correlation function at nonvanishing temperatures. As any magnetic ordering breaks the continuous  $SU(2)$  spin symmetry the theorem strongly disfavours the above assumption of antiferromagnetism at low temperatures. This would suggest that we have to reject the two dimensional Hubbard model as an adequate description of real high temperature superconductors and that we have to include e.g. interlayer coupling into the model turning it into a three dimensional one. Fortunately there is a way around this: one may assume that on scales accessible to the experiments there are large clusters showing magnetic ordering and only when averaging over even larger scales this ordering is washed out. This mechanism will be clarified in our investigation with renormalisation group equations.

In the last few years an increasing number of renormalisation group studies of the Hubbard model have been published [46, 20, 23, 19]. They have shown very encouraging results and indeed suggest that antiferromagnetism dominates close to half filling while for stronger doping the superconducting instability is the leading one.

However, all these studies are done by directly investigating the scale dependence of the four fermion coupling. Symmetry breaking is here identified by a divergence of the coupling in various momentum channels. Therefore these techniques are limited to the symmetric regime. Furthermore couplings between more than four fermions which are not considered in these studies should play an important role at low energy scales.

We believe that it is preferable to introduce the low energy degrees of freedom more explicitly. This can be achieved by a partial bosonisation, i.e. by rewriting the original action in a form where fermions couple via a Yukawa like interaction to the interesting degrees of freedom represented by bosonic fields appropriate for condensates of an even number of fermions. The symmetry breaking then manifests itself in a nonvanishing expectation value for one of these bosons. At the onset of a second order phase transition one will observe a vanishing of the mass of this boson. This then allows to expand the investigation to the broken phase. Furthermore multi-fermion couplings translate into interactions between bosonic fields which may conveniently be enclosed in an effective potential term.

Another advantage of this formalism is the possibility to investigate the interplay of different degrees of freedom by deliberately blocking some of the bosonic channels. An investigation in this direction has been performed in parallel to the present work [12]. Although this has shown encouraging results, the renormalisation of the Yukawa couplings between bosons and fermions have been neglected thus severely limiting its predictive power.

The present work is dedicated mostly to the investigation of how the flow of these couplings may be incorporated into the study. It turns out, however, that several obstacles have to be overcome in order to get a satisfactory result. An alternative bosonisation procedure than applied in our former studies greatly simplifies the calculational tasks and makes the inherent structure of the bosonised theory much more transparent.

## 1.4 Dissertation outline

In chapter 2 we rewrite the partition function in path integral form. By suitably rewriting this expression we are able to define a theory that is equivalent to the Hubbard model but where its purely fermionic interaction is mediated by bosonic fields that represent interesting degrees of freedom.

We then pursue a mean field analysis of the bosonised Hubbard model in chapter 3. Although oversimplified this gives a first impression of the phase diagram. However, it also reveals that a certain reparametrisation invariance of the bosonic

couplings induced by the bosonisation procedure strongly affects the mean field results.

This arbitrariness should be lifted if bosonic fluctuations are taken into account properly. A way to do this is by renormalisation group techniques. The renormalisation group formalism for the average effective action is presented in chapter 4.

Some loop calculations are done in chapter 5. Their purpose is twofold. First they are to give a hint towards suitable truncation schemes for the renormalisation group study. Second, the full renormalisation group equations may be formally deduced from a one loop equation.

Chapter 6 is dedicated to the application of the renormalisation group formalism to the Hubbard model. A way to incorporate unwanted four fermion interactions developed under the flow into the running of Yukawa couplings is described. We investigate two truncations. The first one deals with antiferromagnetism close to half filling and a second one investigates the parametrisation dependence induced by the bosonisation procedure of the final result.

# Chapter 2

## The partition function

The equilibrium properties of a thermodynamic system connected to a heat bath and a particle reservoir are described completely by its grand canonical partition function

$$Z = \text{Tr} \exp(-\beta[\hat{H} - \mu\hat{N}]), \quad (2.1)$$

where  $\beta = \frac{1}{T}$  is the inverse temperature,  $\hat{H}$  the Hamiltonian operator governing the system,  $\mu$  the chemical potential and  $\hat{N}$  the particle number operator. The trace runs over all many-particle states the system can access. For many applications it is very useful to rewrite this partition function as a path integral. In this way one can make contact to quantum field theory and the wealth of techniques known in this field.

In this chapter we briefly review the steps leading to the coherent state path integral description of fermionic systems. Excellent reviews of this topic can be found in e.g. [34, 38]. This formalism is then applied to the Hubbard model. We proceed by rewriting the purely fermionic theory as a mixed theory containing both fermionic and bosonic degrees of freedom coupled by a Yukawa-like interaction.

### 2.1 Quantum many particle systems

Consider a quantum mechanical one-particle system. Suppose it lives in a Hilbert space  $\mathcal{H}_1$  which is spanned by a complete orthonormal set of states  $|\nu\rangle$

$$\sum_{\nu} |\nu\rangle\langle\nu| = \mathbb{1}, \quad \langle\nu|\nu'\rangle = \delta_{\nu\nu'}. \quad (2.2)$$

Now consider a system composed of  $N$  noninteracting copies of these particles. Suppose the  $i$ th particle is in the state  $|\nu_i\rangle$ . Then the  $N$  particle state is described

by

$$|\nu_1 \nu_2 \dots \nu_N\rangle = |\nu_1\rangle \otimes |\nu_2\rangle \otimes \dots \otimes |\nu_N\rangle. \quad (2.3)$$

The fundamental assumption of many particle quantum mechanics is that a system composed of  $N$  copies of some particle can be described by a superposition of the states (2.3) even if an interaction is present, i.e. that in this case the Hilbert space is  $\mathcal{H}_N = \mathcal{H}_1 \otimes \mathcal{H}_1 \otimes \dots \otimes \mathcal{H}_1$ . The states (2.3) form a basis for the Hilbert space  $\mathcal{H}_N$  with completeness and orthogonality relations deduced from the properties of the one particle case.

However, for identical particles this space is too large as physical observables are independent of an interchange of two particles, i.e. the way the particles are ordered in (2.3). Hence only symmetrised or antisymmetrised states are necessary, forming their respective Hilbert spaces  $\mathcal{H}_N^{s/a}$ . Particles having the former property are called bosons and the latter are called fermions. This has remarkable consequences: whereas any number of bosons may occupy a given state fermions are celibatory, i.e. two of them may not be in the same state.

Because of this property many particle systems may be very conveniently described in terms of creation and annihilation operators as states "created" from the vacuum in this way automatically fulfil the above symmetry properties. As these operators change the particle number they are defined on the so called *Fock space* given by a direct sum of symmetrised/antisymmetrised Hilbert spaces with all particle numbers including the vacuum state  $|0\rangle$  which contains zero particles (not to be confused with the null vector). States with different particle content are supposed to be orthogonal and hence completeness and orthogonality are induced by the properties of the  $N$  particle Hilbert spaces. The creation operator  $a_\mu^+$  adds a particle with quantum numbers  $\mu$  to a given state ket, i.e. maps between  $\mathcal{H}_N$  and  $\mathcal{H}_{N+1}$

$$a_\mu^+ |\nu_1 \nu_2 \dots \nu_N\rangle = |\mu \nu_1 \nu_2 \dots \nu_N\rangle. \quad (2.4)$$

Let us restrict ourselves to fermions in the following. Two fermionic creation operators anticommute, that is

$$\{a_\mu^+, a_\nu^+\} = a_\mu^+ a_\nu^+ + a_\nu^+ a_\mu^+ = 0 \quad (2.5)$$

and hence the Fock space is spanned by the states

$$|\nu_1 \dots \nu_n \dots\rangle = a_{\nu_1}^+ \dots a_{\nu_n}^+ \dots |0\rangle \quad (2.6)$$

which automatically obey the right symmetry properties with respect to an interchange of two particles. By using completeness and orthogonality in the Fock space one shows that the hermitian conjugate of the creation operator  $a_\mu = (a_\mu^+)^\dagger$  obeys the anticommutation relations

$$\{a_\mu, a_\nu\} = 0, \quad \{a_\mu, a_\nu^+\} = \delta_{\mu\nu} \quad (2.7)$$

and maps from  $\mathcal{H}_N$  to  $\mathcal{H}_{N-1}$ , i.e. destroys a particle in state  $\mu$ . Hence the name destruction (or annihilation) operator for it.

Because all possible states are formed as a superposition of the states (2.6), any operator acting in this space can be described by a product (and sum) of creation and annihilation operators. E.g. a one particle operator has the matrix elements

$$\langle \alpha_1 \cdots \alpha_N | \hat{T} | \beta_1 \cdots \beta_N \rangle = \sum_{i,j=1}^N \langle \alpha_i | \hat{T} | \beta_j \rangle \prod_{\substack{k \neq i \\ l \neq j}} \langle \alpha_k | \beta_l \rangle \equiv \sum_{i,j=1}^N T_{\alpha_i \beta_j} \prod_{\substack{k \neq i \\ l \neq j}} \langle \alpha_k | \beta_l \rangle \quad (2.8)$$

and can therefore be expressed as<sup>1</sup>

$$\hat{T} = \sum_{\alpha\beta} T_{\alpha\beta} a_{\alpha}^{\dagger} a_{\beta}, \quad T_{\alpha\beta} = \langle \alpha | \hat{T} | \beta \rangle \quad (2.9)$$

in terms of creation and annihilation operators. Similarly a two particle operator has the form

$$\hat{V} = \frac{1}{2} \sum_{\alpha\beta\gamma\delta} V_{\alpha\beta\gamma\delta} a_{\alpha}^{\dagger} a_{\beta}^{\dagger} a_{\delta} a_{\gamma}, \quad V_{\alpha\beta\gamma\delta} = \langle \alpha\beta | \hat{V} | \gamma\delta \rangle. \quad (2.10)$$

## 2.2 Coherent state path integral

### 2.2.1 Coherent states

In order to derive a path integral formulation of the partition function in statistical physics, it is useful to consider coherent states. A coherent state is defined as an eigenstate of the destruction operator

$$a_{\alpha} |\psi\rangle = \psi_{\alpha} |\psi\rangle. \quad (2.11)$$

For fermions a subtlety arises here. Because destruction operators anticommute the same property must hold for the eigenvalues

$$\{\psi_{\alpha}, \psi_{\beta}\} = 0, \quad \{\psi_{\alpha}, a_{\beta}\} = 0. \quad (2.12)$$

---

<sup>1</sup>Then the matrix elements are the same as in (2.8)

$$\langle \alpha | \hat{T} | \beta \rangle = T_{\gamma\delta} \langle 0 | a_{\alpha} a_{\gamma}^{\dagger} a_{\delta} a_{\beta}^{\dagger} | 0 \rangle = T_{\gamma\delta} \langle 0 | (-a_{\gamma}^{\dagger} a_{\alpha} + \delta_{\alpha\gamma}) (-a_{\beta}^{\dagger} a_{\delta} + \delta_{\beta\delta}) | 0 \rangle = T_{\gamma\delta} \delta_{\alpha\gamma} \delta_{\beta\delta} = T_{\alpha\beta}$$

Anticommuting numbers like these are termed Grassmann numbers (for excellent introductions to this field see [9, 41]). It is easy to check that the eigenvalue equation (2.11) is solved by

$$|\psi\rangle = e^{-\sum_{\alpha} \psi_{\alpha} a_{\alpha}^{\dagger}} |0\rangle = \prod_{\alpha} (1 - \psi_{\alpha} a_{\alpha}^{\dagger}) |0\rangle \quad (2.13)$$

which can be verified by direct calculation (in order to enhance readability we restrict the calculations in this section to a single quantum number)

$$a|\psi\rangle = a|0\rangle - a\psi a^{\dagger}|0\rangle = \psi a a^{\dagger}|0\rangle = \psi|0\rangle = \psi(|0\rangle - \psi a^{\dagger}|0\rangle) = \psi|\psi\rangle.$$

We are thus forced to generalise the Fock space by allowing Grassmann valued coefficients in linear combinations of states.

In the same way as above we introduce left-eigenstates of the creation operator

$$\langle\psi^*|a_{\alpha}^{\dagger} = \langle\psi^*|\psi_{\alpha}^*, \quad \langle\psi^*| = \langle 0|e^{-\sum_{\alpha} a_{\alpha} \psi_{\alpha}^*} = \langle 0| \prod_{\alpha} (1 - a_{\alpha} \psi_{\alpha}^*) \quad (2.14)$$

and demand that the eigenvalues  $\psi, \psi^*$  anticommute mutually and with all creation and destruction operators

$$\{\psi_{\alpha}^{(*)}, \psi_{\beta}^{(*)}\} = 0, \quad \{\psi_{\alpha}^{(*)}, a_{\beta}^{(+)}\} = 0.$$

Although the notation is reminiscent of complex conjugation we treat  $\psi$  and  $\psi^*$  as independent variables.

We are now able to calculate some properties of states and operators in the generalised Fock space. The *scalar product* of two coherent states is

$$\langle\psi^*|\psi\rangle = \prod_{\alpha} (1 + \psi_{\alpha}^* \psi_{\alpha}) = e^{\sum_{\alpha} \psi_{\alpha}^* \psi_{\alpha}}. \quad (2.15)$$

Let us define a normal ordered operator as one with all creation operators to the left of the destruction operators, e.g.  $A = a_{\alpha}^{\dagger} a_{\beta}^{\dagger} a_{\gamma} a_{\delta}$ . Then the matrix elements of a normal ordered operator are easily calculated to be

$$\langle\psi^*|A[a_{\alpha}^{\dagger}, a_{\beta}]|\psi\rangle = e^{\sum_{\gamma} \psi_{\gamma}^* \psi_{\gamma}} A[\psi_{\alpha}^*, \psi_{\beta}]. \quad (2.16)$$

We can also derive a completeness relation in the space of coherent states. For this we define integrals over Grassmann variables as follows<sup>2</sup>

$$\int d\psi \, 1 = 0, \quad \int d\psi \, \psi = 1, \quad \int d\psi d\psi' \, \psi' \psi = 1 = - \int d\psi' d\psi \, \psi' \psi.$$

<sup>2</sup>The definition is such that the integrals over Grassmann variables are translation invariant

$$b = \int d\psi (a + b\psi) = \int d\psi' ((a + b\eta) + b\psi'), \quad \psi = \psi' + \eta.$$



The *completeness relation* then reads

$$\int \prod_{\alpha} d\psi_{\alpha}^* d\psi_{\alpha} e^{-\sum_{\gamma} \psi_{\gamma}^* \psi_{\gamma}} |\psi\rangle\langle\psi^*| = \mathbb{1}_{\text{Fock space}}, \quad (2.17)$$

where the identity operator resides in the usual Fock-space (*not* in the generalised one). Let us do the calculation

$$\begin{aligned} \int d\psi^* d\psi e^{-\psi^* \psi} |\psi\rangle\langle\psi^*| &= \int d\psi^* d\psi (1 - \psi^* \psi) \{(|0\rangle - \psi|1\rangle)\langle 0| - \langle 1|\psi^*\rangle\} \\ &= \int d\psi^* d\psi (-\psi^* \psi |0\rangle\langle 0| + \psi|1\rangle\langle 1|\psi^*) = |0\rangle\langle 0| + |1\rangle\langle 1|. \end{aligned}$$

As a last ingredient we need the *trace* of a bosonic operator, i.e. one that contains an even number of creation and annihilation operators

$$\text{Tr} A = \sum_n \langle n|A|n\rangle = \int \prod_{\alpha} d\psi_{\alpha}^* d\psi_{\alpha} e^{-\sum_{\gamma} \psi_{\gamma}^* \psi_{\gamma}} \langle -\psi^* | A | \psi \rangle. \quad (2.18)$$

Again the calculation is simple with only one quantum number

$$\sum_n \langle n|A|n\rangle = \int d\psi^* d\psi e^{-\psi^* \psi} \sum_n \langle n|A|\psi\rangle \langle\psi^*|n\rangle = \int d\psi^* d\psi e^{-\psi^* \psi} \langle -\psi^* | \underbrace{\sum_n |n\rangle\langle n|}_1 A | \psi \rangle.$$

Especially note the minus sign in  $\langle -\psi^* |$  due to the interchange of Grassmann numbers. It will force the fields to have anti-periodic boundary conditions in the path integral representation as we will shortly see.

## 2.2.2 Path integral formalism

In the following we derive a path integral expression for the (grand canonical) partition function of a system governed by the Hamiltonian  $\hat{H}$  at temperature  $T = 1/\beta$  and chemical potential  $\mu$

$$Z = \text{Tr} e^{-\beta(\hat{H} - \mu \hat{N})} = \text{Tr} e^{-\beta \hat{H}}, \quad (2.19)$$

where  $\hat{N} = \sum_{\alpha} a_{\alpha}^{\dagger} a_{\alpha}$  is the particle number operator. We will assume that  $\hat{H}[a^{\dagger}, a]$  is normal ordered. The exponential  $e^{-\beta \hat{H}}$ , however, will in general not be normal ordered, so we cannot apply (2.18) with (2.16) directly. Therefore we rewrite the exponential as ( $\epsilon = \beta/N$ )

$$e^{-\beta \hat{H}} = (e^{-\beta \hat{H}/N})^N = \lim_{N \rightarrow \infty} (1 - \epsilon \tilde{H})^N = \underbrace{(1 - \epsilon \tilde{H}) \cdots (1 - \epsilon \tilde{H})}_{N \text{ times}}, \quad \epsilon = \beta/N.$$

Now insert the completeness relation (2.17) between each factor and use

$$\langle \psi_i^* | 1 - \epsilon \tilde{H}[a^+, a] | \psi_{i-1} \rangle = e^{\sum_{\alpha} \psi_{\alpha,i}^* \psi_{\alpha,i-1}} e^{-\epsilon \tilde{H}[\psi_i^*, \psi_{i-1}]} + \mathcal{O}(\epsilon^2).$$

Defining the “endpoints” of the trace (2.18) as  $\psi_{\alpha,0}^{(*)} = -\psi_{\alpha,N}^{(*)} = \psi_{\alpha}^{(*)}$  we may now write the partition function as

$$\begin{aligned} Z &= \lim_{\epsilon \rightarrow 0} \int \prod_{i=1}^N \prod_{\alpha} d\psi_{\alpha,i}^* d\psi_{\alpha,i} \\ &\times \exp \left[ -\epsilon \sum_{k=1}^N \left\{ \sum_{\alpha} \psi_{\alpha,k}^* \left( \frac{\psi_{\alpha,k} - \psi_{\alpha,k-1}}{\epsilon} - \mu \psi_{\alpha,k-1} \right) \right\} + H[\psi_{\alpha,k}^*, \psi_{\alpha,k-1}] \right]. \end{aligned} \quad (2.20)$$

One often adopts a continuum notation for this expression by writing  $\psi_{\alpha,i}^{(*)} = \psi_{\alpha}^{(*)}(\tau = \epsilon i)$

$$\frac{\psi(\tau) - \psi(\tau - \epsilon)}{\epsilon} \rightarrow \partial_{\tau} \psi(\tau), \quad \sum_{k=1}^N \epsilon \rightarrow \int_0^{\tau} d\tau \quad \text{for } \epsilon \rightarrow 0. \quad (2.21)$$

The partition function then reads

$$\begin{aligned} Z &= \int_{\substack{\psi_{\alpha}(\beta) = -\psi_{\alpha}(0) \\ \psi_{\alpha}^*(\beta) = -\psi_{\alpha}^*(0)}} \mathcal{D}(\psi_{\alpha}^*, \psi_{\alpha}) \exp(-S[\psi_{\alpha}^*, \psi_{\alpha}]), \\ S[\psi_{\alpha}^*, \psi_{\alpha}] &= \int_0^{\beta} d\tau [\psi_{\alpha}^*(\tau) (\partial_{\tau} - \mu) \psi_{\alpha}(\tau) + H[\psi_{\alpha}^*(\tau), \psi_{\alpha}(\tau)]]. \end{aligned} \quad (2.22)$$

One has to keep in mind, however, that (2.22) is a shorthand notation for the discrete version (2.20). Indeed, there is no sense in which the difference  $\psi_k - \psi_{k-1}$  in (2.21) is small and can be replaced by a derivative since the objects are Grassmann numbers and thus do not even have any numerical value.

Note that the antiperiodic boundary conditions stem from the fact that we are dealing with fermions. For bosonic fields one encounters exactly the same partition function as (2.22) but with an integral over fields having periodic boundary conditions.

It is often convenient to use a Fourier expansion of the functions  $\psi^{(*)}(\tau)$  with respect to the “time” variable  $\tau$ . Since the functions are antiperiodic we may expand

$$\begin{aligned} \psi_{\alpha}(\tau) &= T \sum_n e^{i\omega_n \tau} \psi_{\alpha n}, \\ \psi_{\alpha}^*(\tau) &= T \sum_n e^{-i\omega_n \tau} \psi_{\alpha n}^*, \\ \omega_n &= \pi T(2n + 1), \quad n \in \mathbb{Z}. \end{aligned} \quad (2.23)$$

The “time derivative” now has the meaning

$$\begin{aligned} \lim_{\epsilon \rightarrow 0} \int_0^\tau d\tau \psi^*(\tau) \left( \frac{\psi(\tau) - \psi(\tau - \epsilon)}{\epsilon} \right) &= \lim_{\epsilon \rightarrow 0} T^2 \sum_{nn'} \psi_n^* \psi_{n'} \int_0^\tau d\tau e^{-i(\omega_n - \omega_{n'})\tau} \left( \frac{1 - e^{-i\omega_n \epsilon}}{\epsilon} \right) \\ &= T \sum_n \psi_n^* \psi_n i\omega_n, \end{aligned}$$

i.e. the integrals over “time” are converted into sums, conventionally called *Matsubara sums*.

### 2.2.3 Application to the Hubbard model

We are now able to write down the partition function for the Hubbard model in path integral formulation. If we adopt a spinor notation

$$\hat{\psi}_i = \begin{pmatrix} \hat{\psi}_{i\uparrow} \\ \hat{\psi}_{i\downarrow} \end{pmatrix}, \quad \hat{\psi}_i^* = \begin{pmatrix} \hat{\psi}_{i\uparrow}^* \\ \hat{\psi}_{i\downarrow}^* \end{pmatrix}, \quad (2.24)$$

the action for the Hubbard model reads

$$\boxed{S_F[\hat{\psi}, \hat{\psi}^*] = \int_0^\beta d\tau \left[ \sum_{ij} \hat{\psi}_i^* ([\partial_\tau - \mu]\delta_{ij} + t_{ij}) \hat{\psi}_j + \frac{U}{2} \sum_i (\hat{\psi}_i^* \hat{\psi}_i)^2 \right]}, \quad (2.25)$$

where we have used the replacement rules given above for the normal ordered Hamiltonian

$$\begin{aligned} H_{\text{int}}(a^\dagger, a) &= U \sum_i n_{i\uparrow} n_{i\downarrow} = -U \sum_i a_{i\uparrow}^\dagger a_{i\downarrow}^\dagger a_{i\uparrow} a_{i\downarrow} \\ \rightarrow H_{\text{int}}[\hat{\psi}^*, \hat{\psi}] &= -U \sum_i \hat{\psi}_{i\uparrow}^* \hat{\psi}_{i\downarrow}^* \hat{\psi}_{i\uparrow} \hat{\psi}_{i\downarrow} = \frac{U}{2} \sum_{i\sigma} \hat{\psi}_{i\sigma}^* \hat{\psi}_{i\sigma} \hat{\psi}_{i,-\sigma}^* \hat{\psi}_{i,-\sigma} = \frac{U}{2} \sum_i (\hat{\psi}_i^* \hat{\psi}_i)^2. \end{aligned}$$

Introducing sources for the fermions, the partition function finally reads

$$\boxed{Z[\eta, \eta^*] = \int_{\substack{\hat{\psi}(\beta) = -\hat{\psi}(0) \\ \hat{\psi}^*(\beta) = -\hat{\psi}^*(0)}} \mathcal{D}(\hat{\psi}^*, \hat{\psi}) \exp \left( -S_F[\hat{\psi}, \hat{\psi}^*] + \eta^* \hat{\psi} + \eta \hat{\psi}^* \right)}, \quad (2.26)$$

where a sum over lattice sites and an integral over “time” is understood in the product  $\eta^* \hat{\psi}$  etc.

It is convenient to look at the Fourier transform of the action as the kinetic term becomes diagonal in Fourier-space. For this purpose we introduce a compact notation combining space and time indices. If we label the lattice sites by a vector

$\mathbf{x}$ , we may write  $\hat{\psi}^{(*)}(X) = \hat{\psi}^{(*)}(\tau, \mathbf{x}) = \hat{\psi}_i^{(*)}(\tau)$  and define a collective notation for time and space or frequency and momentum respectively

$$X = (\tau, \mathbf{x}), \quad Q = (\omega_n, \mathbf{q}), \quad QX = \omega_n \tau + \mathbf{xq}. \quad (2.27)$$

Generalised sums and corresponding delta functions then read

$$\begin{aligned} \sum_X &= \int_0^\beta d\tau \sum_{\mathbf{x}}, & \sum_Q &= T \sum_n \int_{-\pi}^\pi \frac{d^2 q}{(2\pi)^2}, \\ \delta(Q - Q') &= \frac{1}{T} \delta_{n, n'} \cdot (2\pi)^2 \delta(\mathbf{q} - \mathbf{q}'), \\ \delta(X - X') &= \delta(\tau - \tau') \cdot \delta(\mathbf{x} - \mathbf{x}'). \end{aligned} \quad (2.28)$$

These definitions apply equally in the fermionic and bosonic case if we remember that

$$\omega_Q \equiv \omega_n = 2\pi nT, \quad n \in \begin{cases} \mathbb{Z} & \text{for bosons} \\ \mathbb{Z} + 1/2 & \text{for fermions.} \end{cases} \quad (2.29)$$

Note that  $\delta(\mathbf{q} - \mathbf{q}')$  is periodic in  $2\pi$ . Similarly,  $\delta(\tau)$  obeys  $\delta(\tau) = \pm\delta(\tau + \beta)$  for bosons/fermions.

The Fourier transforms of the fermionic fields can now be expressed in a very compact form:

$$\hat{\psi}(X) = \sum_Q e^{iQX} \hat{\psi}(Q), \quad \hat{\psi}^*(X) = \sum_Q e^{-iQX} \hat{\psi}^*(Q). \quad (2.30)$$

We will restrict ourselves to a square lattice in two dimensions and specify the hopping matrix as

$$t_{ij} = \begin{cases} -t & \text{for NN (nearest neighbours)} \\ -t' & \text{for NNN (next-NN)} \\ 0 & \text{else.} \end{cases} \quad (2.31)$$

The kinetic part of the action (i.e. the part quadratic in the fields) then reads in Fourier space

$$\begin{aligned} S_{F, \text{kin}} &= \sum_Q \hat{\psi}^*(Q) [i\omega_Q + \epsilon_Q - \mu] \hat{\psi}(Q), \\ \epsilon_Q &= -2t(\cos q_x + \cos q_y) - 4t' \cos q_x \cos q_y. \end{aligned} \quad (2.32)$$

The inverse fermionic propagator  $P_F(Q) = i\omega_Q + \epsilon_Q - \mu$  has zeroes for  $T = 0$  and  $\epsilon_Q = \mu$ . This is of course expected and we recognise the condition for the Fermi surface. Figure 2.1 shows the Fermi surface for different values of  $\mu$  for  $t' = 0$  (left) and for  $t' = -0.1t$  (right). The line of quadratic shape in the left figure corresponds

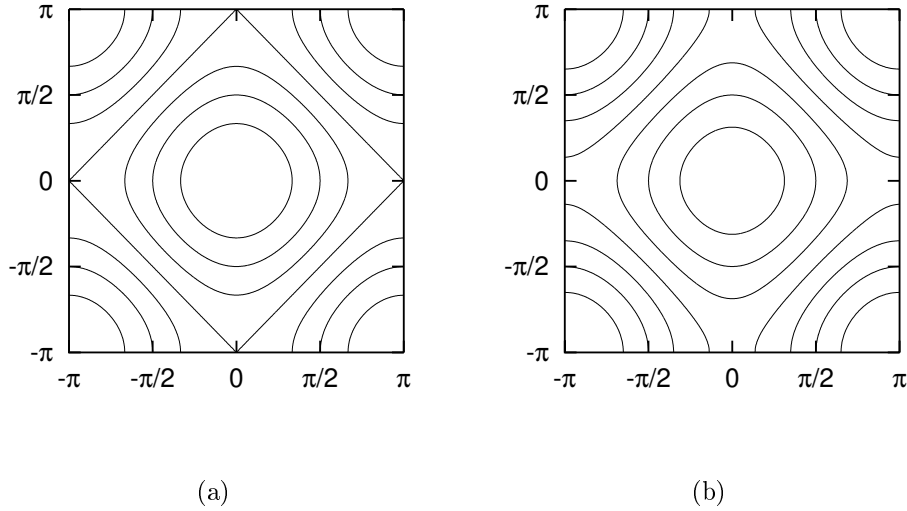


Figure 2.1: Fermi surfaces  $\epsilon_Q = \mu$  of the non-interacting Hubbard model for  $t' = 0$  (left) and  $t' = -0.1t$  (right). The contours correspond to various values of the chemical potential  $\mu = \pm\{0, \frac{1}{2}, 1, \frac{3}{2}\}t$ .

to  $\epsilon_Q = \mu = 0$ . In this case there are as many states above the Fermi surface as there are below, i.e. exactly half of the states are occupied and the average number of electrons per lattice site is one.  $\mu = 0$  is therefore referred to as *half filling*. A doped system, i.e. one where electrons have been added or removed, is therefore described by a nonzero chemical potential.

## Symmetries

Let us take a look at the symmetries obeyed by the action of the Hubbard model (2.25).

The most obvious symmetries are maybe the symmetries of the underlying lattice, which are of course also respected by the Hubbard action. For a square lattice they are translation, rotation and reflection. A  $U(1)$  symmetry<sup>3</sup>

$$\hat{\psi}(X) \rightarrow e^{i\theta} \hat{\psi}(X), \quad \hat{\psi}^*(X) \rightarrow \hat{\psi}^*(X) e^{-i\theta}$$

provides for charge conservation and a  $SU(2)$  symmetry acting in spinor space

$$\hat{\psi}(X) \rightarrow e^{i\vec{\sigma}\vec{\theta}} \hat{\psi}(X), \quad \hat{\psi}^*(X) \rightarrow \hat{\psi}^*(X) e^{-i\vec{\sigma}\vec{\theta}}$$

<sup>3</sup>Do not expect to see gauge bosons corresponding to a *local*  $U(1)$  symmetry. We are dealing with an effective theory in which photons are supposed to have been integrated out.

reflects invariance under spin rotations.

Another symmetry is reminiscent of time reversal

$$\hat{\psi}_i(\tau) \rightarrow -\hat{\psi}_i(\beta - \tau), \quad \hat{\psi}_i^*(\tau) \rightarrow \hat{\psi}_i^*(\beta - \tau), \quad t_{ij} \rightarrow -t_{ij}, \quad \mu \rightarrow -\mu.$$

Assuming appropriate transformations of the sources the partition function will be invariant under this transformation.

For special choices of the underlying lattice and hopping matrix  $t_{ij}$  other symmetries may arise. Consider a square lattice  $I$  and a hopping matrix  $t_{ij}$  which has entries for nearest neighbours only. We may then split the lattice  $I$  into two sublattices  $I_1$  containing the lattice points  $\vec{x} = (2\mathbb{Z}, 2\mathbb{Z})$  and  $I_2 = I/I_1$  containing the rest; the hopping matrix  $t_{ij}$  then has nonvanishing elements only if  $i$  and  $j$  reside on different sublattices. Such a lattice is often called a bipartite lattice. The mapping (together with an appropriate mapping of the sources)

$$\begin{aligned} \hat{\psi}_{i \in I_1} &\rightarrow \hat{\psi}_{i \in I_1}, & \hat{\psi}_{i \in I_2} &\rightarrow -\hat{\psi}_{i \in I_2}, \\ \hat{\psi}_{i \in I_1}^* &\rightarrow \hat{\psi}_{i \in I_1}^*, & \hat{\psi}_{i \in I_2}^* &\rightarrow -\hat{\psi}_{i \in I_2}^*, \\ & & t_{ij} &\rightarrow -t_{ij} \end{aligned}$$

again leaves the partition function invariant. Together with time reversal invariance we therefore conclude that for a bipartite lattice we may restrict ourselves to positive  $\mu$  and  $t$ .

At half filling the Hubbard model on a bipartite lattice even has another  $SU(2)$  symmetry (*pseudospin*) which for  $\mu \neq 0$  breaks down to the  $U(1)$  fermion number symmetry mentioned above [47].

Also note that the partition function is invariant under the rescaling ( $\alpha \in \mathbb{R}_+$ )

$$\tau \rightarrow \tau/\alpha, \quad T \rightarrow \alpha T, \quad \mu \rightarrow \alpha\mu, \quad t \rightarrow \alpha t, \quad U \rightarrow \alpha U,$$

and can therefore only depend on the dimensionless ratios  $T/t$ ,  $\mu/t$  and  $U/t$ .

## 2.3 Partial bosonisation

Under a renormalisation group transformation the interaction term of the Hubbard model will acquire a complex momentum dependence. Also vertex functions containing more than 4 fermionic operators will appear. Interesting physical phenomena (e.g. the emergence of quasiparticles) are encoded in this momentum dependence. If one of these degrees of freedom acquires a nonzero expectation value, a symmetry is possibly broken. It would be nice if one could somehow make these degrees of freedom explicit in the formalism. This can be achieved by partial bosonisation.

In the purely fermionic formalism spontaneous symmetry breaking is characterised by a divergence of the four fermion coupling in certain momentum channels. This limits this formalism to the study of the symmetric phase. Furthermore it is difficult to include higher vertex functions that are likely to play an important role close to the phase transition. In the partially bosonised theory this divergence is translated into a vanishing of the mass term of a bosonic field if the phase transition is of second order. The bosonic fields correspond to composite operators consisting of an even number of fermionic fields, e.g. the magnetisation density is described by  $\tilde{m}_i = \hat{\psi}_i^* \vec{\sigma} \hat{\psi}_i$  with the Pauli matrices  $\sigma^i$ .

Partial bosonisation, or Hubbard–Stratonovic transformation, is nothing but an inclusion of a suitable  $\mathbb{1}$  under the functional integral, usually chosen to be a Gaussian integral over some auxiliary field. By a suitable shift in the integration variable corresponding to a fermion bilinear like e.g.  $\tilde{m}_i$  one may be able to cancel the interaction term of the purely fermionic theory and end up with a Yukawa–type theory with bosonic fields coupled to the fermionic fields. To see how this works we first proceed by decomposing the Hubbard interaction into fermion bilinears.

Note that the interaction can be written in many different ways. To display a few, define fermion bilinears corresponding to charge density, magnetisation and Cooper pairs in different channels

$$\tilde{\rho}(X) \equiv \tilde{\rho}_i = \hat{\psi}_i^* \hat{\psi}_i, \quad (2.33)$$

$$\tilde{m}(X) \equiv \tilde{m}_i = \hat{\psi}_i^* \vec{\sigma} \hat{\psi}_i, \quad (2.34)$$

$$\tilde{s}(X) \equiv \tilde{s}_i = \hat{\psi}_i \epsilon \hat{\psi}_i, \quad \tilde{s}^*(X) \equiv \tilde{s}_i^* = -\hat{\psi}_i^* \epsilon \hat{\psi}_i^*, \quad (2.35)$$

$$\tilde{c}_x(X) \equiv \tilde{c}_{xi} = \hat{\psi}_i \epsilon \hat{\psi}_{i+\hat{e}_x}, \quad \tilde{c}_x^*(X) \equiv \tilde{c}_{xi}^* = -\hat{\psi}_{i+\hat{e}_x}^* \epsilon \hat{\psi}_i^*, \quad (2.36)$$

where  $\epsilon$  is the two dimensional completely antisymmetric tensor ( $\epsilon = i\sigma^2$ ) and  $\hat{e}_x$  is the unit vector in  $x$ -direction. We also define a  $\tilde{c}_y$  similar to  $\tilde{c}_x$ . With these definitions we may rewrite the interaction term as follows<sup>4</sup>

$$(\hat{\psi}_i^* \hat{\psi}_i)^2 = \tilde{\rho}_i^2 = -\frac{1}{3} \tilde{m}_i^2 = -\tilde{m}_{3,i}^2 = \frac{1}{2} \tilde{s}_i^* \tilde{s}_i \quad (2.37)$$

and further note the identity

$$-\tilde{\rho}_i \tilde{\rho}_{i+\hat{e}_x} + \tilde{m}_i \tilde{m}_{i+\hat{e}_x} + 2\tilde{c}_{xi}^* \tilde{c}_{xi} = 0 \quad (2.38)$$

and similar for  $x \rightarrow y$ .

Let us now introduce auxiliary fields  $\hat{B} = (\hat{\rho}, \hat{m}, \hat{s}^{(*)}, \hat{c}_x^{(*)}, \hat{c}_y^{(*)})$  and add a term quadratic in these fields to the action such that the four fermion interaction is just

<sup>4</sup>Appendix B.1 may be useful for spinor gymnastics.

cancelled:

$$S[\hat{\psi}, \hat{\psi}^*, \hat{B}] = S[\hat{\psi}, \hat{\psi}^*] + \Delta S_{int}[\hat{\psi}, \hat{\psi}^*, \hat{B}] \quad (2.39)$$

$$\begin{aligned} \Delta S_{int} = \sum_X \left\{ \frac{1}{2} \alpha_\rho (\hat{\rho}_i - \tilde{\rho}_i)^2 + \frac{1}{2} \alpha_m (\hat{m}_i - \tilde{m}_i)^2 + \alpha_s (\hat{s}_i^* - \tilde{s}_i^*) (\hat{s}_i - \tilde{s}_i) \right. \\ \left. + \alpha_x [(\hat{c}_{xi}^* - \tilde{c}_{xi}^*) (\hat{c}_{xi} - \tilde{c}_{xi}) \right. \\ \left. - \frac{1}{2} (\hat{\rho}_i - \tilde{\rho}_i) (\hat{\rho}_{i+\hat{e}_x} - \tilde{\rho}_{i+\hat{e}_x}) + \frac{1}{2} (\hat{m}_i - \tilde{m}_i) (\hat{m}_{i+\hat{e}_x} - \tilde{m}_{i+\hat{e}_x}) \right] \\ \left. + \alpha_y [x \rightarrow y] \right\}. \end{aligned} \quad (2.40)$$

Restricting the couplings to the range

$$\begin{aligned} \alpha_i &> 0, \\ \alpha_\rho, \alpha_m &> \alpha_x + \alpha_y, \\ 3\alpha_m - \alpha_\rho - 2\alpha_s &= U \end{aligned} \quad (2.41)$$

ensures that the auxiliary fields are Gaussian and can be integrated out after a shift of variables (first and second conditions) and furthermore the four fermion interaction in the original action is exactly cancelled (third condition). These conditions thus ensure that the partition function containing bosonic fields

$$Z[\eta, \eta^*] = \int \mathcal{D}(\hat{\psi}^*, \hat{\psi}, \hat{B}) \exp \left( -S[\hat{\psi}, \hat{\psi}^*, \hat{B}] + \eta^* \hat{\psi} + \eta \hat{\psi}^* \right)$$

is indeed equivalent to (2.26).

We emphasise, however, that the choice of the parameters  $\alpha_i$  is not unique. A wide range of choices thus describe the same fermionic model and physical results should be independent of this arbitrariness. Nevertheless, when doing approximations it is hard to preserve this invariance. It is therefore a good check for the validity of any approximation scheme to investigate if and how strongly the final result depends on the initial choice of parameters.

Collecting terms in (2.39) we see that as promised we are now dealing with a theory of fermions coupled to bosons via a Yukawa interaction. In Fourier space the bosonised action reads

$$S[\hat{\psi}, \hat{\psi}^*, \hat{B}] = S_{kin}[\hat{\psi}, \hat{\psi}^*, \hat{B}] + S_Y[\hat{\psi}, \hat{\psi}^*, \hat{B}] \quad (2.42)$$

$$\begin{aligned} S_{kin} = \sum_Q \left\{ \hat{\psi}^*(Q) [i\omega_Q - \mu - \overbrace{-2t(\cos q_x + \cos q_y) - 4t' \cos q_x \cos q_y}^{=\epsilon_Q = \epsilon_q}] \hat{\psi}(Q) \right. \\ \left. + \frac{1}{2} (\alpha_\rho - \alpha_x \cos q_x - \alpha_y \cos q_y) \hat{\rho}(-Q) \hat{\rho}(Q) \right. \\ \left. + \frac{1}{2} (\alpha_m + \alpha_x \cos q_x + \alpha_y \cos q_y) \hat{m}(-Q) \hat{m}(Q) \right. \\ \left. + \alpha_s \hat{s}^*(Q) \hat{s}(Q) + \alpha_x \hat{c}_x^*(Q) \hat{c}_x(Q) + \alpha_y \hat{c}_y^*(Q) \hat{c}_y(Q) \right\} \end{aligned} \quad (2.43)$$



$$\begin{aligned}
S_Y = & - \sum_{KQQ'} \left[ \delta(K - Q + Q') \right. \\
& \left. \left\{ (\alpha_\rho - \alpha_x \cos k_x - \alpha_y \cos k_y) \hat{\rho}(K) \hat{\psi}^*(Q) \hat{\psi}(Q') \right. \right. \\
& \left. \left. + (\alpha_m + \alpha_x \cos k_x + \alpha_y \cos k_y) \hat{m}(K) \hat{\psi}^*(Q) \vec{\sigma} \hat{\psi}(Q') \right\} \right. \\
& + \delta(K - Q - Q') \\
& \left. \left\{ \alpha_s [\hat{s}^*(K) \hat{\psi}(Q) \epsilon \hat{\psi}(Q') - \hat{s}(K) \hat{\psi}^*(Q) \epsilon \hat{\psi}^*(Q')] \right. \right. \\
& \left. \left. + \alpha_x \cos \frac{q_x - q'_x}{2} [\hat{c}_x^*(K) \hat{\psi}(Q) \epsilon \hat{\psi}(Q') - \hat{c}_x(K) \hat{\psi}^*(Q) \epsilon \hat{\psi}^*(Q')] \right. \right. \\
& \left. \left. + \alpha_y \cos \frac{q_y - q'_y}{2} [\hat{c}_y^*(K) \hat{\psi}(Q) \epsilon \hat{\psi}(Q') - \hat{c}_y(K) \hat{\psi}^*(Q) \epsilon \hat{\psi}^*(Q')] \right\} \right], \tag{2.44}
\end{aligned}$$

where we have used the Fourier transforms (2.30) for the fermions and (using the conventions (2.28))

$$\hat{\chi}(X) = \sum_Q e^{iQX} \hat{\chi}(Q), \quad \hat{\chi}^*(X) = \sum_Q e^{-iQX} \hat{\chi}^*(Q) \tag{2.45}$$

for  $\hat{\chi}^{(*)} = (\hat{\rho}, \hat{m}, \hat{s}^{(*)})$ , while for  $\hat{c}, \hat{c}^*$  we use:

$$\hat{c}_x(X) = \sum_Q e^{i(QX + q_x/2)} \hat{c}_x(Q), \quad \hat{c}_x^*(X) = \sum_Q e^{-i(QX + q_x/2)} \hat{c}_x^*(Q) \tag{2.46}$$

and similar for  $\hat{c}_y^{(*)}$ . At this point it is convenient to define the momentum space bilinears

$$\begin{aligned}
\tilde{\rho}(Q) &= \sum_X e^{-iQX} \tilde{\rho}(X) = \sum_K \hat{\psi}^*(K) \hat{\psi}(K + Q), \\
\tilde{s}(Q) &= \sum_X e^{-iQX} \tilde{s}(X) = \sum_K \hat{\psi}(K) \epsilon \hat{\psi}(K - Q), \\
\tilde{c}_x(Q) &= \sum_X e^{-i(QX + q_x/2)} \tilde{c}_x(X) = \sum_{KK'} \delta(Q - K - K') \cos \frac{k_x - k'_x}{2} \hat{\psi}(K) \epsilon \hat{\psi}(K')
\end{aligned} \tag{2.47}$$

and so forth.

In the bosonised theory a broken symmetry will now manifest itself in a nonzero expectation value of one of the bosonic fields. For example there is strong evidence for the fact that at low temperatures and close to half filling the Hubbard model describes an antiferromagnet, i.e. that the sign of the magnetisation density alternates between neighbouring lattice sites. In Fourier space this translates into a nonzero expectation value of the  $\vec{m}(\mathbf{q} = (\pi, \pi))$ -mode of the spin density. Another important excitation seems to be connected to Cooper pairs having  $d$ -wave symmetry. In the following section we will therefore construct a boson reflecting these symmetries from  $\hat{c}_x$  and  $\hat{c}_y$ .

### 2.3.1 $d$ -wave operators

In order to get an operator that has  $d$ -wave symmetry perform the transformation of variables

$$\begin{aligned}\hat{e} &= (\hat{c}_x + \hat{c}_y), & \hat{c}_x &= \frac{1}{2}(\hat{e} + \hat{d}), \\ \hat{d} &= (\hat{c}_x - \hat{c}_y), & \hat{c}_y &= \frac{1}{2}(\hat{e} - \hat{d}),\end{aligned}\quad (2.48)$$

and similar for  $\hat{e}^*, \hat{d}^*$ . Then sums and products of these variables translate as

$$\begin{aligned}\hat{c}_x^* \hat{c}_x + \hat{c}_y^* \hat{c}_y &= \frac{1}{2}(\hat{e}^* \hat{e} + \hat{d}^* \hat{d}), \\ \eta_x \hat{c}_x + \eta_y \hat{c}_y &= \frac{1}{2}(\eta_x + \eta_y) \hat{e} + \frac{1}{2}(\eta_x - \eta_y) \hat{d}.\end{aligned}\quad (2.49)$$

If we insert this variable transformation into the action (2.42) and put  $\alpha_x = \alpha_y = \alpha_c$  we obtain for the  $e$  and  $d$  dependent part of the action:

$$\begin{aligned}S^{e,d} &= \sum_Q \frac{1}{2} \alpha_c \{ \hat{e}^*(Q) \hat{e}(Q) + \hat{d}^*(Q) \hat{d}(Q) \} \\ &\quad - \sum_{KQ Q'} \delta(K - Q - Q') \\ &\quad \left\{ \frac{\alpha_c}{2} \left( \cos \frac{q_x - q'_x}{2} + \cos \frac{q_x - q'_y}{2} \right) [ \hat{e}^*(K) \hat{\psi}(Q) \epsilon \hat{\psi}(Q') - \hat{e}(K) \hat{\psi}^*(Q) \epsilon \hat{\psi}^*(Q') ] \right. \\ &\quad \left. + \frac{\alpha_c}{2} \left( \cos \frac{q_x - q'_x}{2} - \cos \frac{q_x - q'_y}{2} \right) [ \hat{d}^*(K) \hat{\psi}(Q) \epsilon \hat{\psi}(Q') - \hat{d}(K) \hat{\psi}^*(Q) \epsilon \hat{\psi}^*(Q') ] \right\}.\end{aligned}\quad (2.50)$$

Integrating out the bosons is equivalent to inserting the solutions of their field equations  $\delta S[\hat{\psi}, \hat{\psi}^*, \hat{B}] / \delta \hat{B} = 0$  (i.e. the saddle point) into the action  $S[\hat{\psi}, \hat{\psi}^*, \hat{B}]$ . For the boson  $\hat{d}$  the solution is

$$\tilde{d}(Q) = \tilde{c}_x(Q) - \tilde{c}_y(Q), \quad (2.51)$$

as expected from the construction of  $\hat{d}$  and it is thus this combination the boson  $\hat{d}$  represents in the fermionic theory (this will become clearer when we introduce sources in the next section).

Let us take a look at the  $\mathbf{q} = (0, 0)$  mode of  $\tilde{d}(Q)$ , i.e. at a spatially homogeneous field. From (2.51) we know that it is a superposition of stripes along the  $x$ - and  $y$ -axis added with opposite signs. A graphical representation is given in figure 2.2 (left) where the solid and dashed lines indicate that two fermionic operators on neighbouring lattice sites are connected with positive or negative sign respectively. To find a “local” expression rewrite

$$\begin{aligned}\tilde{d}(Q=0) &= \sum_K (\cos k_x - \cos k_y) \hat{\psi}(K) \epsilon \hat{\psi}(-K) \\ &= \frac{1}{2} \sum_X \left\{ \hat{\psi}(X) \epsilon \hat{\psi}(X + \hat{e}_x) + \hat{\psi}(X) \epsilon \hat{\psi}(X - \hat{e}_x) \right. \\ &\quad \left. - \hat{\psi}(X) \epsilon \hat{\psi}(X + \hat{e}_y) - \hat{\psi}(X) \epsilon \hat{\psi}(X - \hat{e}_y) \right\}\end{aligned}\quad (2.52)$$

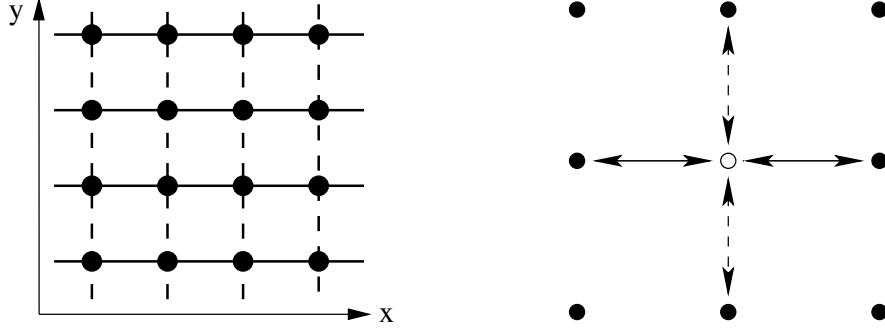


Figure 2.2: The  $\mathbf{q} = \mathbf{0}$  mode of  $\tilde{d}(Q)$  in its global (left) and local (right) form. Solid and dashed lines indicate that two fermionic operators on neighbouring lattice sites are connected with positive or negative sign respectively.

so at each lattice site we find an operator of the form shown in figure 2.2 (right). We see that indeed this boson may serve as a lattice representation of  $d_{x^2-y^2}$  symmetry as it changes its sign under rotation by  $90^\circ$  but not under reflection at the  $x$  or  $y$  axes (see also [37]).

### 2.3.2 Introducing sources for bosonic fields

Let us now introduce source terms for the fermionic and bosonic fields<sup>5</sup>

$$S_j = - \sum_X \left\{ \eta^*(X) \hat{\psi}(X) + \eta(X) \hat{\psi}^*(X) + l^\rho(X) \hat{\rho}(X) + \vec{l}^m(X) \hat{m}(X) + l^{s^*}(X) \hat{s}(X) + l^s(X) \hat{s}^*(X) + [s^{(*)} \rightarrow (c_x^{(*)}, c_y^{(*)}) \text{ or } (e^{(*)}, d^{(*)})] \right\}. \quad (2.53)$$

The logarithm of the partition function

$$Z[\eta, \eta^*, \{l^B\}] = \int \mathcal{D}(\hat{\psi}^*, \hat{\psi}, \hat{B}) \exp(-S[\hat{\psi}, \hat{\psi}^*, \hat{B}] - S_j[\hat{\psi}, \hat{\psi}^*, \hat{B}]) \quad (2.54)$$

is then the generating functional of connected Green functions [34]. In particular we find

$$B = \langle \hat{B} \rangle = \frac{\delta}{\delta l^B} \ln Z[\eta, \eta^*, \{l^B\}]. \quad (2.55)$$

<sup>5</sup>It may sometimes be favourable to absorb the chemical potential  $\mu$  into the source of  $\rho$  by exchanging  $l^\rho(X) \rightarrow l^\rho(X) + \mu$  and adding appropriate factors  $\sim \mu^2$  in the action [4].

However, if we first integrate out the bosonic fields, we find

$$\begin{aligned}
Z[\eta, \eta^*, \{l^B\}] &= \int \mathcal{D}(\hat{\psi}^*, \hat{\psi}) \exp(-S_F[\hat{\psi}, \hat{\psi}^*] - \tilde{S}_j[\hat{\psi}, \hat{\psi}^*]) \\
\tilde{S}_j[\hat{\psi}, \hat{\psi}^*] &= - \sum_Q \left\{ \eta^*(Q) \hat{\psi}(Q) + \eta(Q) \hat{\psi}^*(Q) \right. \\
&\quad + l^\rho(-Q) \tilde{\rho}(Q) + \frac{1}{2} (\alpha_\rho - \alpha_c (\cos q_x + \cos q_y))^{-1} l^\rho(-Q) l^\rho(Q) \\
&\quad + \cdots + l^{s^*}(Q) \tilde{s}(Q) + l^s(Q) \tilde{s}^*(Q) + \alpha_s^{-1} l^{s^*}(Q) l^s(Q) \\
&\quad \left. + \cdots + l^{a^*}(Q) \tilde{d}(Q) + l^d(Q) \tilde{d}^*(Q) + 2\alpha_c^{-1} l^{a^*}(Q) l^d(Q) \right\},
\end{aligned} \tag{2.56}$$

i.e. for every composite field there is a usual source term and a term quadratic in the sources. This is exactly what we want: for vanishing sources the expectation values of the bosonic fields and their corresponding fermionic bilinears exactly coincide

$$B = \langle \hat{B} \rangle = \langle \tilde{B} \rangle = \left. \frac{\delta}{\delta l^B} \ln Z[\eta, \eta^*, \{l^B\}] \right|_{l^B=0};$$

thus if we find a nonvanishing expectation value of a bosonic field we know that the corresponding symmetry is also broken in the purely fermionic description.

## 2.4 The effective action

In this section we introduce the important concept of the effective action. In order to make the notation more concise we combine fields and sources into a vector notation<sup>6</sup>:

$$\begin{aligned}
\hat{\chi}(X) &= (\hat{\rho}, \hat{m}, \hat{s}, \hat{s}^*, \dots, \hat{\psi}, \hat{\psi}^*)(X), \\
J(X) &= (l^\rho, \vec{l}^m, l^{s^*}, l^s, \dots, \eta^*, \eta)(X).
\end{aligned} \tag{2.57}$$

Now define *classical fields* as expectation values of the corresponding quantum operators

$$\chi := \langle \hat{\chi} \rangle = \frac{\delta}{\delta J} \ln Z[J]. \tag{2.58}$$

The *effective action* is defined as the Legendre transform of the generating functional of connected Green functions,  $W[J] = \ln Z[J]$ , with respect to the classical fields

$$\boxed{\Gamma[\chi] = -W[J] + \sum_X J \chi, \quad J = J[\chi],} \tag{2.59}$$

<sup>6</sup>If we define the Fourier transform as in (2.45), i.e.  $\hat{\chi}(X) = \sum_Q e^{iQX} \hat{\chi}(Q)$ , we obtain  $\hat{\chi}(Q) = (\hat{\rho}(Q), \hat{m}(Q), \hat{s}(Q), \hat{s}^*(-Q), \dots, \hat{\psi}(Q), \hat{\psi}^*(-Q))$ .

where  $J[\chi]$  is a solution of the field equation (2.58). From this definition we immediately find the field equations<sup>7</sup>

$$\begin{aligned} \frac{\delta}{\delta\chi_i}\Gamma[\chi] &= -\frac{\delta J_j}{\delta\chi_i}\frac{\delta\ln Z}{\delta J_j} + \frac{\delta J_j}{\delta\chi_i}\chi_j + M_{ij}J_j = M_{ij}J_j = J_jM_{ji}, \\ M &= \text{diag}(1, 1, 1, 1, \dots, -1, -1). \end{aligned} \quad (2.60)$$

Sometimes it is useful to write the effective action in a more implicit way. Using (2.59) and the definition of the partition function  $Z[J]$  we may also write

$$e^{-\Gamma[\chi]} = \int \mathcal{D}\hat{\chi} e^{-S[\hat{\chi}] + J(\hat{\chi} - \chi)} = \int \mathcal{D}\hat{\chi} e^{-S[\hat{\chi} + \chi] + J\hat{\chi}}, \quad (2.61)$$

where  $J = M\frac{\delta}{\delta\chi}\Gamma$  (alternatively,  $J = \frac{\delta\Gamma}{\delta R\chi}$  for right-derivatives). We further note the identity<sup>8</sup>

$$\Gamma_{ij}^{(2)} W_{jk}^{(2)} = M_{jl} \frac{\delta J_l}{\delta\chi_i} \frac{\delta\chi_k}{\delta J_j} = M_{ik}, \quad (2.62)$$

stating that the second functional derivative of the effective action is the inverse propagator.

The effective action is a very powerful concept in field theory. It is the generating functional of one particle irreducible (1PI) Green functions [34]. Since by the reduction formulae one can construct all  $S$ -matrix elements from the Green functions, calculating the effective action is equivalent to solving a quantum theory. It is not hard to imagine that calculating the effective action thus is a very difficult task.

Note that for vanishing sources the field equations (2.58) exactly correspond to the ones derived by a classical action principle (hence the terms ‘‘classical field’’ and ‘‘effective action’’).

<sup>7</sup>We make use of the chain rule for left-derivatives:  $f[g[\chi_0 + \chi]] = f[g[\chi_0] + \chi g^{(1)}[\chi_0] + \dots] = f[g[\chi_0]] + \chi g^{(1)}[\chi_0] f^{(1)}[g[\chi_0]] + \dots$ .

<sup>8</sup>This identity holds irrespective of whether we define the second functional derivatives as containing only left derivatives or as containing both right and left derivatives:

$$F[\chi_0 + \chi] = F[\chi_0] + \chi_\alpha F_\alpha^{(1)}[\chi_0] + \frac{1}{2}\chi_\alpha F_{\alpha\beta}^{(2)}[\chi_0]\chi_\beta + \dots = \dots + \frac{1}{2}\chi_\beta\chi_\alpha \hat{F}_{\alpha\beta}^{(2)}[\chi_0] + \dots \quad (2.63)$$

# Chapter 3

## A mean field calculation

In order to get a first impression of which structures might arise in a quantum theory one often relies on some kind of mean field approximation. In a mean field approach one replaces some fluctuating quantity by its average value and tries to solve the resulting equations in a self consistent way, thereby obtaining an equation for the size of the average value. However, there is not *the* way to make a mean field approximation. Several may exist and lead to different results. Furthermore, mean field theory is grossly inadequate in the critical region of some phase transition where fluctuations play an increasingly important role. The larger the space-dimensionality of the system, however, the better mean field theory works. Nevertheless, mean field theory is often a starting point for a more sophisticated approximation.

Let us look at a crude derivation of a mean field equation. Consider a theory with action

$$S[\psi, \psi^*] = \psi_A^* P_{AB} \psi_B + \frac{1}{2} f_{ABCD} \psi_A^* \psi_B \psi_C^* \psi_D, \quad (3.1)$$

where for notational convenience we have extended the summation convention also to include momentum indices etc. We may then approximate the two point function (propagator) by replacing products of fields by their respective expectation value in the interaction term

$$\begin{aligned} \langle \psi_\beta \psi_\alpha^* \rangle &\approx \int \mathcal{D}(\psi^*, \psi) \psi_\beta \psi_\alpha^* e^{-\psi_A^* P_{AB} \psi_B - f_{ABCD} (\psi_A^* \psi_B \langle \psi_C^* \psi_D \rangle - \psi_A^* \psi_D \langle \psi_C^* \psi_B \rangle)} \\ &\approx [P_{\alpha\beta} + (f_{\alpha\beta CD} - f_{\alpha DC\beta}) \langle \psi_C^* \psi_D \rangle]^{-1}. \end{aligned}$$

We have converted the many-particle problem into a one-particle problem for which the solution is known. Making some ansatz for the propagator leads to a self consistency equation since the two point function occurs on both sides of the equation. The above equation is nothing but the Hartree-Fock mean field equation [34] and may be regarded as the one-loop part of the Schwinger-Dyson equation for the propagator. We will return to this at the end of this chapter.

In the kind of mean field approach we are going to pursue we replace the bosonic fields by some constant value. By constant we do not necessarily mean spatially uniform. For example we will assume the spin density to alternate in sign between neighbouring lattice sites corresponding to an antiferromagnet which is believed to be the ground state of the Hubbard model near half filling.

### 3.1 Calculation of the effective potential

When considering constant field distributions it is possible to pull out a volume factor from the effective action. We will consider vanishing expectation values of the fermionic fields and define the *effective potential* as

$$\mathcal{V}U(B) = \Gamma[\psi^{(*)} = 0, B = \text{const.}], \quad (3.2)$$

where  $\mathcal{V} = \sum_X 1$  is the two dimensional volume divided by temperature. By minimising the effective potential we are able to find the ground state of the system.

In our mean field approximation calculating the effective potential amounts to performing only the fermionic part of the functional integral for the partition function (2.54) while the bosonic fields are fixed. This integral is Gaussian and may be performed leading to a functional determinant.

We now want to calculate the fermionic functional determinant at fixed bosonic fields ( $\boldsymbol{\pi} = (\pi, \pi)$ )

$$\rho = \hat{\rho}(\mathbf{q} = 0), \quad \vec{a} = \hat{m}(\mathbf{q} = \boldsymbol{\pi}), \quad d^{(*)} = \hat{d}^{(*)}(\mathbf{q} = 0), \quad (3.3)$$

while all other fields vanish, i.e. we assume that they do not gain a nonvanishing expectation value. The fermionic part of the action at fixed bosonic fields can be written as

$$S_2[\psi, \psi^*] = \frac{1}{2} \sum_{QQ'} [\psi(-Q), \psi^*(Q)] S^{(2)}(Q, Q') \begin{bmatrix} \psi(Q') \\ \psi^*(-Q') \end{bmatrix}, \quad (3.4)$$

which defines  $S^{(2)}$  and yields<sup>1</sup>

$$S^{(2)}(Q, Q') = \begin{pmatrix} B^+(Q)\delta(Q - Q') & -A^T(-Q, -Q') \\ A(Q, Q') & B(Q)\delta(Q - Q') \end{pmatrix}, \quad (3.5)$$

---

<sup>1</sup>We set  $t' = 0$  in this calculation.

$$\begin{aligned}
A(Q, Q') &= [i\omega_Q + \epsilon_Q - \tilde{\mu}] \delta(Q - Q') - \vec{A} \otimes \vec{\sigma} \delta(\boldsymbol{\pi} - Q + Q'), \\
\epsilon_Q &= \epsilon_{-Q} = -\epsilon_{Q+\boldsymbol{\pi}} = -2t(\cos q_x + \cos q_y), \\
\tilde{\mu} &= \mu + \underbrace{(\alpha_\rho - 2\alpha_c)}_{=:h_\rho} \rho = \mu + h_\rho \rho, \quad \vec{A} = \underbrace{(\alpha_m - 2\alpha_c)}_{=:h_a} \vec{a} = h_a \vec{a}, \\
B(Q) &= D(\mathbf{q}) \otimes \epsilon, \quad B^+(Q) = -D^+(\mathbf{q}) \otimes \epsilon, \\
D^{(+)}(\mathbf{q}) &= D^{(+)}(-\mathbf{q}) = -D^{(+)}(\mathbf{q} + \boldsymbol{\pi}) = \alpha_c (\cos q_x - \cos q_y) d^{(*)}.
\end{aligned} \tag{3.6}$$

The integral-correction to the effective potential now reads (see appendix B.4 and B.5)  $\Delta U = -\ln \int \mathcal{D}(\psi, \psi^*) \exp(-S_2) = -\frac{1}{2} \ln \det S^{(2)}$ . Using  $\epsilon \vec{\sigma}^T \epsilon^{-1} = -\vec{\sigma}$  we can simplify the determinant as follows

$$\begin{aligned}
\ln \det S^{(2)} &= \frac{1}{2} \ln \det \left[ S^{(2)}(Q, Q') \begin{pmatrix} 0 & \mathbb{1} \\ \mathbb{1} & 0 \end{pmatrix} S^{(2)}(-Q', -Q'') \begin{pmatrix} 0 & \mathbb{1} \\ \mathbb{1} & 0 \end{pmatrix} \right] \\
&= \ln \det [B^+(Q)B(-Q)\delta(Q - Q'') + A(Q, Q')A(-Q', -Q'')] \\
&= \ln \det \left[ (\omega_Q^2 + (\epsilon_Q - \tilde{\mu})^2 + \vec{A}^2 + D^+(\mathbf{q})D(\mathbf{q})) \delta(Q - Q'') \right. \\
&\quad \left. + 2\tilde{\mu} \vec{A} \vec{\sigma} \delta(Q - Q' + \boldsymbol{\pi}) \right] \\
&\equiv \ln \det [a_q \delta_{qq'} + \vec{b} \vec{\sigma} \delta_{q-\pi, q'}],
\end{aligned} \tag{3.7}$$

where in the last line we have adopted an obvious shorthand notation in momentum space. We will now calculate this determinant in two ways: first directly and then in a matrix notation showing the relation of the present formalism to the ‘‘coloured Hubbard model’’ [4].

First note that by  $SU(2)$  rotation invariance one has  $\det(a + \vec{b} \vec{\sigma}) = \det(a - \vec{b} \vec{\sigma})$  and hence<sup>2</sup>

$$\begin{aligned}
\ln \det [\delta_{q, q'} - \underbrace{\vec{m}_q \vec{\sigma} \delta_{q, q' - \pi}}_{M_{qq'}}] &= \frac{1}{2} \ln \det [(\delta_{qq'} - M_{qq'})(\delta_{q'q''} + M_{q'q''})] \\
&= \frac{1}{2} \ln \det [\delta_{qq''} - M_{qq'} M_{q'q''}] = \frac{1}{2} \ln \det [(1 - \vec{m}_q \vec{m}_{q-\pi}) \delta_{q, q'}].
\end{aligned} \tag{3.8}$$

In a similar way we get (remember that all functions are periodic  $a_q = a_{q+2\pi}$ )

$$\begin{aligned}
\ln \det [a_q \delta_{qq'} - \vec{b} \vec{\sigma} \delta_{q, q' + \pi}] &= \ln \det [a_{q+\pi} \delta_{q+\pi, q'+\pi} - \vec{b} \vec{\sigma} \delta_{q+\pi, q'}] \\
&= \frac{1}{2} \ln \det \{ [a_q \delta_{qq'} - \vec{b} \vec{\sigma} \delta_{q, q' + \pi}] [a_{q+\pi} \delta_{q, q'} + \vec{b} \vec{\sigma} \delta_{q+\pi, q'}] \} \\
&= \frac{1}{2} \ln \det [(a_q a_{q+\pi} - \vec{b} \cdot \vec{b}) \delta_{q, q'}],
\end{aligned} \tag{3.10}$$

<sup>2</sup>Alternatively, you might want to calculate this by expanding the logarithm:

$$\text{tr} \ln [\delta_{q, q'} - \underbrace{\vec{m}_q \vec{\sigma} \delta_{q, q' - \pi}}_{M_{qq'}}] = -\frac{1}{2} \text{tr} \sum_n \frac{(M^2)^n}{n} = \frac{1}{2} \text{tr} \ln [(1 - \vec{m}_q \vec{m}_{q-\pi}) \delta_{q, q'}]. \tag{3.9}$$



where we have used  $[\text{tr} \ln a_q \delta_{qq'} = \sum_q \ln a_q = \sum_q \ln a_{q+\pi} = \text{tr} \ln a_{q+\pi} \delta_{qq'}]$  and similar relations.

Before turning to the other calculation of the determinant show by induction that

$$\left| \begin{array}{cccc} \ddots & & & \\ & a_2 & & \\ & & a_1 & 1 \\ & & & a_{-1} & 1 \\ & & & & a_{-2} \\ & & & & & \ddots \end{array} \right| = \prod_n (a_{-n} a_n - 1). \quad (3.11)$$

Now split up the integration regions in different quadrants  $[0, \pm\pi] \times [0, \pm\pi]$  such that the function under the determinant becomes a  $4 \times 4$  matrix as in [4]<sup>3</sup>:

$$\begin{aligned} & \int_{-\pi}^{\pi} \frac{d^2 q}{(2\pi)^2} \frac{d^2 q'}{(2\pi)^2} \ln \det(a_q \delta_{qq'} + \vec{b} \vec{\sigma} \delta_{q, q' + \vec{\pi}}) \\ &= \int_{-\pi/2}^{\pi/2} \frac{d^2 q}{(2\pi)^2} \ln \det \left\{ \left( \begin{array}{ccc} a_q & & \\ & a_{q+\pi \hat{e}_1} & \\ & & a_{q+\pi \hat{e}_2} \\ & & & a_{q+\vec{\pi}} \end{array} \right) \otimes \mathbf{1}_{\text{spin}} + |\vec{b}| \left( \begin{array}{ccc} & & 1 \\ & 1 & \\ 1 & & \end{array} \right) \otimes \sigma^2 \right\} \\ &= \int_{-\pi/2}^{\pi/2} \frac{d^2 q}{(2\pi)^2} 2 \ln \left\{ (a_q a_{q+\vec{\pi}} - \vec{b}^2) (a_{q+\pi \hat{e}_1} a_{q+\pi \hat{e}_2} - \vec{b}^2) \right\} \\ &= \frac{1}{2} \int_{-\pi}^{\pi} \frac{d^2 q}{(2\pi)^2} \text{tr}_{\text{spin}} \ln \left\{ (a_q a_{q+\vec{\pi}} - \vec{b}^2) \right\}, \end{aligned} \quad (3.12)$$

where in the last line we took the liberty to extend the integration region to  $[-\pi, \pi] \times [-\pi, \pi]$  again. Of course this result coincides with (3.10).

Let us now continue the calculation of the fermionic determinant ( $D_Q^2 = D^+(\mathbf{q})D(\mathbf{q})$ )

$$\begin{aligned} \ln \det S^{(2)} &= \frac{1}{2} \text{tr} \ln \{ (\omega_Q^2 + \epsilon_Q^2 + \tilde{\mu}^2 + \vec{A}^2 + D_Q^2)^2 - 4(\epsilon_Q^2 + \vec{A}^2) \tilde{\mu}^2 \} \\ &= \frac{1}{2} \text{tr} \ln \{ [(\omega_Q^2 + \epsilon_Q^2 + \tilde{\mu}^2 + \vec{A}^2 + D_Q^2) + 2\sqrt{\epsilon_Q^2 + \vec{A}^2} \tilde{\mu}] \\ &\quad [(\omega_Q^2 + \epsilon_Q^2 + \tilde{\mu}^2 + \vec{A}^2 + D_Q^2) - 2\sqrt{\epsilon_Q^2 + \vec{A}^2} \tilde{\mu}] \}, \end{aligned} \quad (3.13)$$

where the trace is in momentum- and spin-space:

$$\text{tr} = T \sum_n \int_{-\pi}^{\pi} \frac{d^2 q}{(2\pi)^2} \text{tr}_{\text{spin}}.$$

<sup>3</sup>Indeed, if we take formula (37) in [4] and use a basis where the symmetric-phase fermionic propagator is diagonal we obtain for matrices  $\Gamma_{\mu\nu} = \sigma_\mu \otimes \sigma_\nu$ ,  $\sigma_0 = \mathbb{1}_2$

$\ln \det S^{(2)} = \ln \det_8 [\omega_n^2 + (2t(c_x \Gamma_{03} + c_y \Gamma_{30}) + h_\rho \rho)^2 + h_a^2 \vec{d}^2 + 2h_\rho \rho h_a \vec{d} \vec{\sigma} \Gamma_{11} + h_d^2 d^* d (c_x \Gamma_{03} - c_y \Gamma_{30})^2]$  which corresponds to (3.7) in “matrix notation”.

If we pull out a (temperature dependent) constant from the functional determinant  $\text{tr} \ln(\omega_Q + \Omega_Q) = \text{tr} \ln(1 + \frac{\Omega_Q}{\omega_Q}) + \text{const}(T)$ , we are able to use [16]

$$2 \ln \cosh(x) = \sum_{n \in \mathbb{Z}} \ln \left( 1 + \frac{x^2}{(n + 1/2)^2 \pi^2} \right) \quad (3.14)$$

and finally obtain for the mean field approximation to the effective potential:

$$U_{\text{pot}} = \frac{1}{2} h_\rho \rho^2 + \frac{1}{2} h_a \vec{a}^2 + \frac{1}{2} \alpha_c d^* d + \Delta U \quad (3.15)$$

$$\Delta U = -\frac{1}{2} \text{tr} \ln S^{(2)} = -T \int_{-\pi}^{\pi} \frac{d^2 q}{(2\pi)^2} \sum_{\epsilon \in \{\pm 1\}} \ln \cosh \frac{\Theta_\epsilon}{2T} \quad (3.16)$$

$$\Theta_\epsilon = \sqrt{\left( \tilde{\mu} + \epsilon \sqrt{4t^2 (\cos q_x + \cos q_y)^2 + h_a^2 \vec{a}^2} \right)^2 + \alpha_c^2 (\cos q_x - \cos q_y)^2 d^* d}. \quad (3.17)$$

For  $h_d = 2\alpha_c$  and  $d^* d = 4\delta$  this can be shown to coincide with the result presented in [4]<sup>4</sup>.

In the next section we will investigate the phase structure implied by this potential. Note again, however, that for given parameters  $\alpha_i$  we are not able to fix the value of the four fermion interaction  $U$  even though only two parameters occur explicitly in the potential:  $h_a = \alpha_m - 2\alpha_c$ ,  $h_d = 2\alpha_c$  (the effective chemical potential  $\tilde{\mu} = \mu + h_\rho \rho$  will be considered as an external parameter governing the electron density of the system). We have not specified  $\alpha_s$ , however, but only made the assumption that  $\hat{s}$  does not gain a nonzero expectation value. (Stated from an other point of view, a specific choice of  $U$  does not uniquely determine the parameters  $\alpha_i$ .)

## 3.2 Spontaneous symmetry breaking

There are two qualitatively different ways in which a phase transition can occur. Let us take a look at a scalar theory with effective potential  $U(\varphi^2)$  at different temperatures. In the first column of figure 3.1 the potential  $U(\varphi^2)$  becomes flatter at the origin when the temperature is lowered, until at some temperature  $T_c$  the potential becomes concave at  $\varphi = 0$  and the minimum smoothly moves outward to

---

<sup>4</sup>If we denote the fields and couplings in [4] by a tilde, we have to set  $\tilde{h}_B^2 = \pi^2 h_B$  and rescale the bosons by  $\tilde{B} = \sqrt{h_B} B / \pi$  in order to get the same results. The parametrisation of the couplings translates as  $\alpha_\rho = U\lambda_2$ ,  $U\lambda_3 = 2\alpha_c$ ,  $U(\lambda_2 + 1) = 3\alpha_m$ ,  $U\lambda_1 = \alpha_s$ . Also note that

$$\int_{-\pi}^{\pi} \frac{d^2 q}{(2\pi)^2} \sum_{\epsilon_i} F[(\cos(q_1/2) \pm \epsilon_i \cos(q_2/2))^2] = 2 \int_{-\pi}^{\pi} \frac{d^2 q}{(2\pi)^2} F[(\cos q_1 \pm \cos q_2)^2].$$

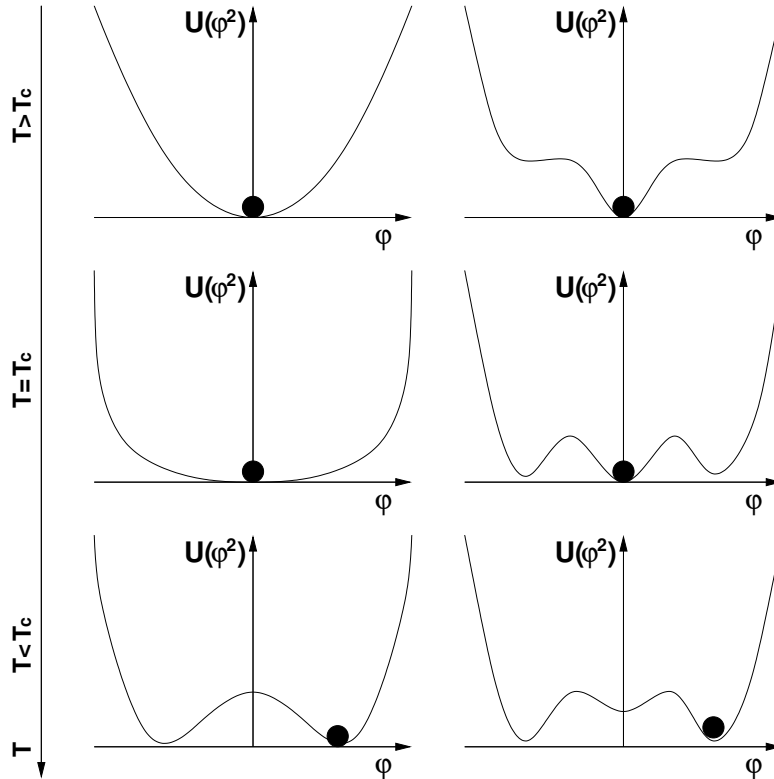


Figure 3.1: Possible scenarios for phase transitions (PT) are continuous PT (left column) and discontinuous PT (right column).

some nonzero value of the field  $\varphi$ . We call such a phase transition *continuous* (or of 2<sup>nd</sup> order) and the temperature  $T_c$  the *critical temperature*. If we define the “mass” of the field  $\varphi$  by  $m_\varphi^2 = 2 \frac{\partial U}{\partial \varphi^2} |_{\varphi=0}$  we observe that the mass vanishes at the phase transition. If as in the case shown in figure 3.1 the potential is symmetric under the transformation  $\varphi \rightarrow -\varphi$  the system has to choose between two energetically equivalent configurations. The symmetry is then said to be *spontaneously broken*.

In a second phase transition scenario the potential develops “pockets” of low energy away from the origin as in the right column of figure 3.1. The minimum of the potential thus jumps away from  $\varphi = 0$  at some transition temperature  $T_c$ . We call such a phase transition *discontinuous* (or of 1<sup>st</sup> order). We see that in this case the mass may still be positive below the phase transition. Negative mass is thus only a sufficient condition for the occurrence of a phase transition but not a necessary one. We will observe symmetry breaking of both kinds in our mean field approximation of the Hubbard model.

Before proceeding with a numerical analysis of the mean field potential (3.15) let us investigate it by analytic means. First note that for large temperature the fluctuation correction  $\Delta U$  to the potential vanishes  $\sim T^{-1}$ . The minimum is therefore

governed by the “classical” potential and the system is in the symmetric phase at  $\vec{a}^2 = 0$  and  $d^*d = 0$ . Furthermore, for large values of the order parameters  $\vec{a}^2$  and  $d^*d$  the classical potential governs the overall behaviour. Thus we know that the minimum of the potential will always be at finite values of the order parameters.

The fluctuations tend to destabilise the symmetric minimum. This can be seen by inspection of the masses of the  $\vec{a}$  and  $d$  bosons defined by

$$\begin{aligned} m_a^2 &= 2 \frac{\partial U_{\text{pot}}}{\partial(\vec{a}^2)} \Big|_{\vec{a}^2=d^*d=0} = h_a - h_a^2 \int \frac{d^2q}{(2\pi)^2} \frac{\tanh(\frac{1}{2T}(\epsilon_{\mathbf{q}} - \tilde{\mu}))}{\epsilon_{\mathbf{q}}}, \\ m_d^2 &= \frac{\partial U_{\text{pot}}}{\partial(d^*d)} \Big|_{\vec{a}^2=d^*d=0} = \frac{\alpha_c}{2} - \frac{\alpha_c^2}{2} \int \frac{d^2q}{(2\pi)^2} \frac{\tanh(\frac{1}{2T}(\epsilon_{\mathbf{q}} - \tilde{\mu}))}{\epsilon_{\mathbf{q}} - \tilde{\mu}} (\cos q_1 - \cos q_2)^2. \end{aligned} \quad (3.18)$$

The fluctuation corrections lower the masses and hence flatten the potential at the origin. The larger the couplings the more pronounced this effect becomes; remember however that there is an arbitrariness in the choice of couplings.

In a similar way we are also able to get some information about the order of the phase transition. Assume that the minimum of the potential is located at  $\vec{a}^2 = 0$  and  $d^*d > 0$ . We know that at the minimum the derivative of the potential vanishes

$$0 \stackrel{!}{=} \frac{\partial U_{\text{pot}}}{\partial(d^*d)} \Big|_{\vec{a}^2=0} = m_d^2 - \frac{\alpha_c^2}{2} \int \frac{d^2q}{(2\pi)^2} (\cos q_1 - \cos q_2)^2 \left\{ \frac{\tanh(\frac{1}{2T} \sqrt{(\epsilon_{\mathbf{q}} - \tilde{\mu})^2 + \alpha_c^2 (\cos q_1 - \cos q_2)^2 d^*d}})}{\sqrt{(\epsilon_{\mathbf{q}} - \tilde{\mu})^2 + \alpha_c^2 (\cos q_1 - \cos q_2)^2 d^*d}} - \frac{\tanh(\frac{1}{2T}(\epsilon_{\mathbf{q}} - \tilde{\mu}))}{\epsilon_{\mathbf{q}} - \tilde{\mu}} \right\}.$$

The term in curly brackets is negative for  $d^*d > 0$  so this equation only has solutions for  $m_d^2 < 0$ . A phase transition from the symmetric to the superconducting phase will therefore be of second order. A similar calculation can be done for the antiferromagnet and indicates that for sufficiently small values of the effective chemical potential the phase transition from the symmetric state is also of second order. However, for large enough  $\tilde{\mu}$  we may well encounter discontinuous phase transitions.

### 3.2.1 Numerical results

We have analysed the phase diagram for different Yukawa couplings numerically. We choose  $U/t = 1$ . It is not clear, however, how the “couplings”  $\alpha_i$  (and thus  $h_i$ ) have to be chosen for a given value of the four fermion coupling  $U$  since all choices respecting (2.41) lead to the same Hubbard model. (Therefore the results may also be interpreted as if the hopping parameter  $t$  is fixed and we perform calculations for different values of the four fermion interaction  $U$ .) Because of our mean field approximation the partition function becomes dependent on the parameters  $\alpha_i$ . The

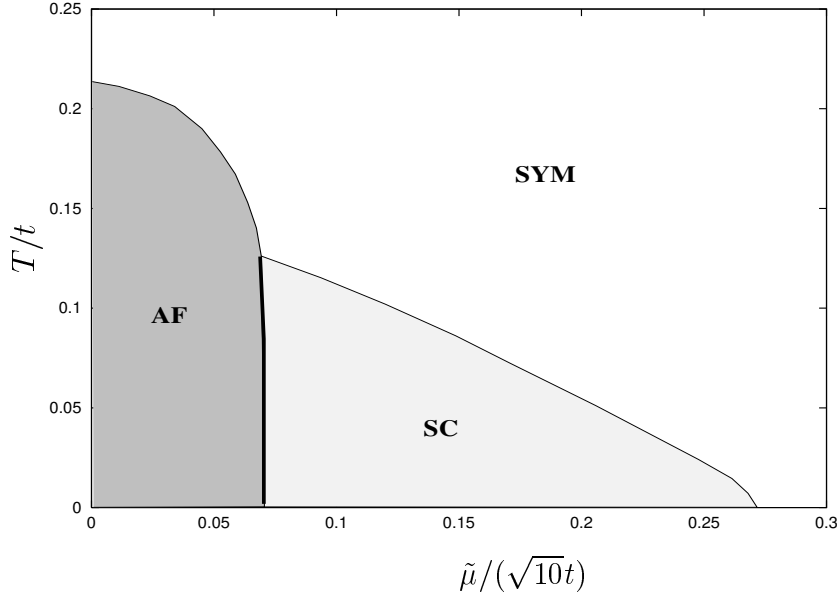


Figure 3.2: The  $T - \tilde{\mu}$  phase diagram for  $h_a = h_d = 10t/\pi^2$  with symmetric (SYM), antiferromagnetic (AF) and superconducting phase (SC). In the region marked by the bold line the phase transition into the antiferromagnetic phase is of first order; all other phase transitions are of second order.

phase diagrams for different choices of the couplings are presented in the figures (3.2) to (3.5); the values chosen are displayed in the respective figure captions. The phases with antiferromagnetic (AF) and superconducting (SC) order are indicated by different fill-patterns. In the symmetric phase (SYM) both operators have a vanishing expectation value. If two regions are separated by a bold line the phase transition between the two is of first order; all other phase transitions are of second order.

The minima were found for fixed temperature and chemical potential by sliding along the gradient of  $U_{\text{pot}}$  into some valley in the phase space spanned by  $\vec{a}^2$  and  $d^*d$ . In order to ensure that the minimum found is not just a local one we have started the minimisation procedure at different values in the phase space. This was necessary for finding the first order transitions where the minimum jumps away from the value obtained at higher temperature.

For equal values of the couplings  $h_a$  and  $h_d$  the phase diagrams (figures 3.2 and 3.3) resemble the ones for a real-life high  $T_c$  superconductor (figure 1.1). However, by increasing one of the couplings  $h_a$  or  $h_d$  the respective boson can be made to dominate the phase diagram, suppressing the regions where the other boson gains a nonvanishing expectation value (figures 3.4 and 3.5). Several features are worth mentioning. Note that there is no region of coexistence of different phases. If one bo-

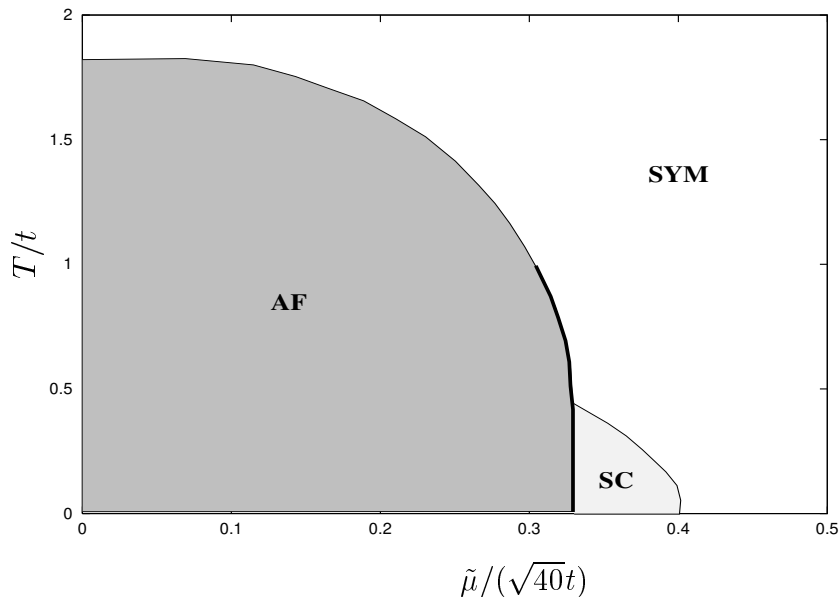


Figure 3.3: The  $T - \tilde{\mu}$  phase diagram for  $h_a = h_d = 40t/\pi^2$  with symmetric (SYM), antiferromagnetic (AF) and superconducting phase (SC). In the region marked by the bold line the phase transition into the antiferromagnetic phase is of first order; all other phase transitions are of second order.

son obtains a nonzero expectation value it tries to prevent the other from obtaining one. Therefore the phase transition between the superconducting and antiferromagnetic region is always of first order. Furthermore, the phase transition between the symmetric phase and the superconducting one is always of second order as already anticipated in the analytic investigation. Similarly there may be a first order phase transition between the symmetric and the antiferromagnetic state for large enough values of the chemical potential. This is also apparent if we plot the value of  $\vec{a}^2$  at the minimum of the potential (figure 3.6), where the discontinuous jump can be seen explicitly.

In conclusion, the mean field approximation for the coloured Hubbard model can give a qualitatively reasonable picture of the phases in high  $T_c$  superconductors. On the other hand, the shortcomings of this approximation are also apparent from the figures. All phase diagrams correspond to different mean field approximations for the same model. It is impossible to resolve this ambiguity within the mean field approximation without additional input on the selection of the Yukawa couplings. The reason is that we have neglected the fluctuations of the bosonic fields. Only if these are included, the different equivalent choices of the Yukawa couplings should lead to the same physical results. The differences between the figures reveal the importance of the neglected bosonic fluctuations.

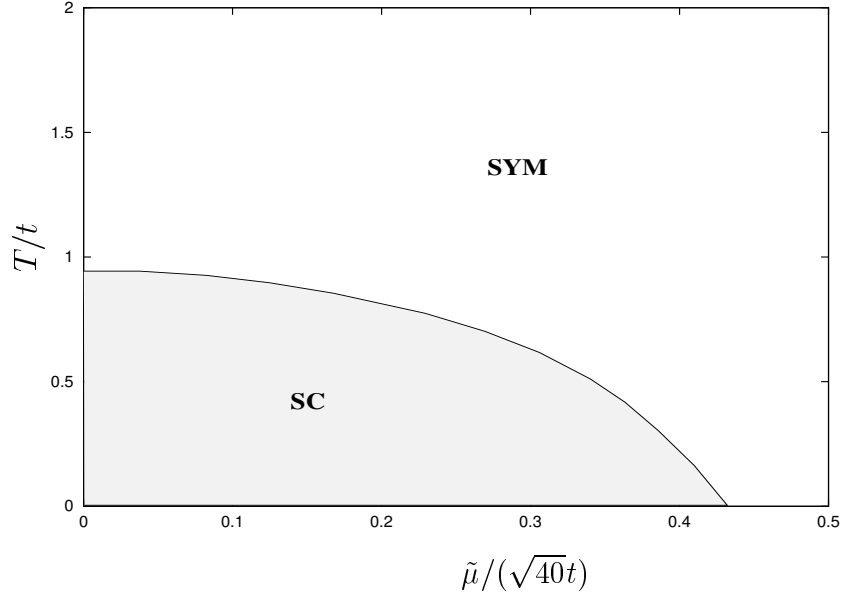


Figure 3.4: The  $T - \tilde{\mu}$  phase diagram for  $h_a = 10t/\pi^2$ ,  $h_d = 40t/\pi^2$  with symmetric (SYM) and superconducting phase (SC). The phase transition is of second order.

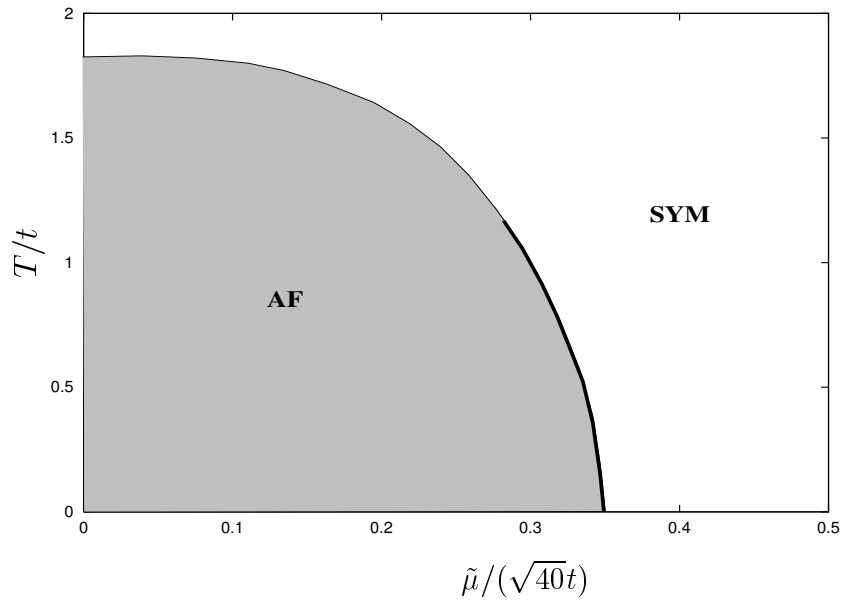


Figure 3.5: The  $T - \tilde{\mu}$  phase diagram for  $h_d = 10t/\pi^2$ ,  $h_a = 40t/\pi^2$  with symmetric (SYM) and antiferromagnetic phase (AF). In the region marked by the bold line the phase transition into the antiferromagnetic phase is of first order, otherwise of second order.

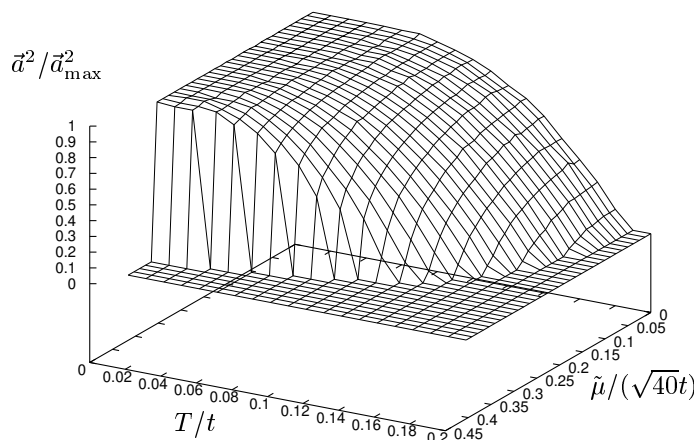


Figure 3.6: The  $T - \tilde{\mu}$  phase diagram for  $h_d = 10t/\pi^2$ ,  $h_a = 40t/\pi^2$ . For large values of the chemical potential the expectation value jumps discontinuously to a non vanishing value when the temperature is lowered.

The inclusion of the bosonic fluctuations is a complex problem which can be attacked by means of nonperturbative renormalisation group equations [11, 43]. Studies for similar QCD-motivated models of fermions with Yukawa coupling to scalars have already been carried out successfully [10, 27]. In the next chapters we will therefore develop renormalisation group equations and apply them in the context of the Hubbard model.

### 3.3 Comparison with Hartree–Fock equations

In the introduction to this chapter we have considered another mean field approach: the Hartree–Fock mean field. It is illuminating to compare the results obtained in the bosonised picture above to this approach which will turn out to be independent of the parametrisation of the interaction term.

Let us first derive the Hartree–Fock equations more formally as the one loop order of a Schwinger–Dyson series. Schwinger–Dyson equations are a simple consequence of the translation invariance of the functional integral<sup>5</sup>

$$\begin{aligned}
 0 &= \int \mathcal{D}\psi \frac{\delta}{\delta\psi_{A'}} \exp(-S[\psi, \psi^*] + \eta^* \psi + \eta \psi^*) \\
 &= \left\{ -\frac{\delta S}{\delta\psi_{A'}} \left[ \psi \rightarrow \frac{\delta}{\delta\eta^*}, \psi^* \rightarrow \frac{\delta}{\delta\eta} \right] - \eta_{A'}^* \right\} Z[\eta, \eta^*].
 \end{aligned} \tag{3.19}$$

<sup>5</sup>This is why the translational invariance was used as defining property of the Grassmann integration in chapter 2.



This is an infinite set of relations between Green functions of different order. For example by a further differentiation with respect to  $\eta_{B'}^*$  we can relate the two point function and the four point function. If we again take an action of the form (3.1), use  $Z = \exp W$  and  $W_{AB}^{(2)} = \frac{\delta^2 W}{\delta \eta_B \delta \eta_A^*}$  etc. and perform the derivatives at vanishing sources  $\eta, \eta^*$  we arrive at

$$\delta_{A'B'} = -P_{AA'} W_{B'A}^{(2)} - f_{ABCA'} \{W_{B'C}^{(2)} W_{BA}^{(2)} - W_{B'A}^{(2)} W_{BC}^{(2)} + W_{B'CB A}^{(4)}\}, \quad (3.20)$$

where we have assumed that  $\frac{\delta^2 W}{\delta \eta \delta \eta}$  etc. vanishes. If we turn towards one particle irreducible (1PI) Green functions (see section 2.4), we finally obtain

$$\begin{aligned} \Gamma_{A'B'}^{(2)} = & P_{A'B'} - (f_{ABA'B'} - f_{A'BAB'}) (\Gamma_{BA}^{(2)})^{-1} \\ & - f_{ABC B'} (\Gamma_{CC''}^{(2)})^{-1} (\Gamma_{BB''}^{(2)})^{-1} (\Gamma_{AA''}^{(2)})^{-1} \Gamma_{A'C'' B'' A''}^{(4)}. \end{aligned} \quad (3.21)$$

These equations have the graphical representation

$$\left( \text{double line} \right)^{-1} = \left( \text{single line} \right)^{-1} + \text{circle with dot} + \text{circle with shaded blob} \quad (3.22)$$

where the double line and shaded blob represent the full propagator and the full vertex respectively. Furthermore we have abbreviated

$$\text{circle with dot} = \text{circle} + \text{dashed arc} \quad (3.23)$$

with  $f_{abcd} = \begin{array}{c} a \\ \diagdown \\ \text{---} \\ \diagup \\ b \end{array} \text{---} \text{---} \begin{array}{c} c \\ \diagup \\ \text{---} \\ \diagdown \\ d \end{array}$  for the “classical” vertex. Sometimes the first term is

called the Hartree term and the second one the Fock term. If we only consider these two terms and neglect the last term of (3.21), which is of two loop order we have rederived the Hartree–Fock equation displayed at the beginning of the chapter. The correction to the propagator  $\Sigma_{AB} = \Gamma_{AB}^{(2)} - P_{AB}$  is often called the *self energy* which we split up in the Hartree and Fock contributions  $\Sigma = \Sigma^H + \Sigma^F$ .

Similar equations can of course be derived for other  $n$ -point functions in the same way. Note that the perturbation series for the  $n$ -point functions can be obtained from these equations by iteratively inserting the right hand side on the left. Indeed the one loop part of (3.21) can also be found in equation (B.32) of appendix B.5, where we deal with one loop corrections to the effective action.

Let us now apply the Hartree–Fock equations to the Hubbard model. We will assume that the fermionic two point function obtains an antiferromagnetic gap

$$\begin{aligned} \Gamma^{(2)}(Q, Q') &= P(Q, Q') + \Sigma(Q, Q') \\ &= (i\omega_Q + \epsilon_Q - \mu) \delta(Q - Q') - \vec{A} \vec{\sigma} \delta(Q - Q' + \boldsymbol{\pi}). \end{aligned} \quad (3.24)$$

This may be inverted and for  $\epsilon_Q = -\epsilon_{Q+\pi}$  one obtains

$$\begin{aligned} (\Gamma^{(2)})^{-1}(Q, Q') &= \mathcal{N}^{-1}(Q)[(-i\omega_Q + \epsilon_Q + \mu)\delta(Q - Q') - \vec{A}\vec{\sigma}\delta(Q - Q' + \boldsymbol{\pi})], \\ \mathcal{N}(Q) &= (\omega_n + i\mu)^2 + \epsilon_Q^2 + \vec{A}^2. \end{aligned} \quad (3.25)$$

We now have to solve the *gap equation*  $\Sigma \stackrel{!}{=} \text{---}\textcircled{\text{---}}\text{---}$  in a self consistent way. As we have seen, the fermionic interaction can be written in different ways, e.g.:

$$\begin{aligned} \frac{U}{2} f_{ABCD} \psi_A^* \psi_B \psi_C^* \psi_D &= \frac{U}{2} \int d\tau \sum_i (\psi_i^* \psi_i)^2 \\ &= -\frac{U}{6} \int d\tau \sum_i (\psi_i^* \vec{\sigma} \psi_i)^2. \end{aligned} \quad (3.26)$$

The Hartree–Fock equations yield the same result independent of the choice of parametrisation of the coupling term as they contain all one loop diagrams. However, in order to get as close to the bosonised description as possible we choose to evaluate the gap equation with the second parametrisation. For the Hartree and Fock terms we find<sup>6</sup>

$$\Sigma_{AB}^H = 2\Sigma_{AB}^F = -2\frac{U}{3} \vec{A}\vec{\sigma}_{AB} \delta(Q_A - Q_B + \boldsymbol{\pi}) \sum_Q \mathcal{N}^{-1}(Q). \quad (3.27)$$

If we set  $\mathcal{M}(Q) = \omega_Q^2 - \mu^2 + \epsilon_Q^2 + \vec{A}^2$  we obtain

$$\begin{aligned} \sum_Q \mathcal{N}^{-1}(Q) &= \sum_Q \frac{\mathcal{M}(Q)}{\mathcal{M}^2(Q) + 4\omega_Q^2 \mu^2} = \frac{1}{2} \partial_{\vec{A}^2} \sum_Q \ln[\mathcal{M}^2(Q) + 4\omega_Q^2 \mu^2] \\ &= \frac{1}{2} \partial_{\vec{A}^2} \sum_Q \ln[(\omega_Q^2 + \epsilon_Q^2 + \mu^2 + \vec{A}^2)^2 - 4(\epsilon_Q^2 + \vec{A}^2)\mu^2]. \end{aligned} \quad (3.28)$$

But we have already evaluated this! It is nothing but the integral in the mean field calculation of  $\Delta U_{\text{pot}}$  familiar from equation (3.13). We thus have

$$\Sigma_{AB}^H = 2\Sigma_{AB}^F = -2\frac{U}{3} \vec{A}\vec{\sigma}_{AB} \delta(Q_A - Q_B + \boldsymbol{\pi}) \partial_{\vec{A}^2} (-\Delta U|_{h_a^2 \vec{a}^2 = \vec{A}^2, d^* d=0}). \quad (3.29)$$

The gap equation thus reads for  $h_a = \alpha_m = U/3$  (in the bosonic language this corresponds to bosonising only with respect to  $\vec{m}$ )

$$1 \stackrel{!}{=} -(1 + \frac{1}{2}) \times 2h_a \partial_{\vec{A}^2} (\Delta U|_{h_a^2 \vec{a}^2 = \vec{A}^2, d^* d=0}) = -(1 + \frac{1}{2}) \times h_a^{-1} [2\partial_{\vec{a}^2} (\Delta U|_{d^* d=0})]. \quad (3.30)$$

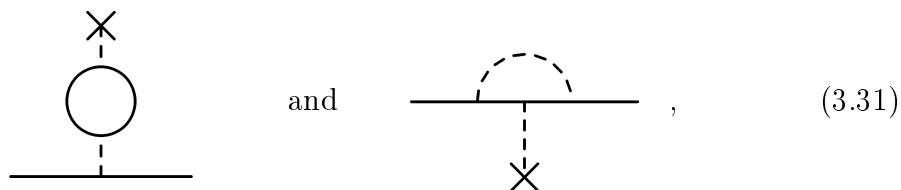
If we compare this with equation (3.18), we find that apart from a factor  $(1 + \frac{1}{2})$  the gap equation is nothing but the condition for the vanishing of the mass  $m_a^2$  (i.e. the onset of spontaneous symmetry breaking) in the mean field calculation for

---

<sup>6</sup>If we had used the first parametrisation, only the Fock term would have contributed and would have been the sum of the two terms in (3.27).

the bosonised Hubbard model. This means that in the Hartree–Fock approach the  $SU(2)$  symmetry is broken at higher values of the temperature compared to what we have seen in the last section.

Let us try to understand where the additional factor of  $\frac{3}{2}$  comes from. If we expand the full propagator to first order in  $\vec{A}$  the interesting part of the Hartree and Fock terms can be visualised as


(3.31)

where the cross denotes the condensate. The calculation of the Hartree Fock results above can be directly translated to the bosonised language for  $\alpha_\rho = \alpha_c = 0$ . Here the dotted lines in the diagrams stand for propagation of bosons and we have a Yukawa coupling at the vertices. We will later see that in this language the fermionic loop (left diagram of (3.31)) exactly corresponds to a change in the bosonic mass, while the right diagram corresponds to a change in the Yukawa coupling. Thus we conclude that in the bosonised theory the mean field results have to be augmented by a corresponding change in the Yukawa couplings in order to obtain parametrisation invariant results. We will later include such a shift of the couplings by using renormalisation group equations where both the bosonic potential and the Yukawa couplings become scale dependent<sup>7</sup>.

A similar calculation of the Hartree and Fock terms above can also be performed for an energy gap with  $d$ -wave symmetry in the particle–particle (or hole–hole) channel, corresponding to superconductivity (equation (2.51)). However, here the “bosonic mean field” results are not reproduced as the momentum integrals vanish.

---

<sup>7</sup>From the results of this section one would expect that the Yukawa coupling should grow during the flow thus leading to larger critical temperatures than found in the simple mean field calculation. The fact that the critical temperatures are actually lowered is due to the fact that the right diagram in (3.31) is not the only contribution to the flow of  $h_a$  that we consider.

# Chapter 4

## Exact renormalisation group equations

In this chapter we will consider the explicit construction of a renormalisation group equation for the (average) effective action [11, 43]. For a review on similar equations and a historical overview see [3].

### 4.1 The average effective action

Let us consider a theory containing a complex bosonic field  $\hat{u}$ ,  $\hat{u}^*$ , a real bosonic field  $\hat{w}$  and a fermionic field  $\hat{\psi}$ ,  $\hat{\psi}^*$ . We collect the fields into generalised fields and define generalised sources for them<sup>1</sup>

$$\begin{aligned}\hat{\chi}_\alpha &= (\hat{u}, \hat{u}^*, \hat{w}, \hat{\psi}, \hat{\psi}^*)_\alpha, \\ J_\alpha &= (j^*, j, l, \eta^*, \eta)_\alpha, \\ S_J[\hat{\chi}] &= -J_\alpha \hat{\chi}_\alpha = -(j^* \hat{u} + j \hat{u}^* + l \hat{w} + \eta^* \hat{\psi} + \eta \hat{\psi}^*).\end{aligned}\tag{4.1}$$

Now we regularise the theory by adding an infrared cutoff

$$\begin{aligned}\Delta S_k[\hat{\chi}] &= \frac{1}{2} \hat{\chi}_\alpha R_{k,\alpha\beta} \hat{\chi}_\beta \\ &= \hat{u}^* R_k^u \hat{u} + \frac{1}{2} \hat{w}^* R_k^w \hat{w} + \hat{\psi}^* R_k^\psi \hat{\psi},\end{aligned}\tag{4.2}$$

$$R_k = \begin{pmatrix} R_k^u & (R_k^u)^T & & \\ & & R_k^w & \\ & & & -(R_k^\psi)^T \\ & & R_k^\psi & \end{pmatrix}\tag{4.3}$$

---

<sup>1</sup>The indices  $\alpha$  run over field type, momentum, internal indices etc.

to the original action  $S[\hat{\chi}]$  and define the  $k$ -dependent functional of the connected Green functions of the regularised theory as

$$W_k[J] = \ln \int \mathcal{D}\hat{\chi} \exp ( - (S[\hat{\chi}] + \Delta S_k[\hat{\chi}]) + J\hat{\chi} ). \quad (4.4)$$

The function  $R_k^\psi$  is to regularise the zero modes of the propagator, i.e. add a mass to the fermions close to the Fermi surface. For momenta far from the Fermi surface (compared to  $k$ )  $R_k^\psi$  is to vanish rapidly so that the behaviour of these modes is essentially unaltered. A similar task is assigned to the bosonic cutoff functions. In the limit  $k \rightarrow 0$  we demand that the regulators vanish so that one recovers the original theory. For  $k \rightarrow \Lambda$ , where  $\Lambda$  is the scale the original theory is defined on, we assume them to diverge

$$\lim_{k \rightarrow 0} R_k^\chi = 0, \quad \lim_{k \rightarrow \Lambda} R_k^\chi = \infty. \quad (4.5)$$

We may now proceed to define an effective action in analogy to the definition (2.59). By a Legendre transform with respect to the classical fields

$$\chi = \langle \hat{\chi} \rangle = \frac{\delta}{\delta J} W_k[J], \quad (4.6)$$

we obtain the functional

$$\tilde{\Gamma}_k[\chi] = J\chi - W_k[J], \quad (4.7)$$

where  $J = J[\chi]$  is a solution of the equation (4.6). As will become clear in a moment it is favourable to subtract the cutoff action from this functional and define the *average effective action* as

$$\boxed{\Gamma_k[\chi] = J\chi - W_k[J] - \Delta S_k[\chi]} \quad (4.8)$$

and establish the relations

$$\begin{aligned} \frac{\delta}{\delta \chi_\alpha} \tilde{\Gamma}[\chi] &= -\frac{\delta J_j}{\delta \chi_\alpha} \frac{\delta W}{\delta J_\beta} + \frac{\delta J_j}{\delta \chi_\alpha} \chi_\beta + M_{\alpha\beta} J_\beta = M_{\alpha\beta} J_\beta, \\ \frac{\delta}{\delta \chi_\alpha} \Gamma[\chi] &= M_{\alpha\beta} J_\beta - R_{k,\alpha\beta} \chi_\beta = (JM)_\alpha - (\chi R_k M)_\alpha, \\ M &= \text{diag}(1, 1, 1, -1, -1). \end{aligned} \quad (4.9)$$

As in (2.61) we may give an equivalent implicit definition of the average effective action:

$$\exp(-\Gamma_k[\chi]) = \int \mathcal{D}\hat{\chi} \exp ( - (S[\hat{\chi} + \chi] + \Delta S_k[\hat{\chi}]) + \frac{\delta \Gamma_k}{\delta \chi} M \hat{\chi} ), \quad (4.10)$$

where we have used the fact  $\Delta S_k$  is quadratic in the fields. We also note the identity (see (2.62))

$$\tilde{\Gamma}_{k,\alpha\beta}^{(2)} W_{k,\beta\gamma}^{(2)} = M_{\alpha\gamma}. \quad (4.11)$$

The average effective action is the effective action of a theory containing an extra “mass” term described by the action  $S[\hat{\chi}] + \Delta S_k[\hat{\chi}]$ . Since the effective action respects all (linearly realised) symmetries of the original action [42], this also applies to  $\Gamma_k[\chi]$  for all  $k$ , if the regulator  $\Delta S_k[\hat{\chi}]$  respects the symmetries. It is thus possible to expand the average effective action in invariants with respect to these symmetries.

The limits (4.5) lead to corresponding limits for the average effective action

$$\lim_{k \rightarrow 0} \Gamma_k[\chi] = \Gamma[\chi], \quad \lim_{k \rightarrow \Lambda} \Gamma_k[\chi] = S[\chi]. \quad (4.12)$$

This is why we chose to subtract the regulator in the definition of  $\Gamma_k[\chi]$ : for large “cutoff”  $k$  this functional is nothing but the original action. If we can somehow smoothly interpolate between a large and a small cutoff we are also able to calculate the effective action by starting with the original action. This is what the “flow equation” described in the next section is all about. The first limit in (4.12) is apparent from the definition (4.8), while the second follows more easily from (4.10) by noting that  $\lim_{R_k \rightarrow \infty} \exp(-\frac{1}{2}\hat{\chi}R_k\hat{\chi})$  essentially acts like a delta functional  $\delta[\hat{\chi}]$  under the integral.

## 4.2 A flow equation

In this section we will derive a differential equation for the cutoff dependence of the average effective action.

We specify the second functional derivative in symmetric form containing both left and right derivatives<sup>2</sup>

$$F[\chi_0 + \chi] = F[\chi_0] + \chi_\alpha F_\alpha^{(1)}[\chi_0] + \frac{1}{2}\chi_\alpha F_{\alpha\beta}^{(2)}[\chi_0]\chi_\beta + \dots \quad (4.13)$$

---

<sup>2</sup>When using only left derivatives  $F[\chi_0 + \chi] = \dots + \frac{1}{2}\chi_\beta\chi_\alpha\hat{F}_{\alpha\beta}^{(2)}[\chi_0] + \dots$ , it is preferable to reparametrise  $\Delta S_k[\hat{\chi}] = \frac{1}{2}\hat{\chi}_\beta\hat{\chi}_\alpha\hat{R}_{k,\alpha\beta} = \hat{u}^*R_k^u\hat{u} + \frac{1}{2}\hat{w}^*R_k^w\hat{w} + \hat{\psi}^*R_k^\psi\hat{\psi}$ . The derivation of the flow equation is essentially identical to the one presented but with  $R_k \rightarrow \hat{R}_k$  and  $F^{(2)} \rightarrow \hat{F}^{(2)}$ . Written out in components this of course leads to the same equation.

For the  $k$ -derivative of  $\tilde{\Gamma}_k$  one now obtains:

$$\begin{aligned}
\partial_k \tilde{\Gamma}_k[\chi]|_\chi &= -\partial_k W_k[J]|_J - \partial_k J \cdot \frac{\delta W_k}{\delta J}|_k + \partial_k J \cdot \chi \\
&= -\partial_k W_k[J]|_J = \langle \partial_k \Delta S_k \rangle = \frac{1}{2} \partial_k R_{k,\alpha\beta} \langle \chi_\alpha \chi_\beta \rangle \\
&= \frac{1}{2} \partial_k R_{k,\alpha\beta} \{ W_{k,\beta\alpha}^{(2)} + \langle \chi_\alpha \rangle \langle \chi_\beta \rangle \} \\
&= \frac{1}{2} \partial_k R_{k,\alpha\beta} W_{k,\beta\alpha}^{(2)} + \Delta S_k[\chi],
\end{aligned} \tag{4.14}$$

where we used the fact that  $W_k[J]$  is the generating functional of connected Green functions, i.e.  $W_{k,\beta\alpha}^{(2)} = \langle \chi_\alpha \chi_\beta \rangle_c = \langle \chi_\alpha \chi_\beta \rangle - \langle \chi_\alpha \rangle \langle \chi_\beta \rangle$ . With the aid of (4.11) we immediately obtain a flow equation for the average effective action

$$\boxed{
\begin{aligned}
\partial_k \Gamma_k[\chi] &= \frac{1}{2} \partial_k R_{k,\alpha\beta} [\Gamma_k^{(2)} + R_k]_{\beta\gamma}^{-1} M_{\gamma\alpha} \\
&= \frac{1}{2} \text{STr} \{ \partial_k R_k [\Gamma_k^{(2)} + R_k]^{-1} \},
\end{aligned}
} \tag{4.15}$$

where the “supertrace” runs over field type, momentum, internal indices etc. (We have collected some properties of the supertrace in appendix B.3.)

This equation is exact – we have only performed formal manipulations. In fact just as exact as the original functional integral definition of the effective action (2.59). However, it is an equation for an infinite number of couplings and hence by no means accessible to an exact solution. The usefulness of (4.15) will only show up if we are able to make sensible approximations to the flow equation. We will come back to this later.

Let us first rewrite the flow equation in a very useful way making contact to perturbation theory. Define the derivative (the index  $i$  counts the field types)

$$\tilde{\partial}_k = (\partial_k R_k^i) \frac{\partial}{\partial R_k^i}. \tag{4.16}$$

With the aid of this derivative the flow equation can be cast in the form

$$\partial_k \Gamma_k[\chi] = \frac{1}{2} \text{STr} \{ \tilde{\partial}_k \ln[\Gamma_k^{(2)} + R_k] \}. \tag{4.17}$$

This has to be compared with the perturbative one loop result

$$\Gamma_k[\chi] = S[\chi] + \frac{1}{2} \text{STr} \ln[S^{(2)} + R_k],$$

where we have regularised the propagators. Performing the  $k$ -derivative of this equation leads to a one loop flow equation. A “renormalisation group improvement”  $S^{(2)} \rightarrow \Gamma_k^{(2)}$  promotes this equation to a non-perturbative exact flow equation. This allows us to identify the right hand side of (4.17) as a sum of one loop diagrams,

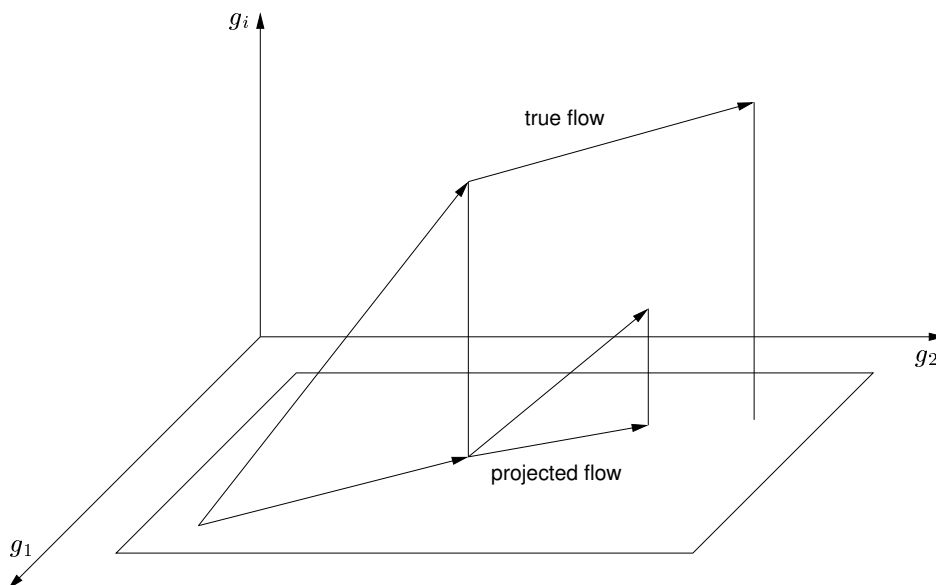


Figure 4.1: The “true” flow through the parameter space will in general not be identical to the truncated one.

where all couplings have been replaced by their renormalised counterparts and momentum integrations, sums over internal indices etc. are performed after the  $\tilde{\partial}_k$  derivative.

Obtaining the flow equation for some coupling thus amounts to summing all one loop diagrams for this coupling, evaluating the  $\tilde{\partial}_k$  derivative and then calculating the trace. However, we may be able to perform parts of the trace first if the cutoff does not depend on it. For example we will later be able to first sum over Matsubara indices before performing the  $\tilde{\partial}_k$  derivative.

The flow equation (4.15) is a complex differential equation for functionals. Let us try to tackle it by expanding the effective action in powers of the fields

$$\Gamma_k[\chi] = \sum_{n=0}^{\infty} \sum_{\alpha_i} \chi_{\alpha_1} \cdots \chi_{\alpha_n} \Gamma_k^{(n)}(\alpha_1, \dots, \alpha_n). \quad (4.18)$$

The flow equations of the  $n$ -point functions  $\Gamma_k^{(n)}$  can easily be derived from (4.15) by appropriate functional derivatives. However, the flow of some  $n$ -point function will in general contain higher  $n$ -point functions. This is a general feature: if we perform a systematic expansion of the effective action, the set of flow equations will not be closed. We have to truncate the expansion at some point.

Let us take a look at this “truncated” flow. The “true” flow through the infinite dimensional parameter space spanned by the couplings  $g$  is defined by the flow



equation (4.15). This leads to a trajectory  $g(k)$ , where  $k$  is the cutoff parameter, winding through this space. If one considers a truncated theory one is confined to an  $m$ -dimensional submanifold of this parameter space. In general the true flow will leave this submanifold. In order to obtain the truncated flow  $\tilde{g}(k)$  one has to project the true flow on to the submanifold after each renormalisation step:  $g(k + dk) \xrightarrow{P} \tilde{g}(k + dk)$ . This is shown schematically in figure 4.1 for two iterations. Observe that in general it is not true that  $g(k') \xrightarrow{P} \tilde{g}(k')$ , because one has to project after each renormalisation group step.

In general one would expect a better agreement between the truncated and the true flow the more couplings  $g$  are considered. It turns out, however, that often the chosen “coordinate system” plays an equally important role. For example, in a system with spontaneous symmetry breaking an expansion around the ( $k$ -dependent) vacuum expectation value leads to far better results than a simple expansion in powers of fields [2].

Note that in the flow equation (4.15) the regulator function  $R_k$  appears in the “numerator” as an infrared regulator as well as in the “denominator”. For an appropriate choice of  $R_k$  this means that effectively only a small interval of momenta contributes to the integrals. In addition our regularisation scheme is thus also able to deal with possible ultraviolet divergencies.

### 4.3 A standard example: the effective potential in $O(N)$ theories

In this section we want to calculate the flow equation for the effective potential in a model with  $O(N)$ -symmetry

$$\Gamma_k[\phi] = \frac{1}{2} \sum_Q Z_\phi \phi_i(-Q) P_{ij}(Q) \phi_j(Q) + \sum_X U(\rho(X)), \quad \rho(X) = \frac{1}{2} \phi_i(X) \phi_i(X) \quad (4.19)$$

where the initial conditions could be standard  $\phi^4$  theory, i.e.  $P(Q) = Q^2$ ,  $Z_\phi = 1$  and  $U(\rho(X)) = \frac{\lambda}{4!} \phi^4(X)$ . The potential  $U(\rho)$  is defined as the part of the effective action for homogeneous values of the fields. The flow for the potential can thus be derived by evaluating the flow equation (4.15) for a constant value of the field  $\phi$ . The matrix of second functional derivatives

$$\Gamma_{ij}^{(2)}(Q) = Z_\phi P(Q) \delta_{ij} + \delta_{ij} U'(\rho) + \phi_i \phi_j U''(\rho) \quad (4.20)$$

has the eigenvalues  $Z_\phi P(Q) + \hat{M}_i^2$  with

$$\hat{M}_i^2 = \begin{cases} U'(\rho) + 2\rho U''(\rho) & \text{for } i = 1 \\ U'(\rho) & \text{for } i = 2 \dots N. \end{cases} \quad (4.21)$$

The flow equation for the effective potential thus reads

$$\begin{aligned} \partial_k U(\rho) &= \frac{1}{2} \sum_{Q,i} \tilde{\partial}_k \ln[Z_\phi P(Q) + \hat{M}_i^2 + R_k(Q)] \\ &= \frac{1}{2} \sum_Q \partial_k R_k(Q) \left\{ \frac{1}{Z_\phi P(Q) + U'(\rho) + 2\rho U''(\rho) + R_k(Q)} + \frac{N-1}{Z_\phi P(Q) + U'(\rho) + R_k(Q)} \right\} \end{aligned} \quad (4.22)$$

or in terms of rescaled and renormalised quantities

$$\tilde{\rho} = Z_\phi k^{2-d} \rho, \quad u(\tilde{\rho}) = k^{-d} U(\rho), \quad t = \ln k, \quad \eta = -\partial_t \ln Z_\phi, \quad (4.23)$$

$$\begin{aligned} \partial_t u(\tilde{\rho}) &= -du(\tilde{\rho}) + k^{-d} \partial_t U(\rho)|_{\tilde{\rho}} \\ &= -du(\tilde{\rho}) + (\eta + d - 2) \tilde{\rho} u'(\tilde{\rho}) + k^{-d} \partial_t U(\rho)|_{\rho}, \end{aligned} \quad (4.24)$$

where we have used the fact that after a change of variables from  $f(x, y)$  to  $f(x, g(x, y))$  the derivatives read  $\frac{\partial f}{\partial x}|_y = \frac{\partial f}{\partial x}|_g + \frac{\partial f}{\partial g}|_x \frac{\partial g}{\partial x}|_y$ .

In equation (4.22) one can clearly see the appearance of the massless Goldstone modes, when the symmetry is spontaneously broken as  $U'(\rho)$  vanishes at the minimum of the potential. The  $O(N)$  symmetry with  $\frac{N(N-1)}{2}$  independent symmetry transformations is broken down to  $O(N-1)$  with  $\frac{(N-1)(N-2)}{2}$  transformations. The number of broken symmetries is just the difference:  $N-1$ . This exactly corresponds to the number of massless modes in (4.22) in accord with Goldstones theorem.

We will later need these equations for the running of the bosonic potential in our description of the Hubbard model.

# Chapter 5

## Loop calculations

As we have seen in the previous chapter, the renormalisation group equation for the effective action has essentially the form of a one loop equation. As a preparation for a renormalisation group study we will therefore take a look at some one loop calculations in this chapter. Our interest in them is twofold: first, a one loop calculation will reproduce the results of a renormalisation group study for large values of the cutoff. We will therefore let us guide by one loop calculations in order to obtain useful truncations. Second, we know that we can obtain the flow equation for some particular coupling from the one loop result by applying the  $\tilde{\partial}_k$  operator to it.

In this chapter we will consider the loop corrections to the bosonic propagator in order to find a suitable truncation and later briefly touch on the loop corrections to four fermion couplings in the bosonised theory as one might hope to obtain some constraint for the choice of parameters  $\alpha_i$  in the bosonisation procedure. More extensive one loop calculations for the Yukawa couplings etc. are listed in appendix B.5.

### 5.1 The bosonic propagator to one loop order

Starting from the action (2.42) (together with (2.50)), we want to calculate the one loop corrections to the bosonic propagators. Due to  $U(1)$  invariance we know that there will be no terms mixing real bosons (corresponding to particle–hole pairs) and complex bosons (corresponding to particle–particle and hole–hole pairs). Similarly, no mixing between the spin triplet and spin singlet bosons occurs because of  $SU(2)$

invariance. The contributing diagrams are

$$(5.1)$$

where the solid lines denote fermions and the dashed bosons. We have collectively called the real bosons  $w$  and the complex bosons  $u$ .

Note that calculating these diagrams is nothing else but calculating the fermionic determinant for fixed external bosonic fields just as we did in the mean field calculation and then expand the determinant in numbers of bosonic fields. However, this time we will allow arbitrary external momenta.

Let us parametrise the action (2.42), (2.50) in the form ( $\chi = (u, u^*, w, \psi, \psi^*)$ )

$$\begin{aligned}
S[\chi] = & \sum_Q \left\{ \psi_\alpha^*(Q) P_{\alpha\beta}^\psi(Q) \psi_\beta(Q) + \frac{1}{2} w_\alpha(Q) P_{\alpha\beta}^w(Q) w_\beta(Q) + u_\alpha^*(Q) P_{\alpha\beta}^u(Q) u_\beta(Q) \right\} \\
& - \sum_{Q'K} \left\{ w_\gamma(K) \psi_\alpha^*(Q) V_{\alpha\beta,\gamma}^w(Q, Q') \psi_\beta(Q') \delta(K - Q + Q') \right. \\
& \quad \left. + (u_\gamma^*(K) \psi_\alpha(Q) V_{\alpha\beta,\gamma}^{u*}(Q, Q') \psi_\beta(Q') + u_\gamma(K) \psi_\alpha^*(Q) V_{\alpha\beta,\gamma}^u(Q, Q') \psi_\beta^*(Q')) \right. \\
& \quad \left. \delta(K - Q - Q') \right\}
\end{aligned} \tag{5.2}$$

with

$$\begin{aligned}
V^\rho(Q, Q') &= h_\rho(Q - Q') \otimes \mathbb{1}_{\text{spin}}, & h_\rho(K) &= \alpha_\rho - \alpha_c(\cos k_x + \cos k_y), \\
V^m(Q, Q') &= h_m(Q - Q') \otimes \vec{\sigma}_{\text{spin}}, & h_m(K) &= \alpha_m + \alpha_c(\cos k_x + \cos k_y),
\end{aligned} \tag{5.3}$$

$$V^{s*}(Q, Q') = h_s \otimes \epsilon_{\text{spin}}, \quad h_s = \alpha_s, \tag{5.4}$$

$$V^{e*,d*}(Q, Q') = h_d \left( \cos \frac{q_x - q'_x}{2} \pm \cos \frac{q_y - q'_y}{2} \right) \otimes \epsilon_{\text{spin}}, \quad h_d = \frac{\alpha_c}{2}$$

and  $V^u(Q, Q') = -V^{u*}(-Q, -Q')$ . The propagators are

$$\begin{aligned}
P^\psi(K) &= i\omega_Q + \epsilon_Q - \mu, & P^\rho(K) &= h_\rho(K), & P^m(K) &= h_m(K), \\
P^s(K) &= h_s, & P^{e,d}(K) &= h_d.
\end{aligned}$$

The fermionic part of the action at fixed bosonic fields can be written as (we suppress the momentum labels – they can be restored in the end of the calculation by momentum conservation)

$$\tilde{S}[\psi, \psi^*] = \frac{1}{2} \sum_{ab} [\psi, \psi^*]_a \underbrace{\begin{pmatrix} -2u_c^* V_{c,c}^{u*} & -(P^\psi - w_c V_{c,c}^w)^T \\ P^\psi - w_c V_{c,c}^w & -2u_c V_{c,c}^u \end{pmatrix}}_{=\tilde{S}^{(2)}}{}_{ab} \begin{bmatrix} \psi \\ \psi^* \end{bmatrix}_b. \tag{5.5}$$

The fermionic one loop correction to the effective action is (c.f. appendix B.5)

$$\Gamma = S + \Delta\Gamma, \quad \Delta\Gamma = -\frac{1}{2}\text{Tr} \ln \tilde{S}^{(2)}. \quad (5.6)$$

Now split  $S^{(2)} = \tilde{P} + \Delta\tilde{P}$  into a part containing only the fermionic propagator and a part containing bosonic fields and expand in the number of bosonic fields

$$\begin{aligned} \Delta\Gamma &= \Delta\Gamma_0 + \Delta\Gamma_1 + \Delta\Gamma_2 + \dots \\ &= -\frac{1}{2}\text{Tr} \ln \tilde{P}(1 + \tilde{P}^{-1}\Delta\tilde{P}) \\ &= -\frac{1}{2}\text{Tr} \ln \tilde{P} - \frac{1}{2}\text{Tr}(\tilde{P}^{-1}\Delta\tilde{P}^{(2)}) + \frac{1}{4}\text{Tr}(\tilde{P}^{-1}\Delta\tilde{P}^{(2)})^2 + \dots \end{aligned} \quad (5.7)$$

The first term is a vacuum graph, the second describes tadpoles and the third yields the loop corrections to the propagators

$$\Delta\Gamma = \text{Diagram} = \text{Diagram} + \text{Diagram} + \text{Diagram} + \dots \quad (5.8)$$

Restoring momenta one obtains for the loop correction of the bosonic propagators

$$\begin{aligned} \Delta\Gamma_2 &= \sum_K \left[ \frac{1}{2}w_i(-K)\Delta\Gamma_{ij}^w(K)w_j(K) + u_i^*(K)\Delta\Gamma_{ij}^u(K)u_j(K) \right], \\ \Delta\Gamma_{ij}^w(K) &= \sum_Q \text{tr}_{\text{spin}} \{ G^\psi(Q)V_i^w(Q, K+Q)G^\psi(K+Q)V_j^w(K+Q, Q) \}, \\ \Delta\Gamma_{ij}^u(K) &= -2 \sum_Q \text{tr}_{\text{spin}} \{ G^\psi(Q)V_j^u(Q, K-Q)G^\psi(K-Q)V_i^{u*}(K-Q, Q) \}, \end{aligned} \quad (5.9)$$

where we have defined  $G^\psi(Q) = [i\omega_Q + \epsilon_Q - \mu]^{-1} = [i\omega_Q + \xi_Q]^{-1}$ . The square of the propagators in (5.9) reads  $(Q = (\omega_n, \mathbf{q}), Q' = (\omega'_n, \mathbf{q}') = K \pm Q)$

$$G^\psi(Q)G^\psi(Q') = \frac{-\omega_n\omega_{n'} + \xi_{\mathbf{q}}\xi_{\mathbf{q}'} + i[\xi_{\mathbf{q}}\omega_{n'} + \xi_{\mathbf{q}'}\omega_n]}{[\omega_n^2 + \xi_{\mathbf{q}}^2][\omega_{n'}^2 + \xi_{\mathbf{q}'}^2]}. \quad (5.10)$$

For  $\omega'_n = \omega_n$ , i.e. vanishing external Matsubara frequency, the imaginary part vanishes due to the Matsubara sum in (5.9). For  $\epsilon_Q = -\epsilon_{Q+\boldsymbol{\pi}}$  and  $\mu = 0$  the imaginary part also vanishes under the momentum integral (the vertex-part is always symmetric under  $Q \rightarrow Q + \boldsymbol{\pi}$ ).

The Matsubara sums in (5.9) can be performed analytically<sup>1</sup>

$$\begin{aligned} S(m; a, b) &= \sum_{n \in \mathbb{Z}} \frac{ab - (2n+1)(2(n+m)+1)}{[a^2 + (2n+1)^2][b^2 + (2(n+m)+1)^2]} \\ &= -\frac{\pi}{2} \frac{(a-b)(\tanh \frac{a\pi}{2} - \tanh \frac{b\pi}{2})}{4m^2 + (a-b)^2}, \end{aligned} \quad (5.11)$$

which has the following limits

$$S(0; a, a) = -\frac{\pi^2}{4} \cosh^{-2} \frac{a\pi}{2}, \quad S(0; a, -a) = -\frac{\pi}{2} \frac{\tanh \frac{a\pi}{2}}{a}. \quad (5.12)$$

We now see that the mass corrections obtained in the mean field approximation (3.18) are of course exactly the same as the bosonic propagator corrections for  $K = (0, \boldsymbol{\pi})$  for the  $\vec{a}$ -boson and  $K = (0, \mathbf{0})$  for the  $d$ -boson. However, here we are able to look at the propagator corrections for different external momenta.

A main reason for calculating the one loop corrections to the bosonic propagators was to get a feeling for the momentum dependence the propagators are likely to obtain under a renormalisation group flow. For example, the boson  $\vec{m}$  has a “classical” (inverse) propagator  $P^m(K) = \alpha_m + \alpha_c(\cos k_x + \cos k_y)$  which is independent of the Matsubara frequency. Furthermore for small or vanishing  $\alpha_c$  the momentum dependence is very weak. In the following we will therefore take a closer look at a numerical evaluation of  $P^m(K) + \Delta\Gamma^m(K)$  for different choices of the external momenta. We will restrict ourselves to  $\epsilon_Q = 2t(\cos q_x + \cos q_y) = -\epsilon_{Q+\boldsymbol{\pi}}$ , i.e. to nearest neighbour hopping of the fermions. Furthermore we choose  $\alpha_m = t$  while the other  $\alpha_i$  vanish; this corresponds to  $U/t = 3$ . The function we are interested in is thus

$$P_{1 \text{ loop}}^m(K = (\omega_m, \mathbf{k})) = h_m(K) + h_m^2(K) \frac{2T}{(\pi T)^2} \int_{-\pi}^{\pi} \frac{d^2q}{(2\pi)^2} S(m, \frac{\epsilon_{\mathbf{q}}}{\pi T}, \frac{\epsilon_{\mathbf{q}+\mathbf{k}}}{\pi T}) \quad (5.13)$$

with  $h_m(K) = \alpha_m$ .

In figure 5.1 we have plotted  $P_{1 \text{ loop}}^m(K)$  for different values of the external momenta at vanishing external Matsubara frequency. The left figure shows the situation well above the critical temperature  $T_c \approx 0.2$ , where the propagator develops a zero mode, while in the right figure the temperature is well below  $T_c$ . Note that the propagator is smallest for  $\mathbf{k} = \boldsymbol{\pi}$ , i.e. the antiferromagnet is the favoured mode of propagation above  $T_c$ . Also notice the development of sharp crests at low temperature (right figure) due to the singularities in the fermionic propagators at the Fermi surface.

Figure 5.2 shows the dependence of  $P_{1 \text{ loop}}^m(K)$  on the external Matsubara frequency  $\omega_m$  for two values of the external momenta. Note that the  $\omega_m = 0$  mode is the one that is changed most. For  $\mathbf{k} = \mathbf{0}$  this is even the only mode that is changed at all, while  $\Delta\Gamma^m$  vanishes in the other cases.

---

<sup>1</sup>This can also be expressed as follows

$$\Re \sum_{n \in \mathbb{Z}} \frac{1}{i\omega_n - \alpha} \frac{1}{i\omega_{n+m} - \beta} = \sum_{n \in \mathbb{Z}} \frac{\alpha\beta - \omega_n\omega_{n+m}}{[\alpha^2 + \omega_n^2][\beta^2 + \omega_{n+m}^2]} = \frac{1}{(\pi T)^2} S(m; \frac{\alpha}{\pi T}, \frac{\beta}{\pi T}) = \frac{[\alpha - \beta][f(\alpha) - f(\beta)]}{(2m\pi T)^2 + (\alpha - \beta)^2},$$

where  $f(x) = \frac{1}{1 + \exp(x)}$  is the Fermi-function.

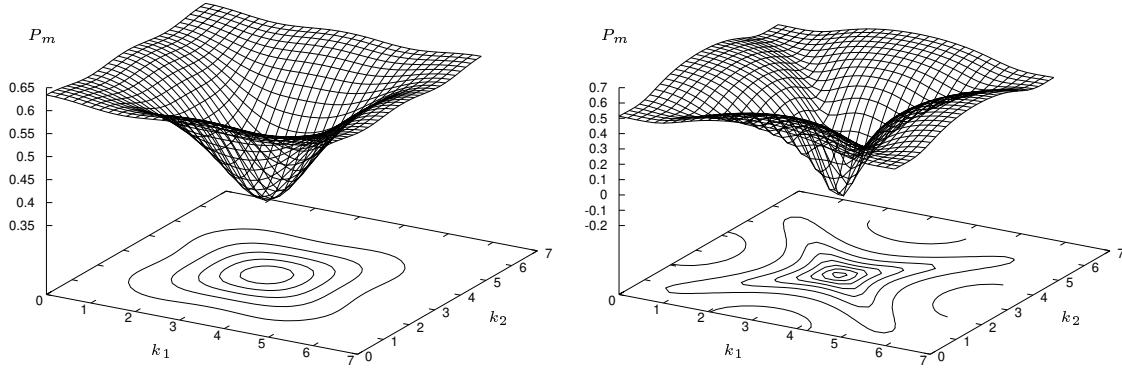


Figure 5.1: The one loop corrected bosonic kinetic term in the effective action for the boson  $\vec{m}$  as a function of the external momenta at  $T = 0.5t$  (left) and  $T = 0.15t$  (right) for  $\omega_m = 0$ ;  $U/t = 3$ .

In the next chapter we will try to make use of the observations of this section in order to formulate suitable truncations for the bosonic propagators. Similar observations can be made for the propagators of the other bosons.

## 5.2 Four fermion terms

Let us take a look at the different one loop graphs that will play an essential role for the flow equations. We again use solid lines for fermions and dashed lines for bosons as in (5.1). However, now we do not put arrows on the lines to indicate the momentum flow. The diagrams can then be interpreted for both real and complex bosons. For the former one fermionic line with ingoing and one with outgoing momentum meet at each vertex, while for the latter two ingoing or two outgoing lines meet. We have collected the algebraic expressions represented by the graphs in appendix B.5. Remember that the renormalisation group equation corresponding to some coupling can be found by applying a derivative with respect to the cutoff function to the one loop result. We will therefore speak of the corrections under the flow by these diagrams in this spirit. The first set of diagrams

(5.14)

are the obvious corrections to the bosonic and fermionic propagators respectively and the vertex corrections. These corrections only change the form of couplings (i.e.

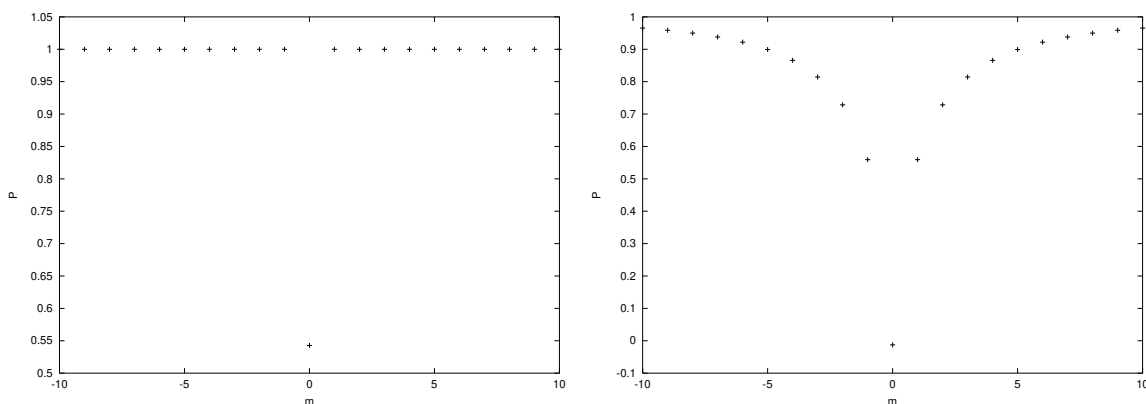


Figure 5.2: The one loop corrected bosonic kinetic term in the effective action for the boson  $\vec{m}$  as a function of the external Matsubara frequency at  $T = 0.2t$  and  $\mathbf{k} = \mathbf{0}$  (left) and  $\mathbf{k} = \boldsymbol{\pi}$  (right);  $U/t = 3$ .

masses, kinetic terms, Yukawa-couplings etc.) already incorporated in the “classical” action (2.42). Nevertheless, there is of course the problem of how the complicated momentum dependence of the corrected couplings can be captured efficiently in a suitable representation.

In a further expansion there will also be diagrams corresponding to a fermionic loop with different numbers of external bosonic fields as in (5.8). We will collect these contributions in an effective potential for the bosonic fields. However, we also have to face purely fermionic diagrams, like

(5.15)

These contributions are certainly unwanted as we tried to get rid of the four fermion terms in the action by a partial bosonisation and would like to deal with a theory of fermions coupled via a Yukawa coupling to bosons that carry the important information about spontaneous symmetry breaking. These four fermion terms are by no means small in comparison with the diagrams generated by the bosonic parts of the action<sup>2</sup>

(5.16)

and will therefore supposedly play an important role in the flow equations.

<sup>2</sup>These diagrams are obtained by solving the bosonic field equation  $\frac{\delta\Gamma}{\delta\bar{B}} = J_B$  for the bosonic fields and inserting the result  $\bar{B}$  into the mixed effective action to obtain a purely fermionic effective action  $\Gamma[\psi, \psi^*] = \Gamma[\psi, \psi^*, \bar{B}]$ .



---

The generation of terms containing higher fermionic vertex functions is a general feature of partially bosonised theories and it is important to develop a method that can deal with them.

In a first attempt we have investigated if it is possible to choose the parameters  $\alpha_i$  parametrising our bosonisation so that the diagrams in (5.15) become small or vanish. This would then correspond to an optimal choice of couplings that pins down the arbitrariness in the parameters to a definite value, thus enlarging the predictive power of the mean field results. However we find that minimising the four fermion loops corresponds to setting  $3\alpha_m - \alpha_\rho = 0$ , i.e.  $U = 0$ . However, noninteracting fermions are not what we wanted to investigate, so we have to find other means of dealing with multi fermion vertices.

A promising formalism for this task was proposed in [18]. The authors use the freedom to redefine the bosonic fields in the course of the renormalisation group flow so that the generated four fermion terms are cancelled. This corresponds to a kind of rebosonisation on the fly. We will deal with this approach in the beginning of the next chapter.

We remark that the diagrams of (5.15) and (5.16) are exactly the ones one obtains in a purely fermionic theory if we reinterpret the dotted lines as the fermionic interaction just as in (3.23). The exact value of each diagram is of course dependent on the special choice of parametrisation chosen for the four fermion coupling. However, if we use the parametrisation as applied in the bosonisation procedure (2.40), there is actually a one to one correspondence between the diagrams in the bosonised and the purely fermionic theory.

# Chapter 6


## Renormalisation group analysis

This chapter is dedicated to the application of the renormalisation group formalism presented in chapter 4 to the Hubbard model in its partially bosonised form. Our initial condition will be the “classical” action of the Hubbard model presented in chapter 2. As has already been discussed in chapter 4 one has to make approximations to the full flow equation in order to be able to solve them, i.e. we will truncate the infinite set of couplings generated under the flow and solve the equations in this subset. For a suitable choice of this truncation we will let us guide by the results obtained in chapter 5 in a one loop study.

In the first section of this chapter we want to present a formalism for translating the four fermion interaction terms generated during the flow into a change of the Yukawa-couplings of the bosonised theory. The following sections deal with specific truncations. In the first one we deal with antiferromagnetism at low chemical potential. A second one investigates the degree of dependence of physical results on the ambiguous choice of parameters  $\alpha_i$  in our truncations.

### 6.1 Rebosonisation of fermionic interactions

As we have seen in the last chapter any partially bosonised theory will generate four fermion interaction terms under a renormalisation group step corresponding to the diagrams


$$(6.1)$$

However, we wanted to capture the complicated behaviour of higher fermion vertices in the bosonic language – this was what the bosonisation procedure was all about. One might suspect that it should be possible to rebosonise the fermionic coupling

obtained after some renormalisation group step by a suitable field redefinition of the bosonic fields. This is indeed the case as was shown in [18] (see also [26]).

Consider a theory with (average effective) action

$$\begin{aligned} \Gamma_k[\psi, \psi^*, \phi] = & \sum_Q \psi^*(Q) P_{\psi,k} \psi(Q) + \frac{1}{2} \sum_Q \phi(-Q) P_{\phi,k}(Q) \phi(Q) \\ & - \sum_Q h_k(Q) \phi(Q) \tilde{\phi}(-Q) + \sum_Q \lambda_k(Q) \tilde{\phi}(Q) \tilde{\phi}(-Q), \end{aligned} \quad (6.2)$$

where  $\tilde{\phi}$  is the fermionic bilinear corresponding to the bosonic field  $\phi$ , e.g.  $\tilde{\phi}_i(K) = \sum_Q \psi^*(Q) \tau^i \psi(Q+K)$ , and the initial condition for the purely fermionic coupling is  $\lambda_{\phi, \bar{k}} = 0$  at some initial scale  $\bar{k}$ .

Now perform a renormalisation group step from the scale  $\bar{k}$  to the scale  $k = \bar{k} - \Delta k$ . The change in scale,  $\Delta k$ , is supposed to be so small that the changes in couplings are also small; they are calculated by the flow equation (4.15) for the truncation (6.2). As we have seen, the four fermion coupling  $\lambda_k$  will in general be different from zero, say  $\Delta \lambda_k$ , at the new scale  $k$ .

We will use our freedom in the definition of our bosonic fields to consider a field redefinition at the scale  $k$  (we put  $\phi_{\bar{k}} = \phi$  at the initial scale)

$$\phi_k(Q) = \phi_{\bar{k}}(Q) + \Delta \alpha_k \tilde{\phi}(Q), \quad (6.3)$$

where  $\Delta \alpha_k$  is an up to now arbitrary function. Inserting this into (6.2) we find:

$$\begin{aligned} \Gamma_k[\psi, \psi^*, \phi_k] = & \sum_Q \psi^*(Q) P_{\psi,k} \psi(Q) + \frac{1}{2} \sum_Q \phi_k(-Q) P_{\phi,k}(Q) \phi_k(Q) \\ & - \sum_Q [h_k(Q) - \Delta \alpha_k(Q) P_{\phi,k}(Q)] \phi_k(Q) \tilde{\phi}(-Q) \\ & + \sum_Q [\Delta \lambda_k(Q) - h_k(Q) \Delta \alpha_k(Q)] \tilde{\phi}(Q) \tilde{\phi}(-Q) + \mathcal{O}[(\Delta \alpha_k)^2], \end{aligned} \quad (6.4)$$

where  $h_k(Q) = h_{\bar{k}}(Q) + \Delta h_k(Q)$ . Due to the field redefinition the change at fixed fields of both the four fermion coupling and the Yukawa coupling is supplemented by a term proportional to the arbitrary parameter  $\Delta \alpha_k$ . The full changes in coupling read

$$\begin{aligned} \bar{\Delta} h_k(Q) &= \Delta h_k(Q) - \Delta \alpha_k(Q) P_{\phi,k}(Q), \\ \bar{\Delta} \lambda_k(Q) &= \Delta \lambda_k(Q) - h_k(Q) \Delta \alpha_k(Q). \end{aligned} \quad (6.5)$$

This is exactly what we need if we want to demand that the four fermion coupling also vanishes at scale  $k$ . We may absorb the change in the four fermion coupling by

adjusting the field redefinition. This in turn leads to the full change of the Yukawa coupling

$$\bar{\Delta}h_k(Q) = \Delta h_k(Q) - \frac{P_{\phi,k}(Q)}{h_k(Q)} \Delta \lambda_k(Q). \quad (6.6)$$

By iterating this procedure after each renormalisation group step from some scale  $k$  to scale  $k - \Delta k$  and so on we may thus demand that the four fermion coupling vanishes for *all* scales by adjusting the parameter  $\Delta \alpha_k$  after each step.

Let us see how we can implement this reasoning into the renormalisation group formalism of chapter 4. In (4.15) the change of scale  $\partial_k \Gamma_k[\chi]|_\chi$  is calculated at fixed fields. Hence if we in addition perform a shift in the fields as above (6.3) corresponding to

$$\partial_k \phi_k(Q) = -\partial_k \alpha_k(Q) \tilde{\phi}(Q), \quad (6.7)$$

the flow equation reads

$$\begin{aligned} \partial_k \Gamma_k[\psi, \psi^*, \phi_k] &= \partial_k \Gamma_k[\psi, \psi^*, \phi_k]|_{\phi_k} + \sum_Q \left( \frac{\delta}{\delta \phi_k} \Gamma[\psi, \psi^*, \phi_k] \right) \partial_k \phi_k \\ &= \partial_k \Gamma_k[\psi, \psi^*, \phi_k]|_{\phi_k} \\ &\quad + \sum_Q \left( -\partial_k \alpha_k(Q) P_{\phi,k}(Q) \phi_k(Q) \tilde{\phi}(-Q) + h_k(Q) \partial_k \alpha_k(Q) \tilde{\phi}(Q) \tilde{\phi}(-Q) \right) \end{aligned} \quad (6.8)$$

and this changes the flow equations for  $h_k$  and  $\lambda_k$  to

$$\begin{aligned} \partial_k h_k(Q) &= \partial_k h_k(Q)|_{\phi_k} - \partial_k \alpha_k(Q) P_{\phi,k}(Q), \\ \partial_k \lambda_k(Q) &= \partial_k \lambda_k(Q)|_{\phi_k} - h_k(Q) \partial_k \alpha_k(Q). \end{aligned} \quad (6.9)$$

Again we may demand that the purely fermionic coupling vanishes for all scales  $k$  which leads to the modified flow equation for the Yukawa coupling

$$\partial_k h_k(Q) = \partial_k h_k(Q)|_{\phi_k} - \frac{P_{\phi,k}(Q)}{h_k(Q)} \partial_k \lambda_k(Q)|_{\phi_k}, \quad (6.10)$$

which exactly corresponds to the adjustment ‘‘by hand’’ done above.

This kind of procedure can also be applied to complex fields and to more than one field.

## 6.2 First truncation: Antiferromagnetic behaviour close to half filling

It is now time to apply the renormalisation group formalism developed in the preceding chapters to the Hubbard model. In this section we will take a look at the

region close to half filling and low temperatures. At and close to half filling the system is dominated by an antiferromagnetic spin density. In this section we will therefore leave aside all bosons apart from the spin density  $\vec{m}(X)$ . There is then no ambiguity how the parameter  $\alpha_m$  is related to the original fermionic coupling  $U$ . However, under the flow couplings with other momentum dependencies will appear that are not included in this simple ansatz.

Let us now try to define a suitable truncation for the effective action. The initial condition for the flow equation (4.15) is the classical action (2.42). In the course of the flow towards lower scales the average effective action will in general pick up all possible couplings that are compatible with the symmetries of the theory. We have to truncate this set of couplings somewhere to make progress. We will make an ansatz containing a fermionic kinetic term  $\Gamma_{\psi,k}$ , a term containing a Yukawa like interaction between fermions and bosons  $\Gamma_{Y,k}$  and a bosonic term. (A term containing a four fermion interaction is to be rebosonised as sketched in the previous section.) As we are mainly interested in antiferromagnetic behaviour we define the boson ( $\boldsymbol{\pi} = (\pi, \pi)$ )

$$\vec{a}(Q) = \vec{m}(Q + \boldsymbol{\pi}), \quad (6.11)$$

whose zero momentum mode  $\vec{a}(0)$  corresponds to an antiferromagnetic spin density.

For the fermionic kinetic term we adopt the classical part unchanged

$$\begin{aligned} \Gamma_{\psi,k}[\psi, \psi^*] &= \sum_Q \psi^*(Q) P_\psi(Q) \psi(Q), \\ P_\psi(Q) &= i\omega_Q + \epsilon_Q - \mu, \quad \epsilon_Q = -2t(\cos q_x + \cos q_y), \end{aligned} \quad (6.12)$$

where we restrict ourselves to nearest neighbour hopping.

Similarly the Yukawa coupling term is taken to be

$$\Gamma_{Y,k}[\psi, \psi^*, \vec{a}] = -\bar{h}_a \sum_{KQQ'} \vec{a}(K) \psi^*(Q) \vec{\sigma} \psi(Q') \delta(K - Q + Q' + \boldsymbol{\pi}) \quad (6.13)$$

with scale dependent (but momentum independent) Yukawa coupling  $\bar{h}_a$ .

As an ansatz for the purely bosonic part we take a kinetic term augmented by an effective potential

$$\Gamma_{a,k}[\vec{a}] = \frac{1}{2} \sum_Q \vec{a}(-Q) P_a(Q) \vec{a}(Q) + \mathcal{V}U[\vec{a}], \quad (6.14)$$

where  $\mathcal{V} = \sum_X 1$  is the two dimensional volume divided by temperature.

Due to  $SU(2)$  symmetry the potential can only depend on the rotation invariant combination

$$\alpha(K, K') = \frac{1}{2} \vec{a}(K) \vec{a}(K'). \quad (6.15)$$

Furthermore we will make an expansion in powers of the field  $\vec{a}$  up to a quartic interaction. We take different truncations in the symmetric regime (SYM) and in the regime with spontaneous symmetry breaking (SSB) as it is preferable to always expand around the minimum of the potential

$$\begin{aligned}
\text{SYM : } \mathcal{V}U[\vec{a}] &= \sum_K \overline{m}_a^2 \alpha(-K, K) \\
&\quad + \frac{1}{2} \sum_{K_1 \dots K_4} \overline{\lambda}_a \delta(K_1 + K_2 + K_3 + K_4) \alpha(K_1, K_2) \alpha(K_3, K_4), \\
\text{SSB : } \mathcal{V}U[\vec{a}] &= \frac{1}{2} \sum_{K_1 \dots K_4} \overline{\lambda}_a \delta(K_1 + K_2 + K_3 + K_4) \\
&\quad (\alpha(K_1, K_2) - \overline{\alpha}_0 \delta(K_1) \delta(K_2)) (\alpha(K_3, K_4) - \overline{\alpha}_0 \delta(K_3) \delta(K_4))
\end{aligned} \tag{6.16}$$

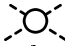
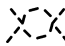
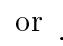
with scale dependent mass  $\overline{m}_a$ , minimum  $\overline{\alpha}_0$  and coupling  $\overline{\lambda}_a$ .

The bosonic propagator on the classical level is simply a mass term in our case (no inclusion of  $e$  and  $d$  bosons, i.e.  $\alpha_c = \alpha_x = \alpha_y = 0$ ). We let us guide by the loop results of chapter 5 for the momentum dependence and take

$$P_a(Q) = Z_a Q^2 = Z_a (\omega_B^2 + [\mathbf{q}]^2), \tag{6.17}$$

where  $Z_a$  is a scale dependent wave function renormalisation and the function  $[\mathbf{q}]^2$  is defined as  $[\mathbf{q}]^2 = q_x^2 + q_y^2$  for  $q_i \in [-\pi, \pi]$  and continued periodically otherwise.

The ansatz  $[\mathbf{q}]^2$  for the spatial part is to mimic the momentum dependence of figure 5.1. The Matsubara dependence is more difficult. A look at figure 5.2 would rather suggest an ansatz where only the part for the smallest frequencies is changed, while the higher frequency modes retain their original mass term. Lowering the scale, the  $\omega_B = 0$  mode will then dominate the propagation more and more. We mimic this behaviour by adding the  $\omega_B^2$  term to the propagator instead and give all modes the same mass.

One would by the way suspect a similar thing for the quartic boson coupling  $\overline{\lambda}_a$ , which at large cutoff is generated by the fermion loop : the low frequency modes are supposedly changed most, while we take  $\lambda_a$  to be independent of  $\omega_B$ . Again the  $\omega_B^2$  term in the propagator will mimic this effect by suppressing all high frequency modes that couple to such a vertex. For example in  or  only low frequency modes will contribute to the loop while others are suppressed by the propagator.

### 6.2.1 Choice of the regulators

In addition to the truncation we still have to specify the regulator functions for the renormalisation group equations.

**Fermionic regulator:**

The fermionic cutoff function is inspired by the fact that at nonvanishing temperature the propagator  $P_\psi(Q) = i\omega_Q + \epsilon_Q - \mu$  has no zero-modes. This means that the temperature itself acts as a regulator. We therefore choose

$$R_k^\psi(Q) = i\omega_Q\left(\frac{T_k}{T} - 1\right) = i2\pi\left(n_Q + \frac{1}{2}\right)(T_k - T), \quad (6.18)$$

which has the effect of replacing the temperature  $T$  by some function  $T_k$  in the fermionic propagator. We will later specify this function to be

$$T_k^2 = T^2 + k^2; \quad \text{then} \quad \partial_k T_k = \frac{k}{T_k} \rightarrow \begin{cases} 1 & \text{if } k \gg T \\ k/T & \text{if } k \ll T \end{cases}, \quad (6.19)$$

which very effectively integrates out the fermions.

**Bosonic regulator:**

For the bosonic regulator we take

$$R_k^a(Q) = Z_a(k^2 - Q^2)\Theta(k^2 - Q^2), \quad (6.20)$$

where  $Q^2$  is defined in (6.17). This leads to a full propagator of the form

$$P_a(Q) + R_k^a(Q) = Z_a \underbrace{(Q^2 \Theta(Q^2 - k^2) + k^2 \Theta(k^2 - Q^2))}_{=: Q_k^2} = \begin{cases} Z_a Q^2 & \text{if } Q^2 > k^2 \\ Z_a k^2 & \text{if } Q^2 < k^2. \end{cases} \quad (6.21)$$

The regulator function (6.20) thus hampers the propagation of modes with small momenta and Matsubara frequencies. Therefore, by lowering  $k$ , we average over larger and larger regions in position space. We may therefore relate properties of the average effective action  $\Gamma_k$  at a given scale  $k$  to properties of size  $1/k$  in position space. However, the cutoff does not allow to perform the Matsubara sums in loops containing bosonic propagators thus slowing down the numerical evaluation.

**6.2.2 The flow equations at half filling****Bosonic potential**

We define the flow of masses and couplings as follows<sup>1</sup>:

$$\begin{aligned} \text{SYM:} \quad \partial_t \bar{m}_a^2 &= \frac{d}{d\alpha} (\partial_k U(\alpha))|_{\alpha=0}, & \partial_t \bar{\lambda}_a &= \frac{d^2}{d\alpha^2} (\partial_k U(\alpha))|_{\alpha=0}, \\ \text{SSB:} \quad \partial_t \bar{\alpha}_0 &= -\frac{1}{\lambda} \frac{d}{d\alpha} (\partial_k U(\alpha))|_{\alpha=\bar{\alpha}_0}, & \partial_t \bar{\lambda}_a &= \frac{d^2}{d\alpha^2} (\partial_k U(\alpha))|_{\alpha=\bar{\alpha}_0}. \end{aligned} \quad (6.22)$$

<sup>1</sup>The flow of the minimum is inferred from the fact that  $U'(\alpha_0) = 0$  and hence  $\frac{d}{dk} U'(\alpha_0) = \partial_k U'(\alpha_0) + U''(\alpha_0) \partial_k \alpha_0 = 0$ .

The flow equation for the potential itself can directly be read off from the results of the mean-field calculation (3.15) and the  $O(N)$ -symmetric model (4.22)

$$\begin{aligned} \partial_t U(\alpha) &= \partial_t U^B(\alpha) + \partial_t U^F(\alpha) \\ &= \frac{1}{2} \sum_{Q,i} \tilde{\partial}_t \ln [P_a(Q) + \hat{M}_i^2(\alpha) + R_{ak}(Q)] - 2T \int_{-\pi}^{\pi} \frac{d^2 q}{(2\pi)^2} \tilde{\partial}_t \ln \cosh y(\alpha), \end{aligned} \quad (6.23)$$

where the “masses”  $M_i^2$  are defined as

$$\hat{M}_i^2(\alpha) = \begin{cases} (\bar{m}_a^2 + 3\bar{\lambda}_a\alpha, \bar{m}_a^2 + \bar{\lambda}_a\alpha, \bar{m}_a^2 + \bar{\lambda}_a\alpha)_i & \text{SYM} \\ \bar{\lambda}(3\alpha - \bar{\alpha}_0, \alpha - \bar{\alpha}_0, \alpha - \bar{\alpha}_0)_i & \text{SSB} \end{cases} \quad (6.24)$$

and we have defined the function

$$y(\alpha) = \sqrt{\epsilon_{\mathbf{q}}^2 + 2\bar{h}_a^2\alpha/Z_{\psi}^2}/(2T_k). \quad (6.25)$$

With the aid of (6.22) we may now derive the flow equations for the parameters in the effective potential. However, first we introduce rescaled and renormalised quantities<sup>2</sup>:

$$m_a^2 = \frac{\bar{m}_a^2}{Z_a k^2}, \quad \alpha_0 = Z_a \bar{\alpha}_0, \quad \lambda_a = \frac{\bar{\lambda}_a}{Z_a^2 k^2}, \quad h_a^2 = \frac{\bar{h}_a^2}{Z_{\psi}^2 Z_a k^2}.$$

With the definitions  $\eta_a = -\partial_t \ln Z_a$  (anomalous dimension),  $t = \ln k$  and  $\overline{\sum_Q} \equiv \sum_Q \Theta(k^2 - Q^2)$  we get in the symmetric (SYM) phase:

$$\begin{aligned} \partial_t m_a^2 &= -\frac{5}{2} \lambda_a \overline{\sum_Q} \frac{2 - \eta_a(1 - Q^2/k^2)}{k^2(1 + m_a^2)^2} \\ &\quad + (k\partial_k T_k) h_a^2 \frac{T}{2T_k^3} \int_{-\pi}^{\pi} \frac{d^2 q}{(2\pi)^2} \left\{ \frac{\tanh y(0)}{y(0)} + \frac{1}{\cosh^2 y(0)} \right\} \\ &\quad - (2 - \eta_a) m_a^2, \end{aligned} \quad (6.26)$$

$$\begin{aligned} \partial_t \lambda_a &= 11 \lambda_a^2 \overline{\sum_Q} \frac{2 - \eta_a(1 - Q^2/k^2)}{k^2(1 + m_a^2)^3} \\ &\quad - k^2 (k\partial_k T_k) h_a^4 \frac{T}{8T_k^5} \int_{-\pi}^{\pi} \frac{d^2 q}{(2\pi)^2} \left\{ \frac{\tanh y(0)}{y^3(0)} + \frac{2y(0) \tanh y(0) - 1}{y^2(0) \cosh^2 y(0)} \right\} \\ &\quad - 2(1 - \eta_a) \lambda_a. \end{aligned} \quad (6.27)$$

---

<sup>2</sup>Note that some of these quantities are *not* dimensionless. However, for small cutoff compared to the temperature the theory becomes essentially two dimensional due to dimensional reduction. In this case the above functions have the desired scale dependence.



In the broken (SSB) phase we get:

$$\begin{aligned} \partial_t \alpha_0 = & \frac{1}{2} \overline{\sum_Q} \frac{2 - \eta_a(1 - Q^2/k^2)}{k^2} \left( \frac{3}{(1 + 2\lambda_a \alpha_0)^2} + 2 \right) \\ & - (k\partial_k T_k) \frac{h_a^2}{\lambda_a} \frac{T}{2T_k^3} \int_{-\pi}^{\pi} \frac{d^2 q}{(2\pi)^2} \left\{ \frac{\tanh y(\alpha_0)}{y(\alpha_0)} + \frac{1}{\cosh^2 y(\alpha_0)} \right\} \\ & - \eta_a \alpha_0, \end{aligned} \quad (6.28)$$

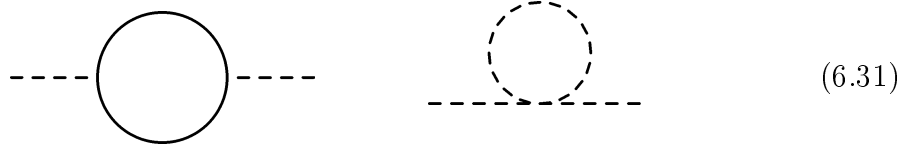
$$\begin{aligned} \partial_t \lambda_a = & \lambda_a^2 \overline{\sum_Q} \frac{2 - \eta_a(1 - Q^2/k^2)}{k^2} \left( \frac{9}{(1 + 2\lambda_a \alpha_0)^3} + 2 \right) \\ & - k^2 (k\partial_k T_k) h_a^4 \frac{T}{8T_k^5} \int_{-\pi}^{\pi} \frac{d^2 q}{(2\pi)^2} \left\{ \frac{\tanh y(\alpha_0)}{y^3(\alpha_0)} + \frac{2y(\alpha_0) \tanh y(\alpha_0) - 1}{y^2(\alpha_0) \cosh^2 y(\alpha_0)} \right\} \\ & - 2(1 - \eta_a) \lambda_a, \end{aligned} \quad (6.29)$$

where

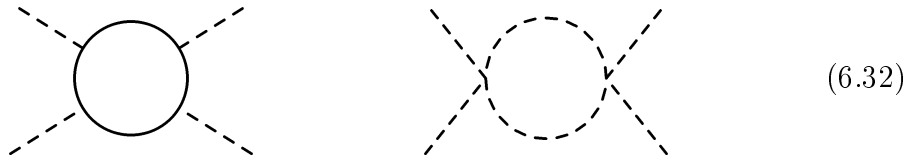
$$y(\alpha_0) = \sqrt{\epsilon_Q^2 + 2k^2 h_a^2 \alpha_0 / (2T_k)}. \quad (6.30)$$

Note that for  $(k < 2\pi T \wedge k < \pi)$  we are able to evaluate the  $\overline{\sum_Q}$ -sum and find  $\overline{\sum_Q} (2 - \eta_a(1 - Q^2/k^2)) = k^2 T (4 - \eta_a) / (8\pi)$ .

These equations all have a simple diagrammatic representation. In the symmetric phase the mass contribution is



and similarly the contribution to the coupling reads



In the SSB phase the inverse fermionic propagator contains terms  $\sim \vec{a}_0 \delta(Q - Q' + \pi)$ ; similarly the field is also present in the bosonic propagator (c.f. the “masses” (6.24)).

### Anomalous dimension

The anomalous dimension  $\eta_a = -k\partial_k \ln Z_a$  is a measure for the change of the wave function renormalisation  $Z_a$  with scale. Therefore we can extract it from the momentum dependence of the bosonic two point function. As we are mainly interested

in the spatial momentum dependence we set

$$Z_a = \mathcal{V}^{-1} \frac{\partial^2}{\partial l^2} \Big|_{l=0} \left\{ \frac{\delta^2}{\delta \vec{a}(-K) \delta \vec{a}(K)} \Gamma_k \right\} \Big|_{\psi, \psi^* = 0, \vec{a} = \vec{a}_0}, \quad K = (\omega_B = 0, \mathbf{k} = l\mathbf{e}_1), \quad (6.33)$$

where  $\vec{a}_0$  is the minimum of the effective potential. In this way we project out the curvature at the minimum in figure 5.1.

In the symmetric phase (SYM) the bosonic propagator is affected by the two diagrams in equation (6.31). However, the bosonic loop is independent of the external momenta and therefore does not contribute to the anomalous dimension. The fermionic loop is well known from our calculation in chapter 5 and we obtain

$$\begin{aligned} \eta_a &= -2h_a^2 T k^2 (k \partial_k T_k) \left[ \partial_{T_k} \partial_l^2 \left\{ \frac{-1}{2T_k} \int_{-\pi}^{\pi} \frac{d^2 q}{(2\pi)^2} \frac{\tanh \frac{\epsilon_{\mathbf{q}}}{2T_k} + \tanh \frac{\epsilon_{\mathbf{q}+l\hat{e}_1}}{2T_k}}{\epsilon_{\mathbf{q}} + \epsilon_{\mathbf{q}+l\hat{e}_1}} \right\} \right]_{l=0} \\ &= \int_{-\pi}^{\pi} \frac{d^2 q}{(2\pi)^2} \frac{-2h_a^2 T k^2 (k \partial_k T_k)}{32T_k^5 \epsilon_{\mathbf{q}}^3 \cosh^4 \frac{\epsilon_{\mathbf{q}}}{2T_k}} \\ &\quad \left[ \left( -2\epsilon_{\mathbf{q}} (T_k^2 + 2\epsilon_{\mathbf{q}}^2) + 2T_k (T_k^2 - 2\epsilon_{\mathbf{q}}^2) \sinh\left(\frac{\epsilon_{\mathbf{q}}}{T_k}\right) \right. \right. \\ &\quad \left. \left. + 2 \cosh\left(\frac{\epsilon_{\mathbf{q}}}{T_k}\right) (-T_k^2 \epsilon_{\mathbf{q}} + \epsilon_{\mathbf{q}}^3 + T_k^3 \sinh\left(\frac{\epsilon_{\mathbf{q}}}{T_k}\right)) \right) (4t^2 \sin^2 q_1) \right. \\ &\quad \left. - T_k \epsilon_{\mathbf{q}} \left( -2T_k \epsilon_{\mathbf{q}} (1 + \cosh\left(\frac{\epsilon_{\mathbf{q}}}{T_k}\right)) \right. \right. \\ &\quad \left. \left. + 2(T_k^2 + \epsilon_{\mathbf{q}}^2 + T_k^2 \cosh\left(\frac{\epsilon_{\mathbf{q}}}{T_k}\right)) \sinh\left(\frac{\epsilon_{\mathbf{q}}}{T_k}\right) \right) (2t \cos q_1) \right]. \end{aligned} \quad (6.34)$$

In the *SSB*-phase we also get a contribution from the bosonic sector. The contribution comes from a bosonic loop with four external legs, where two external legs are connected to the condensate (denoted by a cross):



$$(6.35)$$

As we will later see, the system enters the broken phase at very small values of the cutoff parameter  $k$ . At these values only the lowest Matsubara frequency ( $\omega_B = 0$ ) contributes in the bosonic propagator (c.f. (6.21)). The diagram above is thus the same as the corresponding one for a simple  $O(3)$  model in two dimensions. Here the anomalous dimension has been calculated to be [44]

$$\eta_a = \frac{16T v_2}{2} \alpha_0 \lambda_a^2 m_{2,2}^2 (2\lambda_a \alpha_0, 0) \quad (6.36)$$

$$= \frac{T}{\pi} \frac{\alpha_0 \lambda_a^2}{(1 + 2\lambda_a \alpha_0)^2}, \quad (6.37)$$

where the function  $m_{2,2}^2(x, y)$  contains the momentum dependence of the loop integral and depends on the regulator  $R_k^a$ . For our choice of regulator it can be calculated explicitly [22] as shown in (6.37).

The contribution from the fermionic loop is much smaller at the values of  $k$  we face in the broken phase; we will therefore neglect this contribution.

### Yukawa coupling

In the symmetric phase the running of the Yukawa coupling is generated by the diagrams

$$(6.38)$$

where the first diagram is the direct contribution, while the last two have to be rebosonised as prescribed in the beginning of this chapter. The extraction of the contribution from the first diagram is performed at vanishing bosonic momentum, while we average over the fermionic momenta  $Q = (\pm\omega_0, \mathbf{0})$  because  $\omega_0 = \pi T_k$  does not vanish except for  $T = 0$ .

We apply the rebosonisation procedure presented in the beginning of this chapter to the two box diagrams. Of course the generated four fermion coupling will in general not factorise as in (6.2). What one obtains instead is rather

$$\begin{aligned} \tilde{m}_Q(K) &= \psi^*(Q)\vec{\sigma}\psi(Q+K), \\ \Delta\Gamma_{\text{box}} &= \sum_{KQ Q'} \lambda_{QQ'}(K)\tilde{m}_Q(K)\tilde{m}_{Q'}(-K) + \dots, \end{aligned} \quad (6.39)$$

i.e. the diagrams depend on all external momenta constrained by overall momentum conservation. The definition of  $\tilde{m}_Q(K)$  is in analogy to the one of  $\tilde{m}(K)$  (c.f. (2.47)). In order to extract the coupling we thus have to fix the momenta at some value. In our calculation we choose to put  $\mathbf{q} = \mathbf{q}' = \mathbf{0}$  and  $\mathbf{k} = \boldsymbol{\pi}$  appropriate for the antiferromagnet and again average over Matsubara frequency  $\pm\omega_0$ .

In the symmetric phase we get for the running of  $h_a$

$$Q_k^2 = Q^2\Theta(Q^2 - k^2) + k^2\Theta(k^2 - Q^2), \quad (6.40)$$

$$\partial_t\omega_n^2 = 2\omega_n^2(\partial_t T_k)/T_k, \quad (6.41)$$

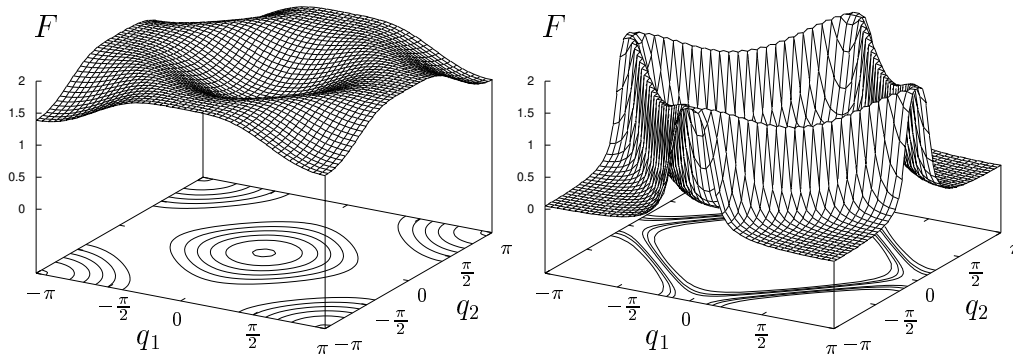


Figure 6.1: The function  $F(q_1, q_2)$  defined in (6.43) for  $T_k/t = 5$  (left) and  $T_k/t = 1/5$  (right).

$$\begin{aligned}
\partial_t h_a^2 = & -2h_a^4 \sum_Q \left\{ \frac{\partial_t \omega_n^2}{(\omega_n^2 + \epsilon_q^2)^2} \frac{1}{Q_k^2/k^2 + m_a^2} \right. \\
& \left. + \frac{1}{\omega_n^2 + \epsilon_q^2} \frac{(2 - \eta_a(1 - Q^2/k^2))\Theta(k^2 - Q^2)}{(1 + m_a^2)^2} \right\} \\
& + 4m_a h_a^4 \sum_Q \left\{ \frac{\partial_t \omega_n^2}{(\omega_n^2 + \epsilon_q^2)^2} \frac{1}{Q_k^2/k^2 + m_a^2} \right. \\
& \left. + \frac{1}{\omega_n^2 + \epsilon_q^2} \frac{(2 - \eta_a(1 - Q^2/k^2))\Theta(k^2 - Q^2)}{(1 + m_a^2)^2} \right\} \\
& \times \frac{1}{(Q + \pi)_k^2/k^2 + m_a^2} \\
& - h_a^2(2 - 2\eta_\psi - \eta_a).
\end{aligned} \tag{6.42}$$

In the phase with spontaneously broken  $SU(2)$ -symmetry (SSB) the change in the Yukawa coupling due to the diagrams (6.38) is negligible as we have checked numerically. Anyhow, we are only interested in the qualitative behaviour in this region, so we will neglect the running of the Yukawa-coupling here; this then amounts to keeping the unrenormalised Yukawa coupling  $\bar{h}_a$  fixed at its value on the scale, where symmetry breaking occurred.

### 6.2.3 Numerical results

Let us first take a look at how the fermionic regulator function works. For this purpose we plot the integrand of the fermionic part of the flow equation for the

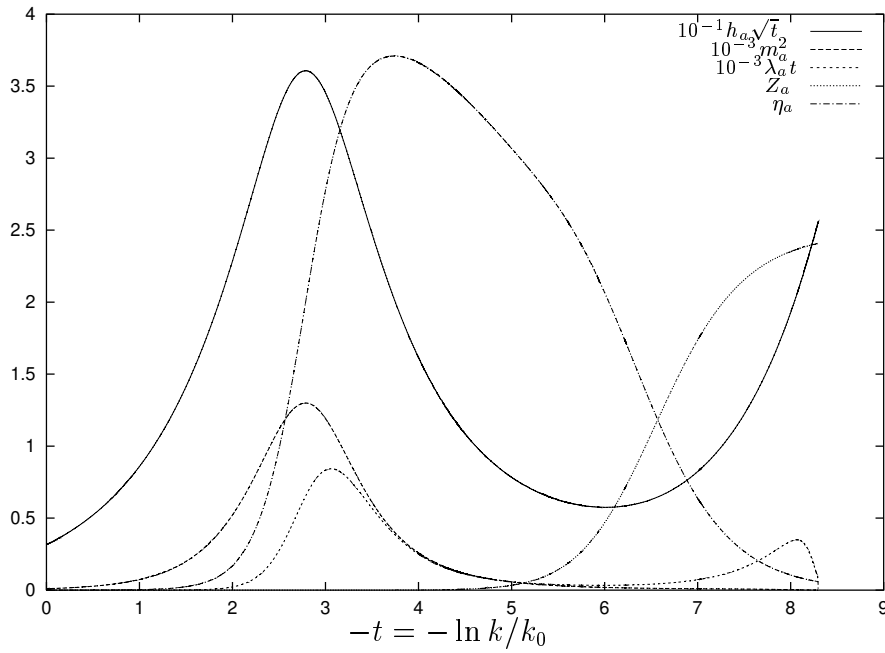


Figure 6.2: Flow of different couplings in the symmetric phase (SYM) at half filling. We have chosen  $U/t = 3$  and  $T/t = 0.18$ .

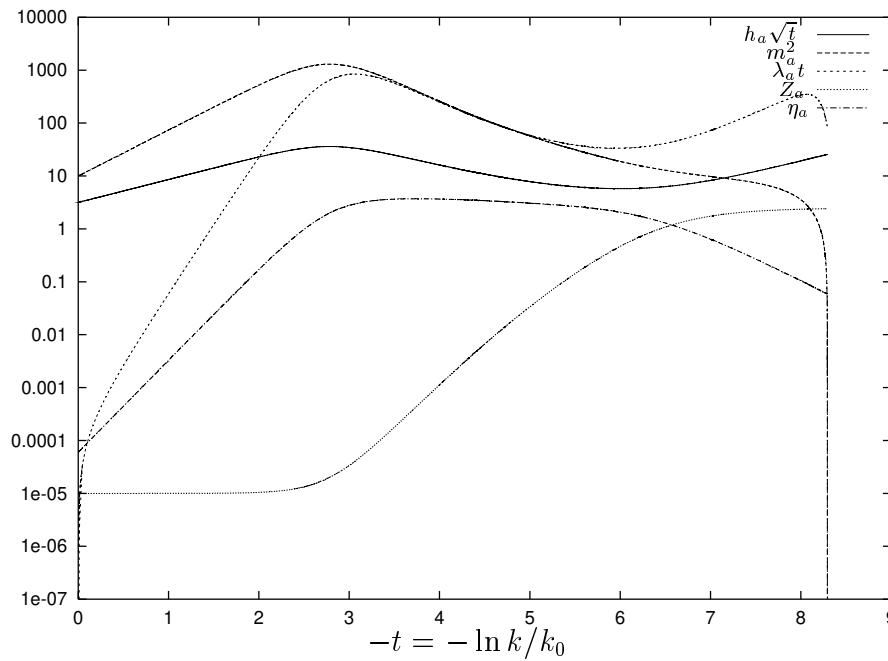


Figure 6.3: Flow of different couplings in the symmetric phase (SYM) at half filling with logarithmic scale. We have chosen  $U/t = 3$  and  $T/t = 0.18$ .

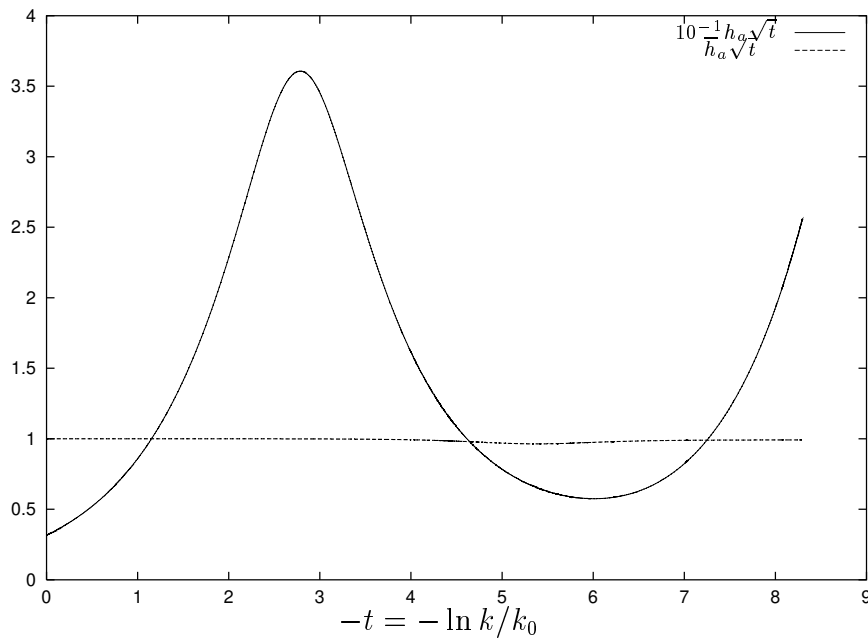


Figure 6.4: Flow of the renormalised and unrenormalised Yukawa couplings in the symmetric phase (SYM) at half filling. We have chosen  $U/t = 3$  and  $T/t = 0.18$ .

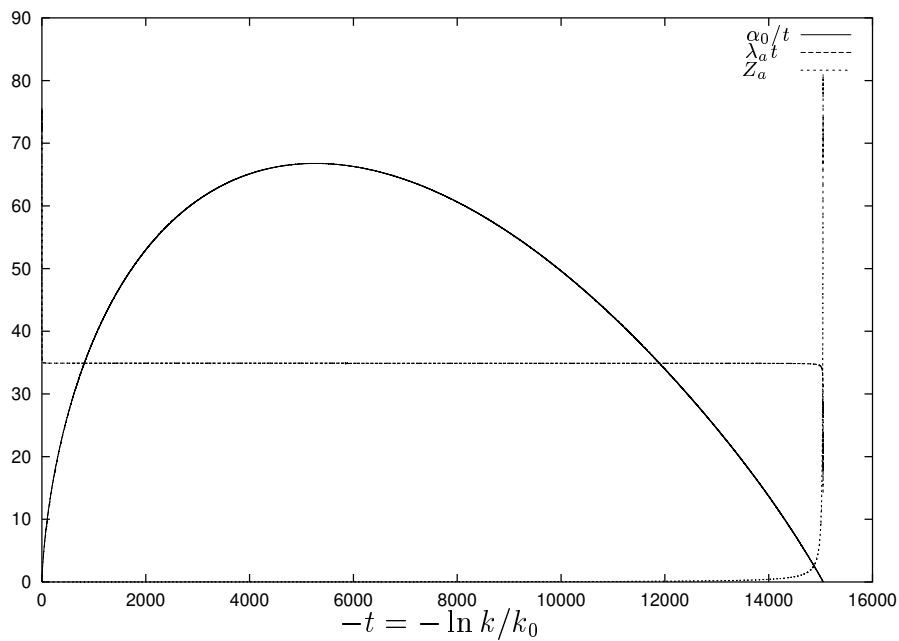


Figure 6.5: Flow of different couplings in the broken phase (SSB) at half filling. We have chosen  $U/t = 3$  and  $T/t = 0.18$ .

bosonic mass, i.e. the function

$$F(q_1, q_2) = \frac{\tanh y}{y} + \frac{1}{\cosh^2 y}, \quad y = \frac{2t(\cos q_1 + \cos q_2)}{T_k} \quad (6.43)$$

for different values of  $T_k/t$ . The left part of figure 6.1 shows  $F(q_1, q_2)$  for fairly large values of  $T_k$  while the right part is for low  $T_k$ . Observe that the contribution to the integral comes from narrower regions around the Fermi-surface the smaller  $T_k$  becomes. This was exactly what was intended by the regulator.

We now turn to a numerical analysis of the above flow equations. For this we set  $U/t = 3$  and take a temperature  $T = 0.18t$  just below the critical temperature. The initial scale  $k_0 = 100t$  is chosen so large that the final results do not depend on it and the one loop results are well produced in the beginning of the flow. The differential equations were integrated by a standard Runge–Kutta like routine [36]. In figures 6.2 and 6.3 we plot the flow of the Yukawa coupling  $h_a$ , the mass  $m_a^2$ , the quartic bosonic coupling  $\lambda_a$ , the wave function renormalisation  $Z_a$  and the anomalous dimension  $\eta_a$  in the symmetric phase (SYM) once with linear and once with logarithmic scale. The reader is cautioned not to mix up the hopping parameter  $t$ , which is kept fixed, and the logarithmic cutoff scale  $t = \ln k/k_0$ , which are denoted by the same letter. For scales below  $t \approx -2.5$  the running is mainly dominated by the simple scaling due to the respective dimensions of the couplings. In an intermediate range up to  $t \approx -6$  the large value of  $\eta_a$  dominates the flow. For even smaller values of  $t$  the flow is mainly driven by the fermionic part of the flow equations. At  $t \approx -8.2$  the bosonic mass  $m_a^2$  vanishes and we enter the broken phase. In figure 6.4 we have plotted both the renormalised and the unrenormalised Yukawa coupling. We observe, that the unrenormalised coupling is almost unaltered from its initial value.

In figure 6.5 we enter the broken phase. In this regime we have kept the unrenormalised Yukawa coupling constant. As we have checked numerically its change due to the flow is negligible. First, we observe that the quartic bosonic coupling reaches a fixed point very soon (the steep initial rise and final decrease is hard to distinguish in the figure). This is because the term  $\sim \lambda_a^2$  in equation (6.29) just compensates the other contributions. A similar thing happens for the minimum of the potential. At the beginning of the flow the fermionic part dominates the flow and the right hand side is negative leading to increasing values of  $\alpha_0$ . However, soon the fermionic part becomes smaller and the bosonic loop dominates. This finally drives the minimum to zero and thus restores the symmetry. When the fermionic part becomes negligible we effectively deal with a bosonic  $O(3)$  model in two dimensions for which the symmetry restoration is a well known feature.

This then reconciles the symmetry breaking with the Mermin–Wagner theorem [32, 33], which states that a continuous symmetry cannot be broken at nonvanishing temperatures in two dimensions and below. As we have found we indeed do not

see any symmetry breaking if we average over larger and larger volumes, i.e. lower the cutoff parameter  $t = \ln k$ . However, for smaller regions there may be clusters in which the symmetry is broken (in a weak sense comparable to domains in a ferromagnet with vanishing net magnetisation). Nevertheless, we find that the symmetry is restored only when averaging over extremely large samples inaccessible to any real experiment<sup>3</sup>.

### 6.2.4 The flow equations for $\mu \neq 0$

Let us take a look at nonvanishing chemical potential in the symmetric phase (i.e.  $\alpha = 0$ ). The bosonic part of the effective potential is not altered, while the fermionic part is. The flow equations for the couplings  $m_a^2$  and  $\lambda_a$  in the **bosonic potential** now read

$$\begin{aligned} \partial_t m_a^2 = & -\frac{5}{2}\lambda_a \overline{\sum_Q} \frac{2 - \eta_a(1 - Q^2/k^2)}{k^2(1 + m_a^2)^2} \\ & + (k\partial_k T_k) h_a^2 \frac{T}{2T_k^3} \int_{-\pi}^{\pi} \frac{d^2 q}{(2\pi)^2} \left\{ \frac{\tanh \tilde{y}(\mu)}{\tilde{y}(0)} + \frac{\tilde{y}(\mu)/\tilde{y}(0)}{\cosh^2 \tilde{y}(\mu)} \right\} \\ & - (2 - \eta_a) m_a^2, \end{aligned} \quad (6.44)$$

$$\begin{aligned} \partial_t \lambda_a = & 11\lambda_a^2 \overline{\sum_Q} \frac{2 - \eta_a(1 - Q^2/k^2)}{k^2(1 + m_a^2)^3} \\ & - k^2 (k\partial_k T_k) h_a^4 \frac{T}{8T_k^5} \int_{-\pi}^{\pi} \frac{d^2 q}{(2\pi)^2} \left\{ \frac{\tanh \tilde{y}(\mu)}{\tilde{y}^3(0)} + \frac{2\tilde{y}(\mu) \tanh \tilde{y}(\mu) - \tilde{y}(-\mu)/\tilde{y}(0)}{\tilde{y}^2(0) \cosh^2 \tilde{y}(\mu)} \right\} \\ & - 2(1 - \eta_a)\lambda_a, \end{aligned} \quad (6.45)$$

with

$$\tilde{y}(\mu) = (\epsilon_{\mathbf{q}} - \mu)/(2T_k). \quad (6.46)$$

The equation for the **anomalous dimension** becomes

$$\eta_a = -2k^3 h_a^2 T (\partial_k T_k) \left[ \partial_{T_k} \partial_l^2 \left\{ \frac{-1}{2T_k} \int_{-\pi}^{\pi} \frac{d^2 q}{(2\pi)^2} \frac{\tanh \frac{\epsilon_{\mathbf{q}+\mu}}{2T_k} + \tanh \frac{\epsilon_{\mathbf{q}+l\hat{e}_1-\mu}}{2T_k}}{\epsilon_{\mathbf{q}} + \epsilon_{\mathbf{q}+l\hat{e}_1}} \right\} \right]_{l=0}, \quad (6.47)$$

which results in a lengthy expression.

---

<sup>3</sup>For  $O(2)$  models in two dimensions there is another possibility to circumvent the Mermin–Wagner theorem mentioned by Kosterlitz and Thouless [29]. It is speculated that this kind of mechanism may play a role in the superconducting region [13].



For the **Yukawa-coupling** we obtain

$$\begin{aligned}
\partial_t h_a^2 = & -2h_a^4 \sum_Q \left\{ -(\partial_t P_{F1}^{-1}(Q)) \frac{1}{Q_k^2/k^2 + m_a^2} \right. \\
& \left. + P_{F1}^{-1}(Q) \frac{(2 - \eta_a(1 - Q^2/k^2))\Theta(k^2 - Q^2)}{(1 + m_a^2)^2} \right\} \\
& + 4m_a h_a^4 \sum_Q \left\{ -(\partial_t P_{F2}^{-1}(Q)) \frac{1}{Q_k^2/k^2 + m_a^2} \right. \\
& \left. + P_{F2}^{-1}(Q) \frac{(2 - \eta_a(1 - Q^2/k^2))\Theta(k^2 - Q^2)}{(1 + m_a^2)^2} \right\} \\
& \times \frac{1}{(Q + \boldsymbol{\pi})_k^2/k^2 + m_a^2} \\
& - h_a^2(2 - 2\eta_\psi - \eta_a),
\end{aligned} \tag{6.48}$$

with

$$P_{F1}^{-1}(Q) = \frac{\omega_Q^2 + \epsilon_Q^2 - \mu^2}{(\omega_Q^2 + \epsilon_Q^2 - \mu^2)^2 + 4\omega_Q^2\mu^2}, \tag{6.49}$$

$$P_{F2}^{-1}(Q) = \frac{\omega_Q^2 + \epsilon_Q^2}{(\omega_Q^2 + (\epsilon_Q + \mu)^2)^2 (\omega_Q^2 + (\epsilon_Q - \mu)^2)^2}. \tag{6.50}$$

### 6.2.5 Numerical results

We have analysed the phase diagram of the Hubbard model for small values of the chemical potential  $\mu$ . The results are plotted in figure 6.6, where again we have chosen  $U = 3t$ . The upper line shows the temperature at which the bosonic mass vanishes in the one loop approximation (c.f. (5.9) for  $\mathbf{k} = \boldsymbol{\pi}$ ). For small enough  $\mu$  this corresponds to the mean field approximation as the phase transition is of second order (c.f. figure 3.2, where  $h_a = 10t/\pi^2 \approx t$ , just as in the example here and so is equivalent as long as no other field acquires a nonzero expectation value). In order to deal with first order phase transitions one would have to treat the bosonic potential in a more complicated truncation so we will restrict ourselves to small values of  $\mu$ .

The lower line in figure 6.6 shows the critical temperature for various values of the chemical potential derived with the aid of the flow equations displayed above. One observes that the critical temperature is lowered compared to the mean field result.

The results found for the critical temperature are in reasonable agreement with results published by other authors [19, 21, 24].

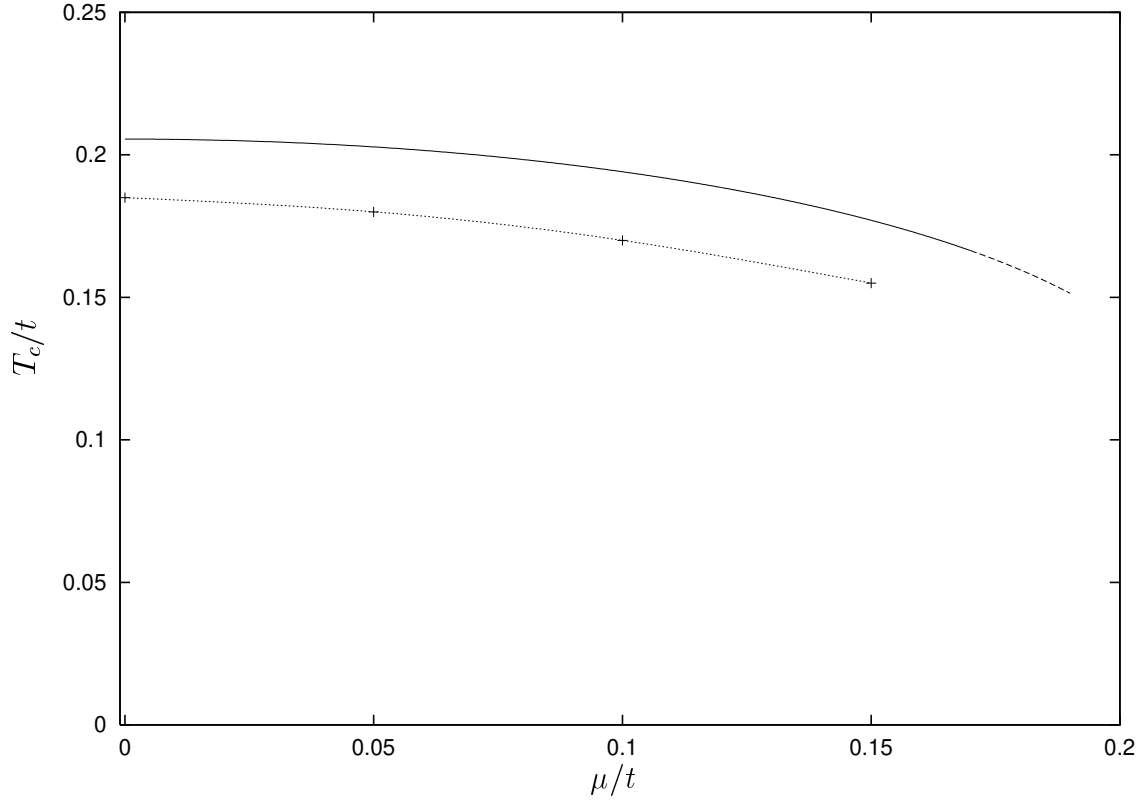


Figure 6.6: Plot of the critical temperature  $T_c$  versus the chemical potential  $\mu$  for  $U/t = 3$  in the mean field approximation (above) and with flow equations (below).

### 6.3 Second truncation: Parametrisation dependence in the bosonised theory

In this section we want to investigate how well the inclusion of running couplings is able to solve the ambiguity with respect to the choice of Yukawa couplings in the bosonisation procedure, which was so annoying in the mean field calculation. For this purpose we add the  $\rho(Q)$  boson corresponding to fluctuations in the charge density to our truncation. To keep things simple, however, we reduce the bosonic effective potential to a simple mass term for each boson.

For the full inverse propagator  $P_{ak}(Q) = P_a(Q) + R_{ak}(Q)$  of the  $\vec{a}$  boson we choose

$$P_{ak}(Q = (\omega_n, \mathbf{q})) = \begin{cases} \bar{m}_{a\Lambda}^2 + R_{ak} \equiv P_{a\Lambda} & \text{for } \omega_n \neq 0 \\ Z_a[\mathbf{q}]^2 + \bar{m}_{ak}^2 + R_{ak} \equiv P_{ak}(\mathbf{q}) & \text{for } \omega_n = 0 \end{cases} \quad (6.51)$$

and similarly for  $P_{\rho k}(Q)$  (however, we fix  $Z_\rho = 1$ ). The function  $[\mathbf{q}]^2$  is defined as below (6.17). This choice reflects the fact that in the one loop calculation we found

that the  $\omega_m = 0$  mode is changed most. Furthermore, if we make an  $\omega_m$ -independent choice of the bosonic regulator, we are able to perform the Matsubara sums in the loops for the Yukawa-couplings, which drastically speeds up the numerics. We choose  $R_{Bk} = k^2$  for both  $\vec{a}$  and  $\rho$ .

The fermionic kinetic part of the truncation is chosen as in section 6.2. Specifically, we restrict ourselves to nearest neighbour hopping. Furthermore we will only consider  $\mu = 0$ . Also the Yukawa part is chosen as in section 6.2, where we have taken the ‘‘classical’’ part with momentum independent couplings.

### 6.3.1 The flow equations

The running of the **anomalous dimension**  $\eta_a$  can be inferred directly from (6.34). The flow of the **masses** is governed by a fermionic loop and reads

$$\partial_k \bar{m}_a^2 = +(\partial_k T_k) \bar{h}_a \frac{T}{2T_k^3} \int_{-\pi}^{\pi} \frac{d^2 q}{(2\pi)^2} \left\{ \frac{\tanh y}{y} + \frac{1}{\cosh^2 y} \right\}, \quad (6.52)$$

$$\partial_k \bar{m}_\rho^2 = +(\partial_k T_k) \bar{h}_\rho \frac{T}{T_k^3} \int_{-\pi}^{\pi} \frac{d^2 q}{(2\pi)^2} \left\{ \frac{1 - y \tanh y}{\cosh^2 y} \right\}, \quad (6.53)$$

where  $y = \frac{\epsilon \mathbf{q}}{2T_k}$ .

The running of the **Yukawa coupling** for the antiferromagnetic boson is

$$\begin{aligned} \partial_k \bar{h}_a = & -\bar{h}_a T \int_{-\pi}^{\pi} \frac{d^2 q}{(2\pi)^2} \tilde{\partial}_k \left[ \right. \\ & \left( -\frac{1}{\omega_{1/2}^2 + \epsilon_{\mathbf{q}}^2} \left\{ \left( \frac{\bar{h}_{ak}^2}{P_{ak}(\mathbf{q})} - \frac{\bar{h}_{a\Lambda}^2}{P_{a\Lambda}} \right) - \left( \frac{\bar{h}_{\rho k}^2}{P_{\rho k}(\mathbf{q})} - \frac{\bar{h}_{\rho\Lambda}^2}{P_{\rho\Lambda}} \right) \right\} \right. \\ & \left. \left. - \frac{\tanh y}{4T_k^2 y} \left\{ \frac{\bar{h}_{a\Lambda}^2}{P_{a\Lambda}} - \frac{\bar{h}_{\rho\Lambda}^2}{P_{\rho\Lambda}} \right\} \right) \right] \\ & - \frac{\bar{m}_{ak}^2}{\bar{h}_a} \times 2T \int_{-\pi}^{\pi} \frac{d^2 q}{(2\pi)^2} \tilde{\partial}_k \left[ \right. \\ & \left( \frac{1}{\omega_{1/2}^2 + \epsilon_{\mathbf{q}}^2} \left\{ \frac{\bar{h}_{ak}^4}{P_{ak}(\mathbf{q})P_{ak}(\boldsymbol{\pi} - \mathbf{q})} - \frac{\bar{h}_{a\Lambda}^4}{P_{a\Lambda}P_{a\Lambda}} \right\} \right. \\ & \left. \left. + \frac{\tanh y}{4T_k^2 y} \times \frac{\bar{h}_{a\Lambda}^4}{P_{a\Lambda}^2} \right) \right] \end{aligned} \quad (6.54)$$

with  $y = \frac{\epsilon_{\mathbf{q}}}{2T_k}$  and  $\omega_{1/2} = \pi T_k$ . Similarly we find for  $\bar{h}_\rho$

$$\begin{aligned}
\partial_k \bar{h}_\rho = & \bar{h}_\rho T \int_{-\pi}^{\pi} \frac{d^2 q}{(2\pi)^2} \tilde{\partial}_k \left[ \right. \\
& \left. \left( \frac{\epsilon_{\mathbf{q}}^2 - \omega_{1/2}^2}{[\epsilon_{\mathbf{q}}^2 + \omega_{1/2}^2]^2} \left\{ \left( \frac{\bar{h}_{\rho k}^2}{P_{\rho k}(\mathbf{q})} - \frac{\bar{h}_{\rho\Lambda}^2}{P_{\rho\Lambda}} \right) + 3 \left( \frac{\bar{h}_{ak}^2}{P_{ak}(\mathbf{q})} - \frac{\bar{h}_{a\Lambda}^2}{P_{a\Lambda}} \right) \right\} \right. \right. \\
& \left. \left. - \frac{1}{4T_k^2 \cosh^2 y} \left\{ \frac{\bar{h}_{\rho\Lambda}^2}{P_{\rho\Lambda}} + 3 \frac{\bar{h}_{a\Lambda}^2}{P_{a\Lambda}} \right\} \right) \right] \\
& - \frac{\bar{m}_{\rho k}^2}{\bar{h}_\rho} \times (-T) \int_{-\pi}^{\pi} \frac{d^2 q}{(2\pi)^2} \tilde{\partial}_k \left[ \right. \\
& \left. \left( \frac{\epsilon_{\mathbf{q}}^2}{(\omega_{1/2}^2 + \epsilon_{\mathbf{q}}^2)^2} \left\{ 3 \left( \frac{\bar{h}_{ak}^4}{P_{ak}^2(\mathbf{q})} - \frac{\bar{h}_{a\Lambda}^4}{P_{a\Lambda}^2} \right) + \left( \frac{\bar{h}_{\rho k}^4}{P_{\rho k}^2(\mathbf{q})} - \frac{\bar{h}_{\rho\Lambda}^4}{P_{\rho\Lambda}^2} \right) \right\} \right. \right. \\
& \left. \left. + \frac{1}{8T_k^2} \left( \frac{\tanh y}{y} - \frac{1}{\cosh^2 y} \right) \left\{ 3 \frac{\bar{h}_{ak}^4}{P_{a\Lambda}^2} + \frac{\bar{h}_{\rho\Lambda}^4}{P_{\rho\Lambda}^2} \right\} \right) \right].
\end{aligned} \tag{6.55}$$

### 6.3.2 Numerical results

The truncation we have defined above is a very primitive one but was chosen to make the numerics relatively fast. We therefore do not expect high precision results but one should be able to see the general features of the flow.

The first check was to see if the corrections to the fermionic coupling  $U$  which can be found from a one loop calculation either in the bosonised or in the purely fermionic theory (see appendix B.5) are reproduced by the above flow equations. For this we start at a large value of the cutoff, follow the flow for a while and integrate out the bosons at their new couplings to obtain the new  $U$ . As expected it turns out that for large enough values of the cutoff this is indeed the case for different choices of the bosonisation parameters  $\alpha_i$ . This of course is no surprise because of the one loop form of the flow equations.

If we follow the flow towards smaller values of the cutoff, the purely fermionic coupling will obtain a complicated momentum dependence and furthermore the loop calculations are no longer adequate as comparison for the quality of the flow. We therefore need another quantity to investigate the invariance of the flow under different reparametrisations of the bosonisation. For this we have chosen the critical temperature where the mass of the boson  $\vec{a}$  corresponding to an antiferromagnetic spin density vanishes, i.e. at the onset of spontaneous symmetry breaking in the antiferromagnetic channel.

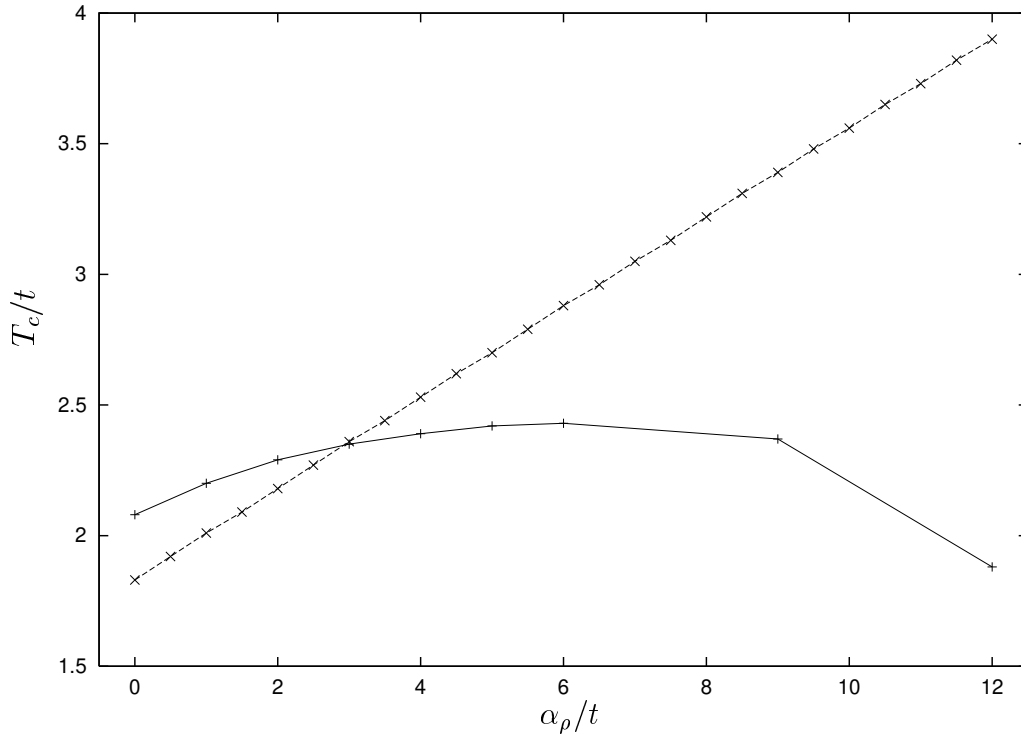


Figure 6.7: Plot of the critical temperature  $T_c$  for different choices of the parameter  $\alpha_\rho$  calculated with flow equations (solid line) and in the mean field approximation (dotted line). The initial fermionic coupling is  $U = 12t = 3\alpha_m - \alpha_\rho$ .

In figure 6.7 we have plotted the critical temperature  $T_c$  at which symmetry breaking into the antiferromagnetic channel takes place for different values of the parameters  $\alpha_m$  and  $\alpha_\rho$  for a fixed value of the initial fermionic coupling  $U = 12t = 3\alpha_m - \alpha_\rho$ . This has been calculated both with flow equations and in the “mean field approximation”, i.e. by searching for the zeroes of the bosonic mass in the loop calculation of the two point function<sup>4</sup>. The fermionic cutoff was chosen to be  $T_k^2 = T^2 + k^2$  for this plot. One observes that the critical temperature is still dependent on the choice of bosonisation. However, this dependence is relatively mild compared to the mean field results and certainly due to our poor truncation. Nevertheless, if we further increase  $\alpha_\rho$ , we will come to a point where the symmetry breaking completely ceases. This is due to the fact that the Yukawa coupling  $\bar{h}_a$  becomes too small at small values of the cutoff and cannot drive the mass  $m_a^2$  to zero sufficiently fast. We mention that the independence of the unrenormalised Yukawa coupling found in figure 6.4 is also found in the present truncation for  $\alpha_\rho = 0$ . For other values of the parameters the unrenormalised Yukawa coupling may indeed change. In the present truncation the flow of  $\bar{m}_a$  is influenced only through  $\bar{h}_a$  (see (6.52)). Therefore, if  $\bar{h}_a$  is altered during the flow this will result in a change of the

final value of  $\overline{m}_a$  and hence the critical temperature.

We also find that the critical temperature is dependent on the choice of the fermionic cutoff if the bosonic cutoff is kept fixed. This is due to different contributions from  $\tilde{\partial}_k$  derivatives of the full fermionic and the full bosonic propagator in the loops contributing to the Yukawa couplings. This dependence is of a size comparable to the parametrisation dependence discussed above if we choose  $T_k = T + k$  instead of the cutoff used for figure 6.7 above.

---

<sup>4</sup>The parametrisation independent Hartree–Fock results correspond to a critical temperature of approximately  $T_c \approx 2.9t$  in this case.

# Chapter 7

## Conclusions

The phase diagram of a high temperature superconductor shows many complicated features. At low doping these materials are antiferromagnetic insulators. Increasing the concentration of electrons or holes turns them into a superconductor with exceptionally high transition temperatures compared to “conventional” superconductors. The mechanism for the binding of electrons into Cooper pairs is so far completely unknown in these materials. Between doping concentrations leading to antiferromagnetic and superconducting behaviour is a region in which a lot of different degrees of freedom seem to play a role. The clarification of the basic degrees of freedom and their interplay in this pseudogap region still needs a lot of experimental and theoretical effort.

The common feature of all high temperature superconductors is their highly anisotropic structure composed of layers of copper oxide ( $\text{CuO}_2$ ) planes. The interesting properties of these materials and the mechanisms for generating them seem to be largely confined to these planes. The two dimensional Hubbard model is a simple attempt to capture this microscopic structure. The model assumes electrons that are able to tunnel from site to site on a lattice and feel a mutual screened Coulomb repulsion. Whether such an oversimplified model is able to reproduce the complex phase structure of a real high temperature superconductor or parts of it still has to be clarified. A lot of theoretical work has been dedicated to this task over the last years but so far the results are still inconclusive.

We try to attack this problem by means of renormalisation group (RG) equations. Earlier RG studies have already revealed the power of this technique in the context of the Hubbard model but derive the properties in a purely fermionic language. We believe that it is favourable to include the interesting degrees of freedom more explicitly. This can be achieved by rewriting the original action of the Hubbard model in a partially bosonised form.

A simple mean field calculation in the partially bosonised Hubbard model leads to very encouraging results. We are able to reproduce a phase diagram that closely resembles the one of a real high temperature superconductor. However, this simple approach also reveals an undesirable drawback of the bosonisation procedure. The couplings are not uniquely fixed by the reformulation procedure but there is an arbitrariness connected to different parametrisations of the coupling term that is also mirrored in the results. Even though the reformulation itself is exact, approximations may break this parametrisation invariance.

In the mean field approximation the fluctuations of the bosonic fields are completely neglected. Taking the bosonic fields into account should dispose of or at least diminish the parametrisation dependence of the results. An inclusion of the bosonic degrees of freedom in the calculation may be performed using renormalisation group equations. We use them in a form generalising the effective action. The bosonised theory then serves as a starting point for the flow of couplings. A loop calculation that for large cutoff reproduces the renormalisation group results serves as a guide for the formulation of suitable truncations schemes and also clarifies the relation between diagrams in the bosonised theory and the original fermionic formulation.

A first truncation deals with antiferromagnetic behaviour at and close to half filling. We are able to observe the breaking of the spin rotation symmetry and may follow the flow further into the broken phase. We obtain a plausible explanation of why antiferromagnetic behaviour may be observed in the two dimensional model despite of the Mermin-Wagner theorem as the system returns to the symmetric state when averaging over extremely large spatial extensions. The observation of antiferromagnetism may thus be regarded as a finite size effect. For low doping concentration we calculate a phase diagram that agrees well with other investigations.

In a second truncation we address the question of how strongly the flow is altered when we change the arbitrary parameters due to the parametrisation invariance of the bosonised model. We still find some dependence but in view of the minimal truncation used the results are encouraging.

We believe that the bosonisation procedure presented and applied to simple cases in this work may be regarded as a suitable starting point for further investigations. As we have shown, multi fermion couplings, corresponding to bosonic interactions in our formulation, may be included efficiently. Furthermore this approach has the advantage to be able to look into the broken phase. Also, the investigation of the interplay of different degrees of freedom is feasible by blocking some of the bosonic channels. Nevertheless, a lot of work still has to be done in order to obtain a unified picture of the phase diagram of the Hubbard model. We hope that our formalism may be able to put in place some of the pieces of this fascinating puzzle.



# Appendix A

## Conventions and notation

We use units with  $\hbar = c = k_B = 1$ . A field is indicated by a  $\hat{\phantom{x}}$  over a symbol, e.g.  $\hat{\psi}$  for a fermion. The symbol without a  $\hat{\phantom{x}}$  denotes the expectation value of the corresponding field. We write a  $\tilde{\phantom{x}}$  over a symbol to indicate composite fields build from two fermionic fields in order to distinguish them from their bosonic counterparts, e.g.  $\tilde{\rho} = \hat{\psi}^* \hat{\psi}$ . Symbols with arrow ( $\vec{m}, \vec{a}, \dots$ ) denote three dimensional vectors, while bold symbols ( $\mathbf{x}, \mathbf{q}, \dots$ ) denote two dimensional vectors. We define generalised momenta and positions by

$$Q \equiv (\omega_n, \mathbf{q}), \quad X \equiv (\tau, \mathbf{x}), \quad QX \equiv \omega_n \tau + \mathbf{xq} \quad (\text{A.1})$$

and generalised sums and corresponding delta functions as follows

$$\begin{aligned} \sum_X &\equiv \int_0^\beta d\tau \sum_{\mathbf{x}}, & \sum_Q &\equiv T \sum_n \int_\pi^\pi \frac{d^2 q}{(2\pi)^2}, \\ \delta(Q - Q') &\equiv \frac{1}{T} \delta_{n,n'} \cdot (2\pi)^2 \delta(\mathbf{q} - \mathbf{q}'), \\ \delta(X - X') &\equiv \delta(\tau - \tau') \cdot \delta(\mathbf{x} - \mathbf{x}'). \end{aligned} \quad (\text{A.2})$$

These definitions apply equally in the fermionic and bosonic case if

$$\omega_n \equiv 2\pi nT, \quad n \in \begin{cases} \mathbb{Z} & \text{for bosons} \\ \mathbb{Z} + 1/2 & \text{for fermions.} \end{cases} \quad (\text{A.3})$$

Note that  $\delta(\mathbf{q} - \mathbf{q}')$  is periodic in  $2\pi$ . The same applies to  $\delta(\tau) = \pm\delta(\tau + \beta)$  for bosons/fermions.

The Fourier transforms of the fermionic fields are:

$$\hat{\psi}(X) = \sum_Q e^{iQX} \hat{\psi}(Q), \quad \hat{\psi}^*(X) = \sum_Q e^{-iQX} \hat{\psi}^*(Q). \quad (\text{A.4})$$

Similar Fourier transforms are used for the bosonic fields (see (2.45) and (2.46)).

# Appendix B

## Useful formulae

### B.1 Pauli matrices

$GL(2, \mathbb{C})$  is the group of all complex  $2 \times 2$ -matrices. They may be constructed from the identity matrix  $\sigma^0 = \mathbb{1}_2$  and the Pauli matrices  $\sigma^1 = \begin{pmatrix} 0 & 1 \\ 1 & 0 \end{pmatrix}$ ,  $\sigma^2 = \begin{pmatrix} 0 & -i \\ i & 0 \end{pmatrix}$ ,  $\sigma^3 = \begin{pmatrix} 1 & 0 \\ 0 & -1 \end{pmatrix}$  and obey the well known relations (roman indices run from  $1 \dots 3$ , greek indices from  $0 \dots 3$ )

$$\{\sigma^i, \sigma^j\} = 2i\epsilon^{ijk}\sigma^k, \quad [\sigma^i, \sigma^j] = 2\delta^{ij}, \quad \sigma^i = (\sigma^i)^\dagger = (\sigma^i)^{-1}. \quad (\text{B.1})$$

It is useful to define a condensed notation and derive the identities ( $\epsilon = i\sigma^2$ ,  $g_{\mu\nu} = \text{diag}(1, -1, -1, -1)$ )

$$\sigma^\mu = (\sigma^0, \vec{\sigma}), \quad \bar{\sigma}^\mu = (\sigma^0, -\vec{\sigma}), \quad (\text{B.2})$$

$$(\sigma^\mu)_{\alpha\beta}(\sigma_\mu)_{\gamma\delta} = 2\epsilon_{\alpha\gamma}\epsilon_{\beta\delta}, \quad \epsilon\sigma^\mu = (\bar{\sigma}^\mu)^T\epsilon, \quad \bar{\sigma}^\mu\sigma_\mu = 4, \quad (\text{B.3})$$

from which we easily derive

$$\sigma_{\alpha\beta}^i\sigma_{\gamma\delta}^i = \delta_{\alpha\beta}\delta_{\gamma\delta} - 2\epsilon_{\alpha\gamma}\epsilon_{\beta\delta} \quad (\text{B.4})$$

$$\sigma^i\sigma^j = \delta^{ij} + i\epsilon^{ijk}\sigma^k \quad (\text{B.5})$$

$$\sigma^i\sigma^j\sigma^i = -\sigma^j \quad (\text{B.6})$$

$$\epsilon\sigma^{iT}\epsilon = \sigma^i, \quad \epsilon\sigma^i\epsilon = \sigma^{iT} \quad (\text{B.7})$$

$$\vec{\sigma}\epsilon\vec{\sigma}^T = \vec{\sigma}^T\epsilon\vec{\sigma} = -3\epsilon \quad (\text{B.8})$$

and  $(\psi^{(*)})$  are Graßmann numbers)

$$(\psi_a^*\epsilon\psi_c^*)(\psi_b\epsilon\psi_d) = -(\psi_a^*\psi_b)(\psi_c^*\psi_d) - (\psi_a^*\psi_d)(\psi_c^*\psi_b) \quad (\text{B.9})$$

$$(\psi_a^*\vec{\sigma}\psi_b)(\psi_c^*\vec{\sigma}\psi_d) = -(\psi_a^*\psi_b)(\psi_c^*\psi_d) - 2(\psi_a^*\psi_d)(\psi_c^*\psi_b). \quad (\text{B.10})$$

## B.2 Matrix relations

Let  $M = \begin{pmatrix} A & B \\ C & D \end{pmatrix}$  be an arbitrary invertible block matrix with square blocks  $A$  and  $D$ . It is often useful to consider the following partitions of the matrix

$$M = \begin{pmatrix} \mathbb{1} & 0 \\ CA^{-1} & D - CA^{-1}B \end{pmatrix} \begin{pmatrix} A & B \\ 0 & \mathbb{1} \end{pmatrix} = \begin{pmatrix} A - BD^{-1}C & BD^{-1} \\ 0 & \mathbb{1} \end{pmatrix} \begin{pmatrix} \mathbb{1} & 0 \\ C & D \end{pmatrix}. \quad (\text{B.11})$$

The determinant of the matrix can then be split up into determinants over submatrices:

$$\det M = \det(D - CA^{-1}B) \det A = \det(A - BD^{-1}C) \det D \quad (\text{B.12})$$

and  $\begin{pmatrix} \mathbb{1} & 0 \\ A & B \end{pmatrix} \begin{pmatrix} \mathbb{1} & 0 \\ -B^{-1}A & B^{-1} \end{pmatrix} = \mathbb{1} = \begin{pmatrix} A & B \\ 0 & \mathbb{1} \end{pmatrix} \begin{pmatrix} A^{-1} & -A^{-1}B \\ 0 & \mathbb{1} \end{pmatrix}$  together with the partitions leads to the inverse

$$M^{-1} = \begin{pmatrix} (A - BD^{-1}C)^{-1} & -(A^{-1}B)(D - CA^{-1}B)^{-1} \\ -(D^{-1}C)(A - BD^{-1}C)^{-1} & (D - CA^{-1}B)^{-1} \end{pmatrix}. \quad (\text{B.13})$$

We often need to expand the inverse of some matrix. For this we calculate (B is supposed to be “small”:  $|A^{-1}B| \ll 1$ ):

$$\begin{aligned} \mathbb{1} &= A^{-1}(A + B - B) = A^{-1}(A + B) - A^{-1}B \\ \Rightarrow (A + B)^{-1} &= A^{-1} - A^{-1}B(A + B)^{-1} \\ &= A^{-1} - A^{-1}BA^{-1} + A^{-1}BA^{-1}BA^{-1} - \dots \end{aligned}$$

The derivative of an inverse matrix can be read of from  $\partial_k(A_k A_k^{-1}) = 0$ :

$$\partial_k A_k^{-1} = -A_k^{-1}(\partial_k A_k)A_k^{-1} \quad (\text{B.14})$$

and under the trace we may use the relations like ( $\text{tr} \ln A = \ln \det A$ )

$$\begin{aligned} \partial_k \text{tr} f(A_k) &= \text{tr}[f'(A_k)\partial_k A_k], \\ \partial_k \text{tr} \ln A_k &= \text{tr} A_k^{-1} \partial_k A_k, \quad \partial_k \det A_k = \text{tr}[A_k^{-1} \partial_k A_k] \det A_k \end{aligned}$$

for matrices depending on some parameter  $k$ .

## B.3 Matrices containing Grassmann numbers

There are many excellent introductions into the field of Grassmann calculus (e.g. [9, 28, 41]). We will only mention a few matters we need for our calculations.

We denote the even (commuting) and odd (anticommuting) parts of a Graßmann algebra  $\mathcal{G}$  by  $\mathcal{G}_+$  and  $\mathcal{G}_-$  respectively.  $\mathcal{G}_+$  are the usual complex numbers  $\mathbb{C}$  (or any field  $\mathbb{F}$ ) and  $\mathcal{G}_-$  contains the “usual” Graßmann numbers.

We will consider matrices in “standard form”:

$$A = \begin{pmatrix} A_{BB} & A_{BF} \\ A_{FB} & A_{FF} \end{pmatrix}, \quad \text{with} \quad \begin{cases} A_{BB,ij}, A_{FF,ij} \in \mathcal{G}_+ \\ A_{BF,ij}, A_{FB,ij} \in \mathcal{G}_- \end{cases}. \quad (\text{B.15})$$

If furthermore  $A_{BB}^T = A_{BB}$ ,  $A_{FF}^T = -A_{FF}$  and  $A_{FB}^T = -A_{BF}$ , we call such a matrix s-symmetric. ( $T$  denotes the usual transposed:  $(A^T)_{ij} = A_{ji}$ ).

Then define

$$\begin{aligned} \text{supertrace:} \quad \text{str} A &= \text{tr} A_{11} - \text{tr} A_{22} \\ \text{superdeterminant:} \quad \text{sdet} A &= \exp(\text{str} \ln A), \end{aligned} \quad (\text{B.16})$$

with the properties

$$\text{str} AB = \text{str} BA \quad (\text{B.17})$$

$$\partial_k \text{str}[f(A_k)] = \text{str}[f'(A_k) \cdot \partial_k A_k] \quad (\text{B.18})$$

$$\text{sdet} AB = \text{sdet} A \cdot \text{sdet} B \quad (\text{B.19})$$

$$\begin{aligned} \text{sdet} A &= [\det(A_{BB} - A_{BF} A_{FF}^{-1} A_{FB})]^{-1} \det A_{FF} \\ &= \det(A_{FF} - A_{FB} A_{BB}^{-1} A_{BF}) [\det A_{BB}]^{-1}. \end{aligned} \quad (\text{B.20})$$

Equation (B.17) is proven easily by direct calculation for two matrices in standard form. (B.18) then follows from (B.17) by expansion of  $f$ .

The supertrace of the commutator of two matrices vanishes because of (B.17). Together with the Baker-Kampbell-Hausdorff formula  $e^A e^B = e^{(A+B+[A,B]/2+\dots)}$  we can prove (B.19) by using the definition of sdet:

$$\text{str} \ln(AB) = \text{str} \ln(e^{\ln A} e^{\ln B}) = \text{str}(\ln A + \ln B) + \text{str}\left(\frac{1}{2}[\ln A, \ln B] + \dots\right),$$

where the linearity of the supertrace was used. The last term only contains commutators and vanishes.

Note that the partitions (B.11) also apply to supermatrices. We thus only need (B.19) to prove (B.20). Note also the similarity between the usual determinant (B.12) and the superdeterminant. An inverse can also be constructed with the aid of the partitions just as we did in (B.13).

The formulae for supertraces and superdeterminants above bear a clear relation to the ones for usual traces and determinants. Another important relation,  $\det A^T = \det A$ , needs the definition of the “supertransposed” matrix  $M^S$  to have a counterpart:

$$A^S = \begin{pmatrix} A_{BB}^T & -A_{FB}^T \\ A_{BF}^T & A_{FF}^T \end{pmatrix}, \quad (AB)^S = B^S A^S, \quad \text{sdet} A^S = \text{sdet} A. \quad (\text{B.21})$$

## B.4 Gaussian integrals

See [41] or [48] for a general discussion of Gaussian integrals. For  $\phi_i, j_i, A_{ij} = A_{ji}, B_{ij} = -B_{ji} \in \mathcal{G}_+$  and  $\theta_i, \eta_i \in \mathcal{G}_-$  one finds

$$\begin{aligned} I_+(A, j) &= \int_{-\infty}^{\infty} \exp\left(-\frac{1}{2}\phi_i A_{ij} \phi_j + j_i \phi_i\right) \prod_i \frac{d\phi_i}{\sqrt{2\pi}} \\ &= \frac{1}{\sqrt{\det(A)}} \exp\left(\frac{1}{2}j_i A_{ij}^{-1} j_j\right), \end{aligned} \quad (\text{B.22})$$

$$\begin{aligned} I_-(B, \eta) &= \int \exp\left(-\frac{1}{2}\theta_i B_{ij} \theta_j + \eta_i \theta_i\right) d\theta_1 \cdots d\theta_n \\ &= \text{pf}(B) \exp\left(-\frac{1}{2}\eta_i B_{ij}^{-1} \eta_j\right), \end{aligned} \quad (\text{B.23})$$

$$\text{pf}^2(B) = \det(B), \quad (\text{B.24})$$

where the "pfaffian" is defined through the integral and can be shown to be related to the determinant as shown.

More general integrals containing both commuting and anticommuting numbers can easily be calculated from these two special cases by first integrating over Grassmann and then over commuting variables (or vice versa). For s-symmetric matrices (see (B.15)) one has

$$\begin{aligned} M &= \begin{pmatrix} A_{BB} & A_{BF} \\ A_{FB} & A_{FF} \end{pmatrix}, \quad \chi = \begin{pmatrix} \phi \\ \eta \end{pmatrix} \\ S[\chi] &= \frac{1}{2}\chi^T M \chi = \frac{1}{2}\phi^T A_{BB} \phi + \phi^T A_{BF} \eta + \frac{1}{2}\eta^T A_{FF} \eta \in \mathcal{G}_+ \end{aligned}$$

$$\begin{aligned} \text{spf}(M) &= \int \exp\left(-\frac{1}{2}\chi^T M \chi\right) \mathcal{D}\chi, \quad \mathcal{D}\chi = \prod_i \frac{d\phi_i}{\sqrt{2\pi}} d\theta_1 \cdots d\theta_n \\ &= \frac{\text{pf}(A_{FF} + A_{BF}^T A_{BB}^{-1} A_{BF})}{\sqrt{\det A_{BB}}} = \frac{\text{pf}(A_{FF})}{\sqrt{\det(A_{BB} + A_{BF} A_{FF}^{-1} A_{BF}^T)}} \end{aligned} \quad (\text{B.25})$$

where again the "super-pfaffian" is defined through the integral. Depending on which integral was performed first one encounters one of the two equivalent representations in terms of determinants. Note the connection with the supertrace (and superdeterminant) for s-symmetric matrices:

$$\text{str} \ln M = \ln \text{sdet} M = -2 \ln \text{spf} M. \quad (\text{B.26})$$

in contrast to  $\text{tr} \ln B = \ln \det B = +2 \ln \text{pf} B$  for "usual" antisymmetric matrices.

## B.5 Loop calculations

We expand the effective action in powers of  $\hbar$ , i.e. in numbers of loops:

$$\begin{aligned}\Gamma[\chi] &= -\hbar \ln \int \mathcal{D}\tilde{\chi} \exp(-S[\tilde{\chi} + \chi] + J[\chi]\chi)/\hbar = \Gamma_0[\chi] + \hbar\Gamma_1[\chi] + \hbar^2\Gamma_2[\chi] + \dots \\ J[\chi] &= \frac{\delta\Gamma[\chi]}{\delta R\chi} = J_0[\chi] + \hbar J_1[\chi] + \hbar^2 J_2[\chi] + \dots\end{aligned}\tag{B.27}$$

(note that the functional derivative is a right-derivative; this is only important for fermions). To lowest order  $\Gamma_0[\chi] = S[\chi]$  and hence  $J_0 = S^{(1)}[\chi]$ . Inserting this together with an expansion of the action

$$S[\chi + \tilde{\chi}] = S[\chi] + S^{(1)}[\chi]\tilde{\chi} + \frac{1}{2}\tilde{\chi}^T S^{(2)}[\chi]\tilde{\chi} + \dots$$

into (B.27) we obtain

$$\Gamma[\chi] = S[\chi] - \hbar \ln \int \mathcal{D}\tilde{\chi} \exp(-\frac{1}{2}\tilde{\chi}^T S^{(2)}[\chi]\tilde{\chi})/\hbar + \mathcal{O}(2\text{-loop}).\tag{B.28}$$

The integral is Gaussian and can be performed both for bosonic and fermionic variables and the mixed case. From  $\Gamma_1[\chi]$  we get  $J_1$  and can proceed calculating the two loop correction. We remark that the source term  $J\chi$  cancels all diagrams in the functional integral that are not one particle irreducible.

We proceed by expanding the one loop result in the bosonic case  $\Gamma_1 = \Delta\Gamma = \frac{1}{2} \ln \det S^{(2)}$  in the number of external legs. For this we rearrange  $S^{(2)} = S_{\text{kin}}^{(2)} + \Delta S^{(2)} = S_{\text{kin}}^{(2)}(1 + (S_{\text{kin}}^{(2)})^{-1}\Delta S_2)$  and expand  $\ln(1-x) = -\sum_{n=1}^{\infty} x^n/n$ . ( $S_{\text{kin}}^{(2)} = \tilde{P}$ )

$$\begin{aligned}\Delta\Gamma &= \Delta\Gamma_0 + \Delta\Gamma_1 + \Delta\Gamma_2 + \dots \\ &= \frac{1}{2}\text{Tr} \ln \tilde{P} + \frac{1}{2}\text{Tr}(\tilde{P}^{-1}\Delta S^{(2)}) - \frac{1}{4}\text{Tr}(\tilde{P}^{-1}\Delta S^{(2)})^2 + \dots\end{aligned}\tag{B.29}$$

The first term is a vacuum graph, the second describes tadpoles and the third yields the loop corrections to the propagators etc. (c.f. (5.8)).

### B.5.1 Fermion-loop corrections in pure fermionic theory

To see how this works consider an action of the form

$$S[\psi, \psi^*] = \psi_A^* P_{AB} \psi_B + \frac{U}{2} f_{ABCD} \psi_A^* \psi_B \psi_C^* \psi_D\tag{B.30}$$

with  $f_{ABCD} = f_{CDAB}$ . We then find (dots indicate the matrix structure  $(f_{AB..})_{\alpha\beta} = f_{AB\alpha\beta}$ )

$$\begin{aligned} S^{(2)}[\psi, \psi^*] &= \underbrace{\begin{pmatrix} & -P^T \\ P & \end{pmatrix}}_{\tilde{P}} + \frac{U}{2} \underbrace{\begin{pmatrix} -2f_{A..C}\psi_A^*\psi_C^* & -2[(f_{AB..} - f_{BA..})\psi_A^*\psi_B]^T \\ 2(f_{AB..} - f_{BA..})\psi_A^*\psi_B & -2f_{B..D}\psi_B\psi_D \end{pmatrix}}_{S_{int}^{(2)}[\psi, \psi^*]} \\ &= \begin{pmatrix} B^+ & -A^T \\ A & B \end{pmatrix} \end{aligned} \quad (\text{B.31})$$

and hence with a relation like (B.29) (for the propagator we write  $G = P^{-1}$ )

$$\begin{aligned} \Delta\Gamma_1[\psi, \psi^*] &= -\frac{1}{2}\text{Tr}(\tilde{P}^{-1}S_{int}^{(2)}[\psi, \psi^*]) \\ &= -U\text{Tr}[G(f_{AB..} - f_{BA..})\psi_A^*\psi_B] \\ \Delta\Gamma_2[\psi, \psi^*] &= \frac{1}{4}\text{Tr}(\tilde{P}^{-1}S_{int}^{(2)}[\psi, \psi^*])^2 \\ &= \frac{U^2}{2}\text{Tr}[G(f_{AB..} - f_{BA..})\psi_A^*\psi_B G(f_{CD..} - f_{DC..})\psi_C^*\psi_D] \\ &\quad - \frac{U^2}{2}\text{Tr}[G^T f_{A..C}\psi_A^*\psi_C^* G f_{B..D}\psi_B\psi_D]. \end{aligned} \quad (\text{B.32})$$

## B.5.2 Mixed bosonic and fermionic fields

We abbreviate  $\chi_A = (u, u^*, w, \psi, \psi^*)_A$  and consider the action:

$$S[\chi] = S_{\text{kin}}^F[\psi, \psi^*] + S^B[u, u^*, w] + S_Y[\chi] \quad (\text{B.33})$$

$$S_{\text{kin}}^F[\psi, \psi^*] = \psi_A^* P_{AB}^F \psi_B, \quad S^B[u, u^*, w] = \frac{1}{2}w_A P_{AB}^w w_B + u_A^* P_{AB}^u u_B, \quad (\text{B.34})$$

$$S_Y[\chi] = -w_C \psi_A^* V_{AB,C}^w \psi_B - u_C^* \psi_A V_{AB,C}^{u^*} \psi_B - u_C \psi_A^* V_{AB,C}^u \psi_B^*. \quad (\text{B.35})$$

Let us parametrise

$$S[\chi + \chi_0] = S^{(0)}[\chi_0] + S_A^{(1)}[\chi_0]\chi_A + \frac{1}{2}\chi_A S_{AB}^{(2)}[\chi_0]\chi_B + \dots, \quad (\text{B.36})$$

then the matrix of second functional derivatives reads

$$S^{(2)}[\chi] = \begin{pmatrix} 0 & P^{uT} & 0 & 0 & -2\psi^* V_{,c}^u \\ P^u & 0 & 0 & -2\psi V_{,c}^{u^*} & 0 \\ 0 & 0 & P^w & -\psi^* V_{,c}^w & V_{,c}^w \psi \\ 0 & -2V_{,c}^{u^*} \psi & \psi^* V_{,c}^w & -2u_c^* V_{,c}^{u^*} & -(P^F - w_c V_{,c}^w)^T \\ -2V_{,c}^u \psi^* & 0 & -V_{,c}^w \psi & P^F - w_c V_{,c}^w & -2u_c V_{,c}^u \end{pmatrix}. \quad (\text{B.37})$$

This matrix is s-symmetric (see (B.15)), therefore to order one-loop we find from the previous sections

$$\Gamma[\chi] = S[\chi] + \Delta\Gamma[\chi] = S[\chi] + \frac{1}{2}\text{str} \ln S^{(2)}. \quad (\text{B.38})$$

As usual we try to perform an expansion of the logarithm:  $\ln(1+x) = x - x^2/2 + x^3/3 - \dots$ . For this we split the matrix into a propagator and an interaction part, e.g. for the fermionic part of the matrix

$$S_{FF}^{(2)} = \tilde{P}_F + \tilde{I}_{FF}. \quad (\text{B.39})$$

It is not always unambiguous how the matrix should be split up. Usually the kinetic or field independent part is taken as propagator and the rest is considered as interaction. However, for some purposes (especially in a phase with broken symmetry) it may be favourable to include some of the “interaction” parts into the propagator.

In the following we relate the lowest order terms of the expansion of  $\Delta\Gamma[\chi]$ . To enhance readability we rename the real and complex fields to  $R$  and  $C$  respectively. The propagators are indicated by a  $G = P^{-1}$  with labels for the respective fields. The vertices are denoted as above.

### Bosonic two point function

$$\begin{aligned} \Delta\Gamma_{BB} = & \sum_K \left[ \frac{1}{2} R_i(-K) R_j(K) \sum_L \text{tr}_{\text{spin}} \{ G^\psi(L) V_i^R(L, K+L) G^\psi(K+L) V_j^R(K+L, L) \} \right. \\ & \left. + C_i^*(K) C_j(K) (-2) \sum_L \text{tr}_{\text{spin}} \{ G^\psi(L) V_j^C(L, K-L) G^\psi(K-L) V_i^{C*}(K-L, L) \} \right] \end{aligned} \quad (\text{B.40})$$

### Fermionic two point function

$$\begin{aligned} \Delta\Gamma_{\psi^*\psi} = & \sum_{QQ'} \psi_\alpha^*(Q) \psi_\beta(Q') \\ & \sum_L \{ -G_{ji}^R(L) V_i^R(Q, Q+L) G^\psi(Q+L, Q'+L) V_j^R(Q'+L, Q') \\ & + 4G_{ji}^C(L) V_i^C(Q, L-Q) G^\psi(L-Q, L-Q') V_j^{C*}(L-Q', Q') \}_{\alpha\beta} \end{aligned} \quad (\text{B.41})$$

### Vertex Corrections

Real:

$$\begin{aligned} \Delta\Gamma_{YR} = & \sum_{KQQ'} R_k(K) \psi_\alpha^*(Q) \psi_\beta(Q') \delta(K-Q+Q') \\ & \sum_L \{ -G_{ji}^R(L) V_i^R(Q, Q+L) G^\psi(Q+L) V_k^R(Q+L, Q'+L) \\ & \quad G^\psi(Q'+L) V_j^R(Q'+L, Q') \\ & + 4G_{ji}^C(L) V_i^C(Q, L-Q) G^\psi(L-Q) [V_k^R(L-Q', L-Q)]^T \\ & \quad G^\psi(L-Q') V_j^{C*}(L-Q', Q') \}_{\alpha\beta} \end{aligned} \quad (\text{B.42})$$



Real-complex:

$$\begin{aligned} \Delta\Gamma_{YC} = & \sum_{KQQ'} C_k(K) \psi_\alpha^*(Q) \psi_\beta^*(Q') \delta(K - Q - Q') \\ & \sum_L \left\{ -G_{ji}^R(L) V_i^R(Q, Q+L) G^\psi(Q+L) V_k^C(Q+L, Q'-L) \right. \\ & \left. [G^\psi(Q'-L)]^T [V_j^R(Q', Q'-L)]^T \right\}_{\alpha\beta} \end{aligned} \quad (\text{B.43})$$

**Box diagrams**

Real-real-1:

$$\begin{aligned} \Delta\Gamma_{B1} = & \sum_{ABCD} \psi_\alpha^*(Q_A) \psi_\beta(Q_B) \psi_\gamma^*(Q_C) \psi_\delta(Q_D) \delta(Q_A - Q_B + Q_C - Q_D) \\ & \frac{1}{2} \sum_L G_{ji}^R(L) G_{kl}^R(L+A-B) \\ & \left\{ -[V_i^R(A, A-L) G^\psi(A-L) V_k^R(A-L, B)]_{\alpha\beta} \right. \\ & \left. [V_l^R(C, D-L) G^\psi(D-L) V_j^R(D-L, D)]_{\gamma\delta} \right\} \end{aligned} \quad (\text{B.44})$$

Real-real-2:

$$\begin{aligned} \Delta\Gamma_{B2} = & \sum_{ABCD} \psi_\alpha^*(Q_A) \psi_\beta(Q_B) \psi_\gamma^*(Q_C) \psi_\delta(Q_D) \delta(Q_A - Q_B + Q_C - Q_D) \\ & \frac{1}{2} \sum_L G_{ji}^R(L) G_{lk}^R(L-A+B) \\ & \left\{ -[V_i^R(A, A-L) G^\psi(A-L) V_l^R(A-L, B)]_{\alpha\beta} \right. \\ & \left. [V_j^R(C, L+C) G^\psi(L+C) V_k^R(L+C, D)]_{\gamma\delta} \right\} \end{aligned} \quad (\text{B.45})$$

Real-complex:

$$\begin{aligned} \Delta\Gamma_{B3} = & \sum_{ABCD} \psi_\alpha^*(Q_A) \psi_\beta(Q_B) \psi_\gamma^*(Q_C) \psi_\delta(Q_D) \delta(Q_A - Q_B + Q_C - Q_D) \\ & \frac{1}{2} \sum_L G_{ji}^R(L) G_{lk}^C(A+C-L) \\ & \left\{ -8[V_i^R(A, A-L) G^\psi(A-L) V_l^C(A-L, C)]_{\alpha\gamma} \right. \\ & \left. [V_k^{C*}(D, B-L) G^\psi(B-L) V_j^R(B-L, B)]_{\delta\beta} \right\} \end{aligned} \quad (\text{B.46})$$

Complex-complex:

$$\begin{aligned} \Delta\Gamma_{B4} = & \sum_{ABCD} \psi_\alpha^*(Q_A) \psi_\beta(Q_B) \psi_\gamma^*(Q_C) \psi_\delta(Q_D) \delta(Q_A - Q_B + Q_C - Q_D) \\ & \frac{1}{2} \sum_L G_{ij}^C(L) G_{kl}^C(L-A+B) \\ & \left\{ -16[V_l^{C*}(B, L-A) G^\psi(L-A) V_i^C(L-A, A)]_{\beta\alpha} \right. \\ & \left. [V_j^{C*}(D, L-D) G^\psi(L-D) V_k^C(L-D, C)]_{\delta\gamma} \right\} \end{aligned} \quad (\text{B.47})$$

# Bibliography

- [1] P.W. Anderson, R. Schrieffer, *Physics Today*, **6**, (1991); P.W. Anderson, *The Theory of Superconductivity in the High- $T_c$  Cuprates*, Princeton University Press (1997)
- [2] K.Aoki, K. Morikawa, W. Souma, J.-I. Sumi, H. Terao, *Prog.Theor.Phys.* **99** (1998) 451
- [3] C. Bagnuls, C. Bervillier, *Phys.Rept.* **348**, 91 (2001) [hep-th/0002034]
- [4] T. Baier, E. Bick and C. Wetterich, *Phys.Rev.* **B62**, 15471 (2000) [cond-mat/0005218]
- [5] T. Baier, E. Bick and C. Wetterich, [cond-mat/0107390]
- [6] J. Bardeen, L.N. Cooper, J.R. Schrieffer, *Phys.Rev.* **106**, 162 (1957) ;*Phys. Rev.* **108**, 1175 (1957)
- [7] B. Batlogg, C.M. Varma, *Phys. World*, 2 (2000)
- [8] J.G. Bednorz, K.A. Müller, *Z.Phys.* **B64**, 189 (1986)
- [9] F.A. Berezin, *Introduction to superanalysis*, Reidel, Dordrecht, 1987
- [10] J. Berges, D.-U. Jungnickel, C. Wetterich, *Phys.Rev.* **D59**, 034010 (1999); *Eur. Phys. J.* **C13**, 323 (2000);
- [11] J. Berges, N. Tetradis, C. Wetterich, *Phys.Rept.* **363**, 223 (2002) [hep-ph/0005122]
- [12] E. Bick, PhD thesis, Heidelberg, 2002
- [13] S. Chandrasekharan, J. Cox, J.C. Osborn, U.-J. Wiese, [cond-mat/0201360]
- [14] U. Ellwanger, C. Wetterich, *Nucl.Phys.* **B423**, 137, (1994); C. Wetterich, *Z.Phys.* **C72**, 139, (1996)

- 
- [15] H. Eschrig, J. Fink, L. Schultz, *Physik Journal*, 45, 1, (2002)
- [16] W. Fischer, I. Lieb, *Funktionentheorie*, Vieweg, Wiesbaden, 1992
- [17] J.F. Gamboa, J.L. Cortes, L.F. Velazquez, *Spektrum d. Wissenschaft*, 6, (1999)
- [18] H. Gies, C. Wetterich, *Phys.Rev.* **D65**, 065001 (2002) [hep-th/0107221]
- [19] I. Grote, E. Koerding, F. Wegner, [cond-mat/0106604]
- [20] C.J. Halboth, W. Metzner, *Phys.Rev.* **B61**, 7364 (2000); *Phys.Rev.Lett.* **85**, 5162 (2000)
- [21] V. Hankevych, F.Wegner, [cond-mat/0207612]
- [22] F. Höfling, Diplomarbeit, Heidelberg, 2002
- [23] C. Honerkamp, M. Salmhofer, N. Furukawa, T.M. Rice, *Phys.Rev.* **B63**, 035109 (2001) [cond-mat/9912358]; M. Salmhofer, C. Honerkamp, *Prog.Theor.Phys.* **105**, 1 (2001); C. Honerkamp, M. Salmhofer, *Phys.Rev.* **B64**, 184516 (2001) [cond-mat/0105218]; C. Honerkamp, M. Salmhofer, T.M. Rice, *Eur.Phys.J.* **B27**, 127 (2002) [cond-mat/0204063]
- [24] C.Honerkamp, M.Salmhofer, T.M.Rice, *Eur.Phys.J.* **B27**, 127 (2002) [cond-mat/0204063]
- [25] J. Hubbard, *Proc.Roy.Soc. (London)* **A 276**, 238 (1963); J. Kanamori, *Prog.Theor.Phys.* **30**, 275 (1963); M. C. Gutzwiller, *Phys.Rev.Lett.* **10**, 159 (1963)
- [26] J. Jäckel, C. Wetterich, [hep-ph/0207094]
- [27] D.-U. Jungnickel, C. Wetterich, [hep-ph/9902316]
- [28] H. Kalka, G. Soff, *Supersymmetrie*, Teubner, Stuttgart, 1997
- [29] J.M. Kosterlitz, D.J. Thouless, *J.Phys.* **C6**, 1181 (1973); J.M. Kosterlitz, *J.Phys.*, **C7**, 1046 (1974)
- [30] L.D.Landau, E.M.Lishitz, *Statistical Physics, Part 2*, Pergamon Press, Oxford, 1988
- [31] E.H. Lieb, F.Y. Wu, *Phys.Rev.Lett.*, **20**, 1445 (1968)
- [32] N.D. Mermin, H.Wagner, *Phys.Rev.Lett.* **17**, 1133 (1966)
- [33] A. Mielke, *Das Hubbardmodell*, lecture notes, Heidelberg, (2002), [<http://www.tphys.uni-heidelberg.de/mielke/>]

- 
- [34] J.W. Negele, H. Orland, *Quantum Many-Particle Systems*, Addison Wesley, Redwood City, 1988
- [35] J.Polchinski, [hep-th/9210046]
- [36] W.H. Press, V.T. Vetterling, S.A. Teukolsky, B.P. Flannery, *Numerical recipes in C*, Cambridge University Press, 1992
- [37] D.J. Scalapino, *Phys.Rep.* **250**, 329 (1995)
- [38] R. Shankar, *Rev.Mod.Phys.* **66**, 1, 129 (1994)
- [39] H. Tasaki, *Prog.Theor.Phys.* **99** (1998) [cond-mat/9712219]; [cond-mat/9512169]
- [40] C.C. Tsuey et al., *Phys.Rev.Lett.* **73**, 593 (1994); J.R. Kirtley et al., *Nature* **373**, 255 (1995)
- [41] F. Wegner, *Graßmann-Variable*, lecture notes, Heidelberg (1998) [<http://www.tphys.uni-heidelberg.de/wegner/>]
- [42] S. Weinberg, *The Quantum Theory of Fields*, vol.2, Cambridge University Press, 1996
- [43] C. Wetterich, *Phys. Lett.* **301B**, 90, (1993); *Z.Phys.* **C48**, 693, (1990); **C 57**, 451, (1993); **C 60**, 461, (1993)
- [44] C. Wetterich, *Z.Phys.*, **C57**, 451 (1993)
- [45] K. G. Wilson, *Phys. Rev.* **B4**, 3174, (1971); 3184; K. G. Wilson, I. G. Kogut, *Phys.Rep.* **12**, 75, (1974); F. Wegner, A. Houghton, *Phys. Rev.* **A8**, 401, (1973); F. Wegner in *Phase Transitions and Critical Phenomena*, vol. 6, eds. C. Domb and M. S. Greene, Academic Press, 1976; J. Polchinski, *Nucl.Phys.* **B231**, 269 (1984)
- [46] D. Zanchi and H. J. Schulz, *Z.Phys.* **B103**, 339 (1997); *Europhys. Lett.* **44**, 235 (1998)
- [47] S. Zhang, *Phys.Rev.Lett.* **65**, 1, 120 (1990)
- [48] J. Zinn-Justin, *Quantum Field Theory and Critical Phenomena*, Clarendon Press, Oxford, 1993

# Dank...

...geht an alle, die mir während der Promotion zur Seite gestanden haben und in der einen oder anderen Weise am Gelingen dieser Arbeit beteiligt sind. Insbesondere gilt mein Dank

Herrn Professor C. Wetterich für freundliche, motivierende, hilfreiche, kompetente und engagierte Betreuung,

Herrn Professor M.G. Schmitt für die tatkräftige Hilfe bei der Beschaffung von Stipendiengeldern und die Übernahme der Zweitkorrektur,

Eike Bick für die freundschaftliche und effektive Zusammenarbeit und für die benutzerfreundliche Implementierung der numerischen Routinen,

Filipe Paccetti und Steffen Weinstock für viele interessante Diskussionen und Hilfestellungen,

Annabella Rauscher, die mir in allen Lebenslagen zur Seite gestanden hat,

und nicht zuletzt meinen Eltern, die mich immer unterstützt haben und ohne die diese Arbeit nie zustande gekommen wäre.